

JUN 21 1977

Cy. 2

Progress
Planning (RR 3)

MAY 10 1976

APR 22 1987



A GENERAL ANALYSIS OF FREE TURBULENT MIXING

Philip T. Harsha
ARO, Inc.

ENGINE TEST FACILITY
ARNOLD ENGINEERING DEVELOPMENT CENTER
AIR FORCE SYSTEMS COMMAND
ARNOLD AIR FORCE STATION, TENNESSEE 37389

May 1974

Final Report for Period June 1969 — June 1973

Approved for public release; distribution unlimited.

Prepared for

AIR FORCE OFFICE OF SCIENTIFIC RESEARCH
1400 WILSON BLVD.
ARLINGTON, VIRGINIA 22209

Property of U. S. Air Force
AEDC LIBRARY
F4U600-74-2-0001

NOTICES

When U. S. Government drawings, specifications, or other data are used for any purpose other than a definitely related Government procurement operation, the Government therby incurs no responsibility nor any obligation whatsoever, and the fact that the Government may have formulated, furnished, or in any way supplied the said drawings, specifications, or other data, is not to be regarded by implication or otherwise, or in any manner licensing the holder or any other person or corporation, or conveying any rights or permission to manufacture, use, or sell any patented invention that may in any way be related thereto.

Qualified users may obtain copies of this report from the Defense Documentation Center.

References to named commercial products in this report are not to be considered in any sense as an endorsement of the product by the United States Air Force or the Government.

**A GENERAL ANALYSIS OF
FREE TURBULENT MIXING**

**Philip T. Harsha
ARO, Inc.**

Approved for public release; distribution unlimited.

FOREWORD

The work reported herein was conducted by the Arnold Engineering Development Center (AEDC), Air Force Systems Command (AFSC) for the Air Force Office of Scientific Research under Program Element 61102F, Project 9711. AFOSR project monitor was Dr. B. T. Wolfson.

This work was done by ARO, Inc. (a subsidiary of Sverdrup & Parcel and Associates, Inc.), contract operator of the Arnold Engineering Development Center (AEDC), Air Force Systems Command (AFSC), Arnold Air Force Station, Tennessee. The investigation was performed under ARO Project Numbers RW5008, RW5108, RW5208 and RF208 from June 1969 to June 1973, and the manuscript was submitted for publication on August 10, 1973.

This technical report has been reviewed and is approved.

MARION L. LASTER
Research and Development
Division
Directorate of Technology

ROBERT O. DIETZ
Director of Technology

ABSTRACT

A general analysis applicable to a variety of free mixing flows of engineering interest is described. An empirical relationship between the turbulent shear stress and the turbulent kinetic energy is used. Solution of the turbulent kinetic energy equation as one of the governing equations yields the turbulent shear stress at all points in the flow field. Algebraic relationships are used to obtain the length scales required to close the turbulent kinetic energy equation. The computer program developed to provide the numerical framework for this analysis is described, and a FORTRAN listing and description of required inputs is included. To demonstrate the capabilities of the analysis, a number of experimental free mixing flows have been calculated, and the results of these calculations are discussed.

CONTENTS

	<u>Page</u>
ABSTRACT	iii
I. INTRODUCTION	1
II. ANALYSIS	4
III. NUMERICAL PROCEDURE	11
IV. DEMONSTRATION OF THE METHOD	17
V. COMPUTER PROGRAM	38
REFERENCES	48

ILLUSTRATIONS

Figure

1. Schematic of Free Mixing Flow Field	1
2. Comparison of Calculated and Experimental Variation of Ratio of Shear Stress to Kinetic Energy	6
3. Coordinate System	12
4. Finite-Difference Grid	16
5. Initial Condition Definition Sketch	18
6. Predicted Effect of Velocity Ratio on Two-Dimensional Shear-Layer Spread Rate, NASA Case 1	21
7. Predicted Variation of Spread Parameter with Mach Number, NASA Case 2	22
8. Variation of Spreading Parameter, with Density Ratio, NASA Case 3	22
9. Comparison of Experimental and Theoretical Velocity Profiles for NASA Case 4 (Incompressible Two-Dimensional Shear Layer, $u_2/u_1 = 0.357$)	23
10. Comparison of Theoretical and Experimental Profiles, Case 5, Compressible ($M = 2$) Two-Dimensional Shear Layer	24
11. Comparison of Prediction with Experimental Data, NASA Case 18, Asymptotic Circular Jet	25
12. Comparison of Profile Predictions with Experimental Data, NASA Case 18, Asymptotic Circular Jet	25
13. Comparison of Prediction with Experimental Data for $M = 0.6$ Circular Jet, NASA Case 6	26
14. Comparison of Prediction with Experiment, $M = 2.22$ Jet, NASA Case 7	26
15. Comparison of Prediction with Experiment, NASA Case 8, Heated $M = 0.7$ Circular Jet	27
16. Comparison of Prediction with Experiment, NASA Case 19, $M_j = 1.4$ Circular Jet	27

<u>Figure</u>	<u>Page</u>
17. Comparison of Prediction with Experiment, NASA Case 13, Two-Dimensional Jet in Moving Stream, $u_j/u_e = 3.29$	28
18. Comparison of Prediction with Experiment, NASA Case 9, Coaxial Air Jets	29
19. Comparison of Predictions with Experiment, NASA Case 20, Coaxial Air Jets	29
20. Comparison of Prediction with Experiment, NASA Case 11, Axisymmetric Jet in Moving Stream, $M_j = 0.90$, $M_e = 1.30$	30
21. Comparison of Predictions with Experiment, NASA Case 10, Hydrogen-Air Jets	31
22. Comparison of Theory with Experiment, NASA Case 21, Hydrogen-Air Jets	31
23. Comparison of Predictions with Experimental Data, NASA Case 12, Hydrogen-Air Jets	32
24. Comparison of Predictions with Experiment, NASA Case 22, Supersonic Hydrogen-Air Jets	32
25. Comparison of Prediction with Experiment, NASA Case 14, Two-Dimensional Incompressible Wake	33
26. Comparison of Measured and Predicted Velocity Profiles, NASA Case 14, Two-Dimensional Wake	34
27. Comparison of Turbulent Shear Stress Profiles, NASA Case 14, Two-Dimensional Wake	35
28. Comparison of Prediction with Experimental Data, NASA Case 15, Axisymmetric Incompressible Wake	35
29. Comparison of Prediction with Experiment, NASA Case 16, Compressible ($M = 2.88$) Two-Dimensional Wake	36
30. Comparison of Prediction with Experiment for NASA Case 17, Compressible Axisymmetric Wake	36
31. Computer Program Flow Diagram	39

TABLES

I. Profile Relations for the Parameter a_1	6
II. Source Terms in the Transformed Equations	13
III. Summary of Initial Conditions	19
IV. Variables Stored in Common Blocks	40
V. Integer Control Inputs	44
VI. Real Variable Control Inputs	44
VII. FORTRAN Variable Names	45

APPENDIX

I. FORTRAN Listing	53
------------------------------	----

NOMENCLATURE

- a Coefficient in general transport equation
- a_1 Ratio of turbulent shear stress to turbulent kinetic energy
- a_2 Turbulent kinetic energy dissipation coefficient
- b Coefficient in general transport equation
- C Jet species concentration
- c Coefficient in general transport equation
- c_1 Density-ratio correction to a_2
- d Coefficient in general transport equation
- H Total enthalpy
- k Turbulent kinetic energy (TKE)
- k_p Constant in Prandtl eddy viscosity model
- λ_k TKE dissipation length scale
- \dot{m}^u Entrained mass flux/unit area
- P Pressure
- Pr_l Turbulent Prandtl number
- Pr_k Turbulent Prandtl number for TKE
- R Gas constant
- r Radial coordinate
- r_i Radius of inner edge of mixing region
- R_T Turbulent Reynolds number
- Sc_T Turbulent Schmidt number
- T_T Total temperature

- u Axial mean velocity component
- \tilde{u} Velocity desired at a flow field edge, entrainment calculation
- u_c Mean velocity on jet centerline at any x
- u_e Mean velocity in surrounding stream
- u_j Mean velocity on jet centerline at nozzle exit
- v Lateral mean velocity component
- x Axial coordinate
- y Lateral coordinate

Greek Symbols

- α Parameter; = 0 for planar flow, = 1 for axisymmetric flow
- Δu Characteristic velocity difference
- ϵ Turbulent eddy viscosity
- ϵ_m Turbulent eddy viscosity at a characteristic point
- θ Angle between flow and x -coordinate
- ρ Fluid density
- ρ_e Density of surrounding stream at nozzle exit
- ρ_{j1} Density of jet at nozzle exit
- σ Two-dimensional shear-layer spread parameter
- σ_0 Value of σ for constant-density, single-stream shear layer
- σ_ϕ Transport coefficient ratio for general variable ϕ
- τ Turbulent shear stress
- ϕ General transportable variable

SECTION I INTRODUCTION

Free turbulent mixing phenomena are of fundamental importance in many flow systems of engineering interest. Applications in which free turbulent mixing phenomena occur include aircraft and missile plumes, jet pumps, wakes, and combustors. The correct prediction of such flows is a basic requirement for the solution of many more complex problems, such as those involving chemical reactions in a flowing system and prediction of exhaust jet noise. The general theory of free turbulent mixing described in this report has been developed to provide an accurate prediction of both the overall mixing rate in a free turbulent flow and the details of the mixing process, such as the profiles of the turbulent shear stress, velocity, total enthalpy, and jet species. The theory is applicable to a broad range of free turbulent flows, including constant and variable density jets and wakes; the required expenditure of computer time is small, approximately one minute for a typical case on an IBM 370/155 computer.

1.1 CAPABILITIES AND LIMITATIONS

The basic approach for the analysis of the free turbulent mixing problems described in this report is developed from the turbulent kinetic energy (TKE) method described in Ref. 1. The method incorporates several of the improvements which were discussed in Ref. 2, as well as certain modifications which have been incorporated since the latter description was written. These modifications allow the use of a single, consistent model for all of the calculations described in Ref. 2. The technique allows the computation of planar and axisymmetric one- and two-stream mixing problems. Referring to Fig. 1 as a schematic of the types of flow field involved, any combination of velocities u_e and u_j may be considered, except u_e or $u_j = 0$. Single-stream flows are approximated by small

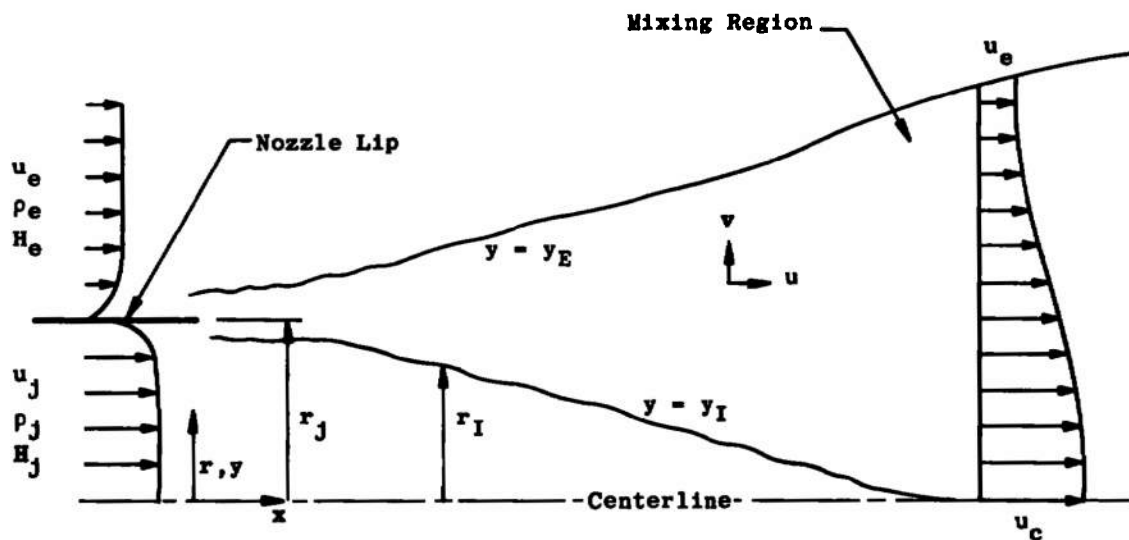


Fig. 1 Schematic of Free Mixing Flow Field

values of the velocity ratio, typically $u_e/u_j \leq 0.01$. The densities of the two streams may be different, and computations have been made successfully for values of the density ratio ρ_e/ρ_j as great as 14. Such cases, in which the center stream density is considerably lower than the outer stream density, are the most difficult to handle because of numerical difficulties associated with the coordinate transformation; no limitations have been observed for $\rho_e/\rho_j \ll 1$. Transport of energy and mass, as well as momentum, can be handled, and nonunity turbulent Prandtl and Schmidt numbers can be assumed. As presently formulated, the turbulent Prandtl and Schmidt numbers are assumed to be constant everywhere, but there is no fundamental reason why axial and radial variations of these transport coefficients could not be prescribed.

The technique is specialized to free turbulent processes, i.e., the mixing field is assumed to exist in a constant-pressure environment remote from walls. A longitudinal pressure gradient may be incorporated with some modifications to the program, but it must be specified a priori. Although compressible flows can be handled, they must be shock free; in general, this limits the computation of supersonic flows to those from correctly expanded nozzles. Only mathematically parabolic flows of the boundary-layer type are considered. In general this limitation implies that the nozzle lip shown in Fig. 1 is thin; otherwise a region of recirculating (and, therefore, mathematically elliptic) flow will exist just downstream of the lip. In practice, this is not a serious limitation since the assumption of a region of small but positive velocity in the lip region will normally suffice for accurate prediction of the mixing field. Finally, the approach is limited to the mixing of two streams. Again, there is no fundamental reason why more than two streams could not be handled. However, such a multi-stream mixing process would require a careful analysis of the problem of merging shear layers with different characteristic length scales; in turn, this would require additional, fairly complex programming logic.

1.2 A BRIEF HISTORY OF APPROACHES

The fundamental problem in the computation of a turbulent shear flow is the specification of the turbulent shear stress, τ . Attempts to solve this problem have occupied a great number of research workers for nearly a century. It was only recently with the availability of high-speed computers, that reliable computations of any but the simplest free turbulent flows have been possible.

Turbulent shear stress models are discussed at some length in Ref. 1, so only a general outline will be given here. Such models can be divided into two classes: those in which the turbulent shear stress is taken to be a function of the local mean velocity and a characteristic mean-flow length scale, and those in which a transport equation is solved to obtain the turbulent shear stress simultaneously with the mean-flow equations describing the problem.

The first class of models includes the mixing length (Ref. 3) and eddy viscosity (Ref. 4) models of Prandtl, as well as the vorticity transport theory of Taylor (Ref. 5) and the "inductive" approach of Reichardt (Ref. 6). More recently, the "displacement

"thickness" model has been proposed by Schetz (Ref. 7). All of these models share a common fault. Although all of them are capable of computing one flow or a few flows well (generally those flows which were used to evaluate the inevitable empirical constants that exist in the models), they cannot be used with confidence in any other flow (Ref. 1). This failure of eddy viscosity models has tended to retard the use of theoretical models for prediction of the free turbulent flows encountered in engineering practice.

The second class of models includes the eddy-viscosity transport equation developed by Nee and Kovasznay (Ref. 8) as well as several turbulent kinetic energy models. The models are based on expressions for the turbulent shear stress which either relate it to the turbulent kinetic energy (such as the present work) or involve a solution of a turbulent shear stress transport equation. In recent years a number of TKE models have been developed. These models can be arranged in a hierarchy, ranked by order of complexity, which ranges from the solution of one additional transport equation, for the turbulent kinetic energy, to the solution of transport equations for the turbulent shear stress, all components of the turbulent kinetic energy, and a characteristic turbulent length scale. The present model fits into the first level of this hierarchy, involving the solution of the TKE transport equation along with an algebraic formulation for the turbulent length scale which enters the problem. The model proposed by Rodi and Spalding (Ref. 9) is at the next level of complexity, involving a TKE equation and a length scale equation. At the most complex level, the approach of Donaldson and Rosenbaum (Ref. 10) involves the solution of five equations in addition to the mean momentum equation (common to all of these approaches) for even the simplest problem.

At no point in the hierarchy is the need for empirical input eliminated. There appears to be an almost religious belief professed by researchers involved in turbulence that as the number of equations increases, so does the profundity of the results; but the fact remains that as the number of equations increases, the number of empirical parameters increases also, and the physical basis for the necessary empirical input becomes more obscure. In the present model the empiricism is used to make the TKE equation soluble, and since the turbulent length scales appear to be directly related to the shear-layer width for most free turbulent flows, algebraic formulae are adopted to relate the characteristic length scale to the shear-layer width. The results of the 1972 NASA-Langley Conference on Free Turbulent Shear Flows (Ref. 11) showed that despite the relative simplicity of the assumptions used in this model, the present model and a closely related one (Ref. 12) were two of the most versatile methods presented.

1.3 LAYOUT OF THE REPORT

In this report the details of the finite-difference turbulent kinetic energy (TKE) model developed by the author will be described. Following this description, a summary of the numerical framework used to solve the equations of motion (based on the technique developed by Patankar and Spalding (Ref. 13)) will be presented. Results of the method as they applied to the test cases from the 1972 NASA-Langley Conference will then be described, followed by a user's manual for the computer program and a complete program listing.

SECTION II ANALYSIS

2.1 THE GOVERNING EQUATIONS

The basic equations to be solved in any analysis of a free turbulent flow (such as that shown schematically in Fig. 1) are the turbulent transport equations for mass, momentum, energy, and species. To this set, the present analysis adds the turbulent kinetic energy equation, as well as several algebraic relationships between the dependent variables. Because all free turbulent mixing problems to be considered involve flow fields in which gradients with y are very much greater than those with x , the boundary-layer approximations may be applied. Thus the governing Navier-Stokes equations are reduced to the following set of parabolic equations:

Continuity:

$$\rho u \frac{\partial u}{\partial x} + \frac{1}{y^\alpha} \frac{\partial}{\partial y} (\rho v y^\alpha) = 0 \quad (1)$$

Momentum:

$$\rho u \frac{\partial u}{\partial x} + \rho v \frac{\partial u}{\partial y} = \frac{1}{y^\alpha} \frac{\partial}{\partial y} (y^\alpha r) - \frac{dp}{dx} \quad (2)$$

Species Transport:

$$\rho u \frac{\partial c}{\partial x} + \rho v \frac{\partial c}{\partial y} = \frac{1}{y^\alpha} \frac{\partial}{\partial y} \left(\frac{\rho \epsilon y^\alpha}{S_c} \frac{\partial c}{\partial y} \right) \quad (3)$$

where

$$\epsilon = (r/\rho) / (\partial u / \partial y) \quad (4)$$

Mean Energy Transport:

$$\rho u \frac{\partial H}{\partial x} + \rho v \frac{\partial H}{\partial y} = \frac{1}{y^\alpha} \frac{\partial}{\partial y} \left\{ \frac{\rho \epsilon y^\alpha}{Pr} \left[\frac{\partial H}{\partial y} + \left(\frac{Pr}{Pr_k} - 1 \right) \frac{\partial k}{\partial y} + (Pr - 1) \frac{\partial}{\partial y} \left(\frac{u^2}{2} \right) \right] \right\} \quad (5)$$

Turbulent Kinetic Energy:

$$\rho u \frac{\partial k}{\partial x} + \rho v \frac{\partial k}{\partial y} = \frac{1}{y^\alpha} \frac{\partial}{\partial y} \left(\frac{\rho \epsilon y^\alpha}{Pr_k} \frac{\partial k}{\partial y} \right) + r \frac{\partial u}{\partial y} - \frac{a_2 \rho k^{3/2}}{\ell_k} \quad (6)$$

For planar flow, $\alpha = 0$, while for axisymmetric flow, $\alpha = 1$.

In writing the species, mean energy, and kinetic energy transport equations, gradient diffusion has been assumed. A similar form for the diffusion term in the momentum equation can be obtained through the use of the Boussinesq hypothesis (Eq. (4)); thus,

$$\frac{\partial}{\partial y} (y^{\alpha} \tau) = \frac{\partial}{\partial y} \left(\rho \epsilon y^{\alpha} \frac{\partial u}{\partial y} \right) \quad (7)$$

and all of the equations may be written in the standard form

$$\rho u \frac{\partial \phi}{\partial x} + \rho v \frac{\partial \phi}{\partial y} = \frac{1}{y^{\alpha}} \frac{\partial}{\partial y} \left(\frac{\rho \epsilon y^{\alpha}}{\sigma_{\phi}} \frac{\partial \phi}{\partial y} \right) + d \quad (8)$$

It must be emphasized that Eq. (4) serves in the present analysis merely to provide a relationship with which to evaluate a momentum diffusion coefficient. Unlike other analyses of turbulent flows, this coefficient is not directly modeled in order to obtain the turbulent shear stress, but it serves simply as a formalism which allows all of the equations of motion to be written in the form of Eq. (8). A model for the turbulent shear stress must still be specified, and this specification is the subject of the following section.

2.2 SHEAR STRESS MODEL

Equations (1) through (6) do not constitute a closed set of equations since there is no relationship yet specified for the turbulent shear stress, τ . In this work, a relationship proposed, after Nevzgljadov, by Dryden (Ref. 14) and used in computations of the turbulent boundary layer by Bradshaw, et al. (Ref. 15), is used:

$$\tau = a_1 \rho k \quad (9)$$

Although there is evidence that in strong shear flows the parameter a_1 is constant with a value of 0.3 over most of the flow (Ref. 16), in certain regions of the flow field it cannot be constant. For example, in the region of the centerline in an axisymmetric flow, the turbulent shear stress must approach zero, yet the turbulent kinetic energy does not. Similarly, in the two-dimensional free shear layer, large variations of a_1 are experimentally observed near the edges of the flow. For these reasons, a semiempirical set of profiles describing the variation of a_1 from its nominal value of 0.3 has been adopted for this work. The relationships used are defined in Table 1 (Eqs. (10) through (13)).

The shape of the a profile predicted by Eqs. (12) and (13) (Table 1) agrees quite well with experimental data for the variation of a_1 in incompressible jets, as Fig. 2 shows. Equation (10) has been verified by the accurate prediction of experimental velocity profiles, and Eq. (11) is inserted at the beginning of the second regime as a simple approximation to the actual transition between Eq. (10) and Eqs. (12) and (13). Little experimental evidence is available for the actual shape of the parameter a_1 through this transition region.

TABLE I
PROFILE RELATIONS FOR THE PARAMETER a_1

Flow Regime	Range	Expression for a_1	Eq.	Remarks
2-D Shear-Layer First Regime of Jets (Fig. 1)	$0.05 \leq \frac{u - u_e}{u_j - u_e} \leq 0.95$	$a_1 = 0.3 \left(\frac{\partial u}{\partial y} \right) / \left \frac{\partial u}{\partial y} \right $	(10)	Ratio of velocity gradients provides proper sign
	$0 \leq \frac{u - u_e}{u_j - u_e} < 0.05$	None	---	u_e held constant at value obtained from Eqs. (4) and (9) at $(u - u_e)/(u_j - u_e) = 0.05$, τ obtained from Eq. (4)
	$0.95 \leq \frac{u - u_e}{u_j - u_e} \leq 1.0$	None	---	u_e held constant at value obtained from Eqs. (4) and (9) at $(u - u_e)/(u_j - u_e) = 0.95$, τ obtained from Eq. (4)
Second Regime of Axisymmetric and Planar Jets (Fig. 1), Wakes	$u_c > 0.9 u_j$	$a_1 = 0.3 \left(\frac{\partial u}{\partial y} \right) / \left \frac{\partial u}{\partial y} \right $	(11)	Ratio of velocity gradients provides proper sign
	$u_c \leq 0.9 u_j$ $y < y_{\max}$	$a_1 = 0.3 \left(\frac{\partial u}{\partial y} \right) / \left \frac{\partial u}{\partial y} \right _{\max}$	(12)	y_{\max} is the value of lateral coordinate at which $ \frac{\partial u}{\partial y} $ is a maximum
	$u_c \leq 0.9 u_j$ $y > y_{\max}$	$a_1 = 0.3 \left(\frac{\partial u}{\partial y} \right) / \left \frac{\partial u}{\partial y} \right $	(13)	Ratio of velocity gradients provides proper sign

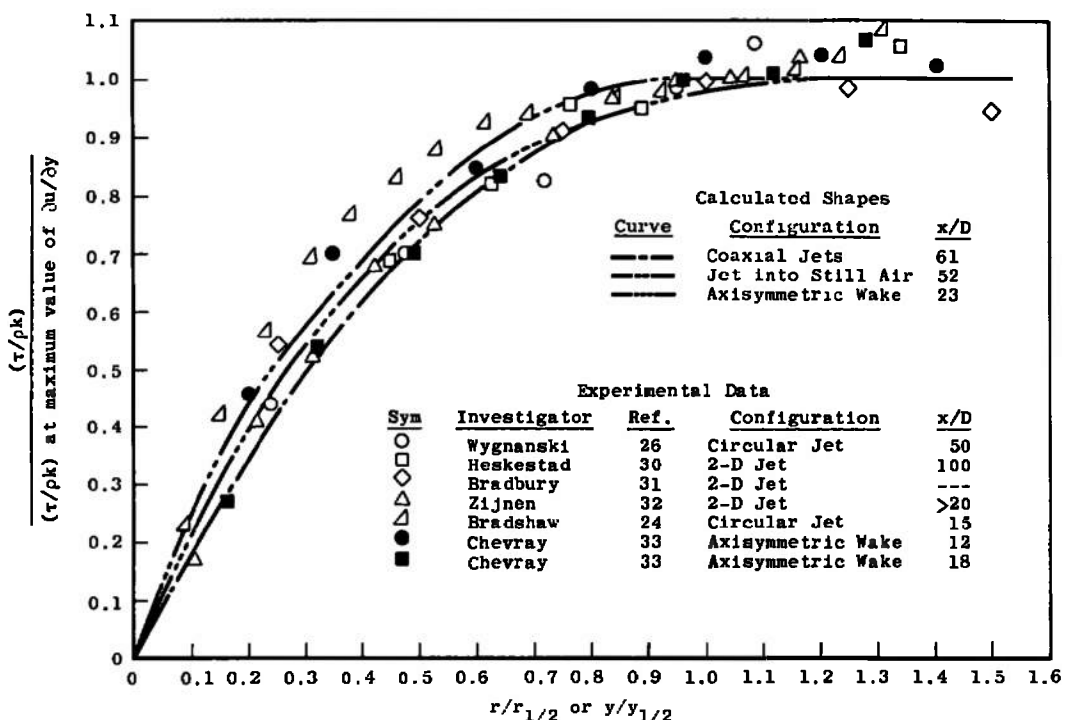


Fig. 2 Comparison of Calculated and Experimental Variation of Ratio of Shear Stress to Kinetic Energy

2.3 MODELING OF THE TURBULENT KINETIC ENERGY EQUATION

2.3.1 The Convection and Production Terms

The turbulent kinetic energy (TKE) equation as written in Section 2.1 (Eq. (6)) incorporates several assumptions. As with any equation for a transportable scalar, this equation can be written

$$\text{convection} = \text{diffusion} + \text{production} - \text{dissipation}$$

Of these four terms, the convection [$\rho u(\partial k/\partial x) + \rho v(\partial k/\partial y)$] and production [$\tau(\partial u/\partial y)$] terms are identically those derived from the Navier-Stokes equations for a turbulent flow, under the boundary-layer assumptions, along with the assumptions that the normal stresses are negligible and that the only significant tangential stress is the term $\tau = \rho u'v'$. The diffusion and dissipation terms are, on the other hand, models used to eliminate higher-order correlations of fluctuating terms (about which little is known) from the equations.

2.3.2 Dissipation

There seems to be little controversy about the dissipation term, which is written as

$$\text{dissipation} = a_2 \rho k^{3/2} / \ell_k \quad (14)$$

based on a suggestion of Kolmogorov (Ref. 17). As Reynolds (Ref. 18) points out, this term does not represent the complete dissipation tensor except in isotropic flow, and thus should be referred to as "isotropic dissipation" perhaps; on the other hand, the use of the term to describe TKE dissipation in general is nearly universal.

The parameter a_2 in Eq. (14) can be looked upon as a factor usable in adjusting the "isotropic dissipation" to apply to nonisotropic flows. In this work an empirical formulation for this parameter, which is based on the empirical formulation developed by Peters and Phares (Ref. 12), has been used. The a_2 relationships used in this work are not identical, however, to those used by Peters and Phares. This is because of differences between the TKE profile development predicted by the method and the profiles assumed in the integral method of Ref. 12.

2.3.3 The Turbulent Reynolds Number and Length Scale

To describe the variation of a_2 , a "turbulent Reynolds number" defined by

$$R_T = \frac{\Delta u \ell_k}{\epsilon_m} \quad (15)$$

is used as the independent variable. This parameter is a function of x only. The term ϵ_m represents the eddy viscosity at the maximum shear point in a lateral profile, i.e.,

$$\epsilon_m = (r_m/\rho_m)/(\partial u/\partial y)_m \quad (16)$$

and ℓ_k is a characteristic length scale, effectively the lateral width of the turbulent flow. This scale, which is also used in the dissipation expression (Eq. (14)), is determined by the following set of relationships:

For the two-dimensional shear layer, or first regime of a jet (see Fig. 1)

$$\ell_k = \Delta y \quad (17)$$

where Δy is the lateral distance between the points at which $(u-u_e)/(u_j-u_e) = 0.95$ and $(u-u_e)/(u_j-u_e) = 0.05$, for profiles which are not fully developed. For fully-developed profiles, which can be approximated by a cosine function,

$$\ell_k = 1.57 \Delta u/(\partial u/\partial y)_m \quad (18)$$

where the subscript m again refers to the position in a lateral profile at which the shear stress is a maximum. Equation (18) provides a characteristic length scale determination which is compatible with the cosine function velocity profiles used in Ref. 12, and which avoids the problem of defining the edge of an asymptotic profile. Because the cosine function is not always a good approximation to the true computed velocity profile, in practice Eq. (18) is only used in place of Eq. (17) wherever the value of ℓ_k determined by it satisfies the inequality $\Delta y \leq \ell_k \leq 1.57 \Delta y$. For a two-dimensional wake, the value of Δy to be used in Eq. (17) is defined as the lateral distance between the centerline and the point at which $(u-u_e)/(u_j-u_e) = 0.05$.

For the second regime of jets (see Fig. 1),

$$\ell_k = 2r_{1/2} \quad (19)$$

where $r_{1/2}$ is the value of r at which $(u-u_e)/(u_c-u_e) = 0.5$.

In the definition of R_T , $\Delta u = u_j-u_e$ in the first regime of jets, or the two-dimensional shear layer, and $\Delta u = u_c-u_e$ in the second regime of jets and in wakes.

The variation of a_2 with R_T was determined by a trial-and-error technique using the variation of the two-dimensional, shear-layer spreading parameter σ with Mach number (Test Case 2 of Ref. 11) as the criterion. Because some controversy over the appropriate variation of σ with M in this case exists, it should be pointed out that for the most part the recommended data from Ref. 11 were used. These data are consistent with the observed variation of velocity potential core length in the submerged jet as a function of Mach number used as a criterion for the variation of a_2 with R_T by Peters and Phares

(Ref. 12). The expressions which resulted from the trial-and-error process undertaken in this work are:

$$\text{For } 0 < R_T \leq 185, \quad a_2 = 1.69 \quad (20)$$

$$\text{For } 185 < R_T \leq 360, \quad a_2 = 0.46 + 0.00762 R_T \quad (21)$$

$$\text{For } R_T > 360, \quad a_2 = 3.20 \quad (22)$$

2.3.4 Modification for the Effects of Density Variation

Equations (20) through (22) describe the axial variation of a_2 . However, further correction is necessary (Ref. 12) to allow for the effects of density gradients. This is obtained by multiplying the parameter a_2 obtained from Eqs. (20) through (22) by the factor $(1/c_1)$, where, for

$$\frac{\rho_{e1}}{\rho_{j1}} > 1 \quad c_1 = 0.984 + 0.016 \frac{\rho_{e1}}{\rho_{j1}} \quad (23)$$

and for

$$\frac{\rho_{e1}}{\rho_{j1}} < 1 \quad c_1 = 0.95 + 0.05 R_e T_{Te} / R_j T_{Tj} \quad (24)$$

In Eqs. (23) and (24), the subscript 1 refers to conditions at the origin of mixing, R_e is the gas constant appropriate to the outer flow, and T_{Te} is the total temperature of that flow. Equation (24) is used when the jet density is greater than the free-stream density in order to preserve the a_2 - R_T relationship for the supersonic shear-layer case, for which the "jet" side is taken to be the high-speed stream. Thus, for the case of compressible but identical-gas mixing problems, the value of c_1 obtained through use of Eq. (24) is unity, while for gases with different molecular weights or stagnation temperatures a nonunity c_1 is obtained.

2.3.5 Significance of the Dissipation Term

There are three points at which empirical information enters the modeling of the turbulent kinetic energy equation: in the diffusion term, in the dissipation term, and in the relationship between the turbulent shear stress and the turbulent kinetic energy. In this paper, the most extensive empiricism has been applied to the dissipation term, rather than to the diffusion term or the τ - k relationship, because, as Bradshaw and others (Ref. 15) point out with reference to the two-dimensional boundary layer, the dissipation parameter is distinctly the most critical term in the modeling. One of the major advantages of a simple TKE analysis such as that described in this report is that the facility with the appropriate empiricism may be introduced. Thus, while the more rigorous analyses such as those proposed by Donaldson and Rosenbaum (Ref. 10), or with somewhat greater simplification by Hanjalic and Launder (Ref. 19), may indeed be more appropriate than

the present analysis for situations in which rapid changes in the turbulent structure occur, they are considerably more difficult to use for predicting the general character of a variety of free turbulent flows. This situation is caused by the complicated interrelationships that exist between the various parameters that still must be modeled in these more rigorous analyses, as well as the remoteness of these parameters from readily available experimental information. The present analysis is intended to provide general predictive (as well as correlative) capability, and thus some approximation of the details of the turbulent structure is accepted in order to provide a more general applicability of the mean flow field prediction.

2.3.6 Diffusion of Turbulent Kinetic Energy

The remaining term to be modeled in the TKE transport equation is the diffusion term, which is here approximated by a gradient diffusion model (Eq. (6)) in order to retain the formal similarity of the equations, discussed in Section 2.1. There is some controversy in the literature over this point, since it is possible to avoid a gradient model, as was done by Bradshaw and others (Ref. 15) for the two-dimensional boundary layer, and by Laster (Ref. 20) for planar and axisymmetric free-turbulent flows. The significance of the approach used by Bradshaw and others and by Laster is that the TKE equation becomes hyperbolic, which both allows the use of the method of characteristics for the numerical solution of the problem and, more significantly, implies that turbulence effects themselves propagate along characteristic lines in a flow. While there is some evidence that this type of behavior is experimentally found in some turbulent flows (see Reynolds (Ref. 18) for a discussion), experimental attempts to determine the nature of the diffusion process in general have not resulted in any conclusive evidence in favor of either hypothesis. In the present work, the TKE is assumed to diffuse in the same manner as any other scalar in the flow field, as is assumed (albeit with a different model for the τ - k relation) by Rodi and Spalding (Ref. 9). This has the advantage of retaining the same form for all of the governing equations.

2.3.7 Turbulent Prandtl Number for Kinetic Energy

A gradient diffusion model requires the specification of a diffusion coefficient. In common with the other scalar transport equations the TKE diffusion coefficient is taken to be related to the momentum diffusion coefficient ϵ ; the TKE "Prandtl number" which provides the constant of proportionality is taken to be constant throughout the flow field, with a value of 0.7.*

2.4 SUMMARY

This analysis of the general free-turbulent mixing problem involves the simultaneous solution of the turbulent transport equations (Eqs. (1) through (6)). In order to solve these equations, the shear stress model given by Eq. (9) is used, in which a parameter

*The solutions have been found to be relatively insensitive to realistic variation in the Prandtl number (Ref. 34).

a_1 appears. This parameter is obtained in different regions of the flow through the relationships given by Eq. (10)-(13). To obtain the turbulent kinetic energy (TKE) necessary in Eq. (9), the TKE transport equation (Eq. (6)) is solved. Equation (6), however, involves models for the TKE diffusion and dissipation. Of these, the latter term is the more important, and a general formulation for it involves the definition of a turbulent Reynolds number, Eq. (15), a turbulent length scale, Eqs. (17) through (19), and a dissipation coefficient, a_2 , Eqs. (20) through (24).

With all the necessary algebraic relationships defined, the system of equations is closed, and a numerical solution can be carried out subject to the specification of the initial and boundary conditions. In the following sections an outline of the numerical procedure will be given, followed by a discussion of the specification of the appropriate initial and boundary conditions. A demonstration of the abilities of the method will then be exhibited, followed by a user's manual to the program and a FORTRAN listing.

SECTION III THE NUMERICAL PROCEDURE

3.1 GENERAL DESCRIPTION

The numerical framework used in the program delineated in this report is a modification of the procedure devised by Patankar and described in Ref. 13. In this technique the governing equations are transformed into nondimensional stream function coordinates, allowing the lateral grid size to be automatically adjusted to account for the growth of the shear region, which can be quite rapid in a free-mixing flow. This grid adjustment feature and the successive substitution method used to evaluate the solution matrix at each downstream step combine to produce an efficient, fast-running program.

Two major modifications were made to the Patankar technique to produce the program described in this report. Relatively straightforward, the first is the incorporation of the turbulent kinetic energy equation and the shear stress model used in this work. The second major modification was made to ensure the satisfaction of the appropriate integral conservation equation, which requires, in the case of a zero pressure gradient free mixing flow, that the momentum excess (or defect) integral be a constant everywhere in the flow. The original technique did not satisfy this requirement, for reasons which are described in Part II of Ref. 13.

In the remainder of this section a brief description of the development of the finite-difference procedure will be given. Because the procedure is described at length by Patankar, only the highlights of the method will be discussed here; it is recommended that the user of this program become familiar with the contents of Ref. 13.

3.2 COORDINATE TRANSFORMATION

To put Eqs. (1) through (6) into a form suitable for rapid numerical computation, a stream function ψ is defined, which satisfies the continuity Eq. (1) identically. Thus, at constant x

$$\rho u r dy = d\psi \quad (25)$$

where $r = r_I + y \cos \theta$ (Fig. 3). Next, a nondimensional stream function, ω , is defined, such that

$$\omega = \frac{\psi - \psi_I}{\psi_E - \psi_I} \quad (26)$$

where E and I represent the external and inner boundaries of the mixing zone, respectively (see Fig. 3). Note that from Eq. (26), $0 \leq \omega \leq 1$. The term $(\psi_E - \psi_I)$ represents the mass flow in the mixing region at a given x , i.e.,

$$\psi_E - \psi_I = \int_{y_I}^{y_E} \rho u r dy \quad (27)$$

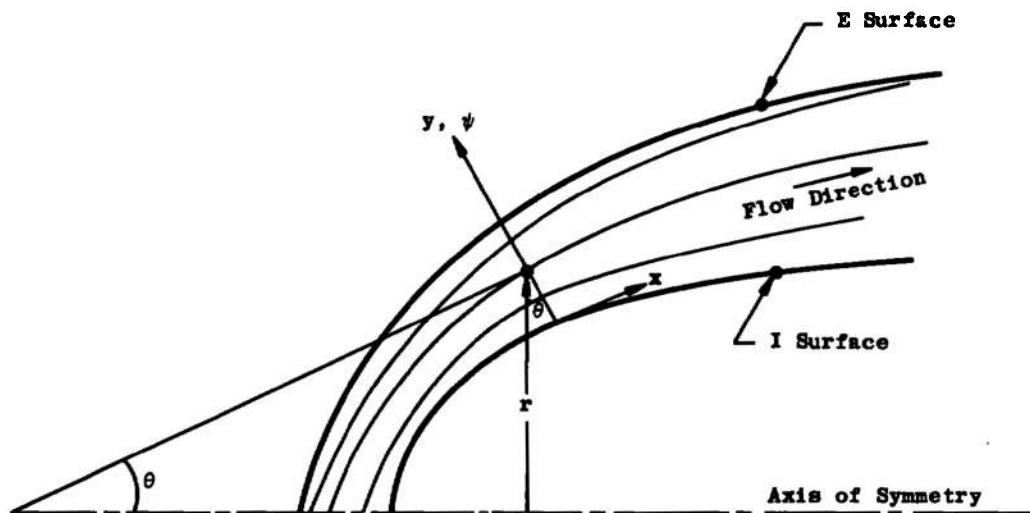


Fig. 3 Coordinate System

After conversion to $x-\omega$ coordinates, each of the Eqs. (2) through (6) can be written in the standard form

$$\frac{\partial \phi}{\partial x} + (a + b\omega) \frac{\partial \phi}{\partial \omega} = \frac{\partial}{\partial \omega} \left(c \frac{\partial \phi}{\partial \omega} \right) + d \quad (28)$$

where

$$a = r_I \dot{m}_I'' / (\psi_E - \psi_I) \quad (29)$$

$$b = (r_E \dot{m}_E'' - r_I \dot{m}_I'') / (\psi_E - \psi_I) \quad (30)$$

$$c = y^{2\alpha} \rho u \epsilon / \sigma_\phi (\psi_E - \psi_I)^2 \quad (31)$$

In these expressions, $\dot{m}_I'' = \rho_I v_I$ represents the mass flux per unit area entrained into the mixing region through the I boundary, while $\dot{m}_E'' = -\rho_E v_E$ is the same quantity evaluated at the E boundary. The definitions of σ_ϕ and d depend on the dependent variable and are given in Table II.

TABLE II
SOURCE TERMS IN THE TRANSFORMED EQUATIONS

ϕ	σ_ϕ	d
u	1	$\frac{1}{\rho u} \frac{dP}{dx}$
k	Pr_k	$\frac{y^{2\alpha} \rho u \epsilon}{(\psi_E - \psi_I)^2} \left(\frac{\partial u}{\partial \omega} \right)^2 - \frac{a_2 k^{3/2}}{\ell_k u}$
C	Sc_T	---
H	Pr_T	$\frac{\partial}{\partial \omega} \left\{ \frac{y^{2\alpha} \rho u \epsilon}{(\psi_E - \psi_I)^2} \left[\left(1 - \frac{1}{Pr_T} \right) \frac{\partial}{\partial \omega} \left(\frac{u^2}{2} \right) + \left(\frac{1}{Pr_k} - \frac{1}{Pr_T} \right) \frac{\partial k}{\partial \omega} \right] \right\}$

3.3 SPECIFICATION OF THE AUXILIARY FUNCTIONS

3.2.1 Entrainment

It is in the evaluation of the terms $(\psi_E - \psi_I)$, $r_E \dot{m}_E''$, and $r_I \dot{m}_I''$ that substantial differences have evolved between the formulations used by Patankar and Spalding (Ref. 13) and those used in this work. In the case of the entrainment rates, the differences have resulted from the use of a shear stress model which does not incorporate a mixing length concept, while the difference in the evaluation of $(\psi_E - \psi_I)$ results from the requirement that the integral momentum equation be exactly satisfied.

The terms $r_E \dot{m}'_E$ and $r_I \dot{m}'_I$ are evaluated from the axial momentum equation, which can be written

$$r_I \dot{m}'_I + \omega_B (r_E \dot{m}'_E - r_I \dot{m}'_I) = \left\{ \frac{\frac{\partial}{\partial \omega} \left[\frac{y^{2\alpha} \rho u \epsilon}{(\psi_E - \psi_I)^2} \frac{\partial u}{\partial \omega} \right]}{\frac{\partial u}{\partial \omega}} \right\}_B - \frac{(\psi_E - \psi_I)}{\left(\frac{\partial u}{\partial \omega} \right)_B} \left(\frac{du_B}{dx} + \frac{1}{\rho_B u_B} \frac{dP}{dx} \right) \quad (32)$$

At the I and E boundaries, $\partial u / \partial \omega \approx 0$ and Eq. (32) cannot be used to obtain the entrainment rates. However, this equation may be applied just inside the edges of the mixing region, for example, at $\omega = 0.05$ and at $\omega = 0.95$. Consider the evaluation at the outer edge, where $\omega = \omega_B = 0.95$. The only term in Eq. (32) which cannot be directly evaluated (assuming a known axial pressure gradient is du_B/dx , since at this point the downstream velocity profile is not known. However, if it is required that at the downstream step the velocity be some desired value, for example, that $\tilde{u}_B = u_I + 0.99 (u_E - u_I)$, then

$$\frac{\partial u_B}{\partial x} \approx \frac{\tilde{u}_B - u_B}{x_B - x_U} \quad (33)$$

where u_B is the value of velocity actually achieved at $\omega = \omega_B$ in the presently known profile. A similar prescription can be formulated for the inner edge, if necessary, and the entrainment rates evaluated from Eq. (32). If one boundary is a wall or an axis of symmetry, Eq. (32) is evaluated at the opposite boundary; if both boundaries are free, the entrainment rates must be obtained at both boundaries simultaneously.

In practice, the most important effect of the entrainment rate specification is on the size of the lateral grid spacing. Clearly, if the grid spacing becomes too large, accuracy is lost, because too many of the computational points will be outside the mixing region of interest. Conversely, if the spacing becomes too small, there will not be enough points available to completely cover the region of interest. In order to keep the grid spacing small enough for accuracy, many controls can be applied: perhaps the most effective is to monitor the nondimensional velocity profile $\phi_u = (u - u_c) / (u_c - u_e)$ at the edges. Then, if at the preceding station this value has decreased below some previously defined Φ_U^* , the current entrainment rate may be multiplied by Φ_U / Φ_U^* . Increasing an entrainment rate which is too low is easily accomplished by alteration of the value of ω_B at which the entrainment is computed.

Too much emphasis should not be placed on the method of specification of the entrainment. It may be obtained from any of the transport equations or in any other way consistent with the physics of the problem, since an incorrect specification is always clearly apparent from the velocity profiles obtained from the solution. The techniques used in the program listing included in this report, in conjunction with the profile shape controls, allow a quite general determination of the entrainment rates; in fact, all of the computations to be described in the following section have been carried out using the

same specification technique. Should the specification fail, however, any alternate technique which allows the computation to proceed smoothly is acceptable.

3.3.2 The Mixing Region Mass Flux

In Patankar's and Spalding's original program (Ref. 13) the mass flux ($\psi_E - \psi_I$) at the downstream station is evaluated as the sum of ($\psi_E - \psi_I$) at the upstream station plus the entrained mass flux over the step. However, inaccuracies in the finite-difference formulation at the edge regions (which are discussed in Part II of Ref. 13) introduce a small error in the determination of the coefficients in the finite-difference version of the equations of motion, which is reflected in a cumulative inaccuracy in the momentum integral at each station. Referring to Fig. 1, the momentum excess (or deficit) integral at any station can be written

$$\rho_j u_j (u_j - u_e) \frac{r_1^2}{2} + \int_{y_1}^{y_E} \rho u (u - u_e) r dy = \text{constant} \quad (34)$$

which, under the transformation of coordinates described above, becomes

$$\rho_j u_j (u_j - u_e) \frac{r_1^2}{2} + (\psi_E - \psi_I) \int_0^1 (u - u_e) d\omega = \text{constant} \quad (35)$$

Thus, Eq. (35) can be used to evaluate ($\psi_E - \psi_I$) subject to the condition, valid for a constant-pressure free turbulent flow, that Eq. (35) is satisfied. Note that Eq. (35) is not appropriate in the case of nonzero axial pressure gradient; however, the appropriate modifications may easily be introduced provided that dp/dx is known externally to the mixing calculations.

3.4 DEVELOPMENT OF THE DIFFERENCE EQUATIONS

The details of the numerical procedure developed by Patankar are described in Ref. 13; it is an implicit procedure similar to the Crank-Nicholson technique. However, Patankar and Spalding's formulation of the difference equations varies sufficiently from other formulations to warrant a brief description.

Consider the finite-difference grid shown in Fig. 4. The points $U-$, U , and $U+$ correspond to the three values ω_{U-} , ω_U , and ω_{U+} ; the corresponding downstream points, at equal values of ω , are denoted by $D-$, D , and $D+$. It is assumed that between grid points the dependent variables ϕ vary linearly with ω , and that along the x -coordinate between x_U and x_D the value of ϕ is ϕ_U except at $x = x_D$, where it becomes, with a step change, ϕ_D . The values of ϕ at $x = x_U$ are all known, and the values of ϕ at $x = x_D$ are to be solved for simultaneously, using these values. If a linear variation in ϕ between x_U and x_D were assumed, the method would correspond to the Crank-Nicholson technique.

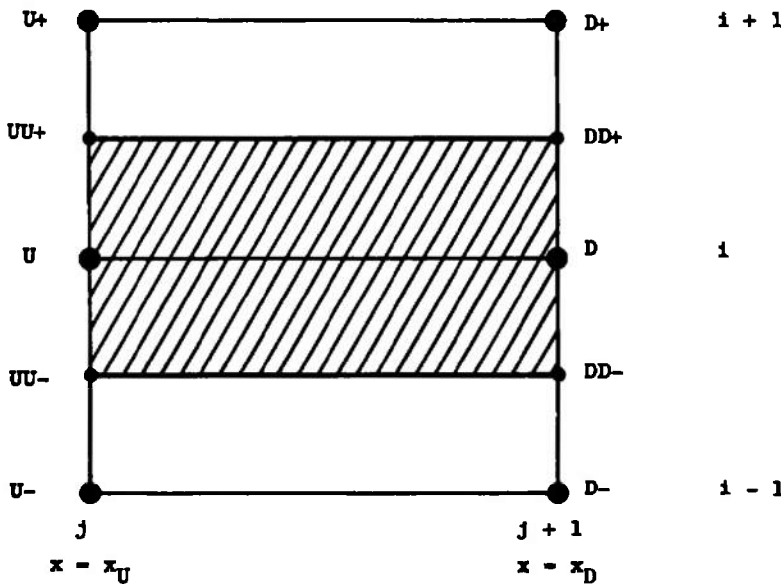


Fig. 4 Finite-Difference Grid

To formulate the difference equation, the values of the derivatives are obtained as mean values integrated over the control volume shown crosshatched in Fig. 4. The points UU-, UU+, DD-, and DD+ are all evaluated halfway between their respective node points on an x - ω grid. In keeping with the formulation of the difference equation as a "miniature integral equation," the fundamental derivatives are expressed as

$$\begin{aligned} \frac{\partial \phi}{\partial x} &\approx \frac{1}{(x_D - x_U)} \left(\frac{1}{\omega_{DD+} - \omega_{DD-}} \right) \int_{x_U}^{x_D} \int_{\omega_{DD-}}^{\omega_{DD+}} \frac{\partial \phi}{\partial x} d\omega dx \\ \frac{\partial \phi}{\partial \omega} &= \frac{1}{(\omega_{DD+} - \omega_{DD-})} \int_{\omega_{DD-}}^{\omega_{DD+}} \frac{\partial \phi}{\partial \omega} d\omega \end{aligned} \quad (36)$$

The integrals are evaluated using the assumed linear profiles between grid points; thus

$$\begin{aligned} \int_{x_D}^{x_U} \int_{\omega_{DD-}}^{\omega_{DD+}} \frac{\partial \phi}{\partial x} d\omega dx &= \int_{\omega_{DD-}}^{\omega_{DD+}} \int_{x_U}^{x_D} \frac{\partial \phi}{\partial x} dx d\omega = \int_{\omega_{DD-}}^{\omega_{DD+}} (\phi_D - \phi_U) d\omega \\ &= \int_{\omega_{DD-}}^{\omega_{DD}} (\phi_D - \phi_U) d\omega + \int_{\omega_{DD}}^{\omega_{DD+}} (\phi_D - \phi_U) d\omega \end{aligned} \quad (37)$$

In general, for

$$\omega_{DD-} \leq \omega \leq \omega_D \quad \phi = \phi_{DD-} + K_1(\omega - \omega_{DD-})$$

and for

$$\omega_D \leq \omega \leq \omega_{DD+} \quad \phi = \phi_D + K_2(\omega - \omega_D)$$

where

$$k_1 = (\phi_{D-} - \phi_{DD-})/(\omega_D - \omega_{DD-}), \text{ etc.}$$

Substituting these expressions into Eq. (37) leads to the expression

$$\frac{\partial \phi}{\partial x} \approx \frac{(\phi_{D-} - \phi_U)(\omega_D - \omega_{D-})}{4(x_D - x_U)(\omega_{D+} - \omega_{D-})} + \frac{3}{4} \frac{(\phi_D - \phi_U)}{(x_D - x_U)} + \frac{(\phi_{D+} - \phi_{U+})(\omega_{D+} - \omega_D)}{4(x_D - x_U)(\omega_{D+} - \omega_{D-})} \quad (38)$$

Similarly, for $\partial\phi/\partial\omega$, evaluation of Eq. (36) yields

$$\frac{\partial \phi}{\partial \omega} \approx \frac{1}{\omega_{DD+} - \omega_{DD-}} \int_{\omega_{DD-}}^{\omega_{DD+}} d\phi$$

so that

$$\frac{\partial \phi}{\partial \omega} \approx \frac{\phi_{D+} - \phi_{D-}}{\omega_{D+} - \omega_{D-}} \quad (39)$$

SECTION IV

A DEMONSTRATION OF THE METHOD

4.1 SPECIFICATION OF INITIAL AND BOUNDARY CONDITIONS

The analysis outlined in the preceding sections allows the rapid computation of a variety of free turbulent mixing problems which are themselves differentiated by the initial and boundary conditions involved. The initial conditions which need to be specified involve beginning profiles of the velocity, concentration, total enthalpy, and turbulent kinetic energy, with specification of the concentration profile necessary only in a two-gas problem and specification of the total enthalpy profile necessary only in nonisoenergetic flow. The appropriate boundary conditions depend on the nature of the problem. Thus, at an axis of symmetry, all lateral gradients are assumed to be zero, while at a free boundary, uniform values of velocity, concentration, total enthalpy, and turbulent kinetic energy are specified. No fundamental changes in the program are necessary to accommodate prescribed axial variation of each of these parameters.

Because of the coordinate system used in this analysis, the initial profiles involved cover only the initial viscous region. In general, if a calculation is started from the nozzle exit plane, power-law initial velocity profiles are used, i.e., $(u/u_B) = (y/\delta)^{1/n}$, where u_B represents either the jet or outer stream velocity. These power-law profiles are patched

together at the nozzle lip assuming a nonzero but small velocity, typically $0.01 u_j$ (see Fig. 5). Uniform (top-hat) profiles of C and H are generally assumed, if required.

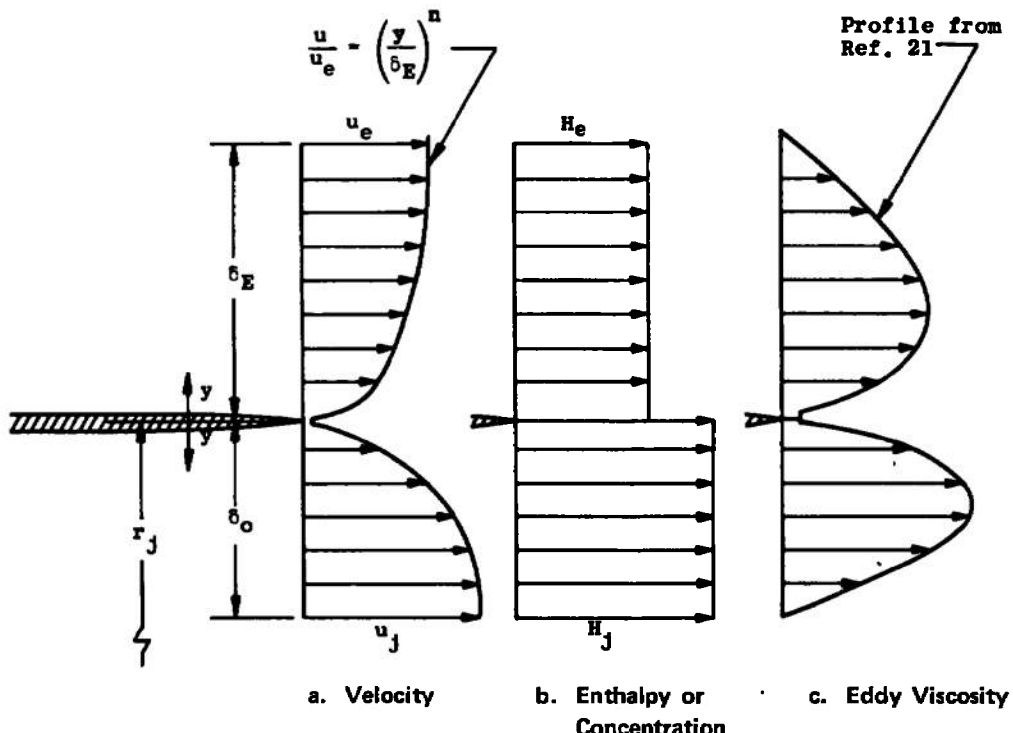


Fig. 5 Initial Condition Definition Sketch

4.1.1 Specification of the Initial Kinetic Energy Profile

Because the turbulent kinetic energy equation is used in this analysis to obtain the turbulent shear stress in the flow field, specification of the initial turbulent kinetic energy profile is required. While the solution downstream is not overly sensitive to this initial specification, some care has to be exercised in providing it, and since initial turbulent kinetic energy levels are not ordinarily part of the specification of a given engineering problem, a general means of developing approximate initial TKE profiles has been developed.

Two techniques for obtaining initial TKE profiles have been used with considerable success in the demonstration of the method which will follow. If the calculation is to begin at the nozzle lip, the eddy-viscosity profiles developed for compressible turbulent boundary layers by Maise and McDonald (Ref. 21) are used to obtain the shear stress and thus the turbulent kinetic energy through use of Eq. (9). Alternatively, if the computation is to begin downstream of the nozzle lip, the Prandtl eddy viscosity model (Ref. 4) is used to obtain the initial shear stress and hence the kinetic energy level. The constants used for this model are shown in Table III. (This level may also be obtained in some cases from experimental data.) One or the other of these techniques has been used for all of the calculations to be presented in the remainder of this section; the specific model used in each case is described in Table III.

TABLE III
SUMMARY OF INITIAL CONDITIONS

(Ref. 11) Case No.	Description	Start Point (CM)	Initial Conditions			
			u	c	h	k
1	Incompressible 2-D shear layer	x = 0	a	N/A	N/A	b
2	Compressible 2-D shear layer	x = 0	a	N/A	c	b
3	Variable density 2-D shear layer	x = 0	a	c	c	b
4	Incompressible 2-D shear layer (Lee)	x = 0	d	N/A	N/A	b
5	Compressible 2-D shear layer (Hill and Page)	x = 2, 5	d	N/A	c	e
6	Circular jet (Maestrello and McDaid)	x/D = 1	d	N/A	N/A	f
7	Supersonic circular jet (Eggers)	x = 0	d	N/A	c	b
8	Compressible circular jet (Heck)	x/D = 2.8	d	N/A	d	f
9	Coaxial air jets with He trace (Forstall)	x/D = 0	d	c	c	b
10	Coaxial H ₂ -air jets (Chriss)	x/D = 0	d	d	d	g
11	Compressible coaxial air-air jets (Eggers and Torrence)	x/D = 0	d	N/A	c	b
12	Compressible coaxial H ₂ -air jets (Eggers)	x/D = 0	d	c	c	b
13	Plane 2-stream jets (Bradbury)	x = 0	a	N/A	N/A	b
14	Incompressible axisymmetric wake (Chevray and Kovasznay)	x/D = 0	d	N/A	N/A	b
15	Incompressible axisymmetric wake (Chevray)	x/D = 0	d	N/A	N/A	f
16	Compressible plane wake (Demetriades)	x = 0.91	d	N/A	c	h
17	Compressible axisymmetric wake (Demetriades)	x = 6.74	d	N/A	c	h
18	Circular jet (Wyynanski and Fiedler)	x/D = 1	i	N/A	N/A	f
19	Compressible circular jet (Heck)	x/D = 2.8	d	N/A	c	f
20	Coaxial air-air jet (Pauk)	x/D = 2.3	d	a	a	f
21	Coaxial H ₂ -air jets (Chriss)	x/D = 2.6	d	a	a	g
22	Coaxial compressible H ₂ -air jets (Eggers)	x/D = 0	d	c	c	b

Legend:

- a. Power-law profile, $n = 1/7$.
- b. Maize and McDonald (Ref. 21) eddy viscosity profile and level.
- c. Constant value based on data sheet (Ref. 11).
- d. Experimental values from data sheet (Ref. 11).
- e. Maize and McDonald (Ref. 21) eddy viscosity on high-velocity side, constant eddy viscosity (equal to one-half adjacent Maize and McDonald value) for low speed side. (Actual value unimportant.)
- f. Prandtl (Ref. 4) eddy viscosity, $k_p = 0.005$.
- g. Constant eddy viscosity, level based on data of Ref. 22.
- h. Constant eddy viscosity, level based on R_T data of Ref. 23.
- i. Data from Ref. 24.

4.2 GENERAL DESCRIPTION OF THE DEMONSTRATION

The data chosen for the demonstration of the method is that used in the 1972 NASA-Langley Working Conference on Free Turbulent Shear Flows (Ref. 11). These data were chosen for two reasons: (1) they represent a compilation of a variety of free mixing experiments against which a variety of models were tested, and (2) the present model represents a modification and improvement of a model presented at that conference (Ref. 2), and thus prediction of the same cases will allow a direct comparison of the present predictions with those of Ref. 2. It should be emphasized that the program listed in Appendix A was used to compute all of the flows shown here; there were no changes made in the empirical information used or to the program structure in order to handle any of the computations.

Four types of flow fields were considered in the data package for the 1972 NASA Conference: the two-dimensional shear layer, circular jets into still surroundings, two-stream jets (both axisymmetric and two-dimensional) and axisymmetric and two-dimensional wakes. In the following subsections the predictions made by the present model for each of these flow classes will be described.

4.3 THE TWO-DIMENSIONAL SHEAR LAYER

Cases 1-3 of the NASA Conference involved the prediction of the behavior of the two-dimensional shear layer spreading rate as a function of velocity ratio, density ratio and Mach number. The spread parameter σ was computed from the standard definition used at the conference:

$$\sigma = 1.855 (X_2 - X_1) / (Y_2 - Y_1) \quad (40)$$

Here, Y_2 represents the lateral distance between the points at which $(u - u_e) / (u_j - u_e) = 0.9$ and $(u - u_e) / (u_j - u_e) = 0.1$ at X_2 , with Y_1 representing a similar distance at X_1 . The subscripts j and e represent the primary and secondary streams.

In the version of this computational approach reported at the NASA Conference (Ref. 2), a special profile of the parameter a_1 was used which was applicable to only the two-dimensional shear layer. Subsequent to the presentation of Ref. 2, the use of a special a_1 function was found to be unnecessary. In the present work the same a_1 function (described by Eq. (10) through (13) has been used for all computations.

Figure 6 shows that the prediction of the variation in the spreading parameter σ with velocity ratio obtained with the present model closely follows the classic expression

$$\frac{\sigma_0}{\sigma} = \frac{1 - u_e/u_j}{1 + u_e/u_j} \quad (41)$$

which is widely accepted as the proper relationship for growth rate as a function of velocity ratio (Birch, in Ref. 11).

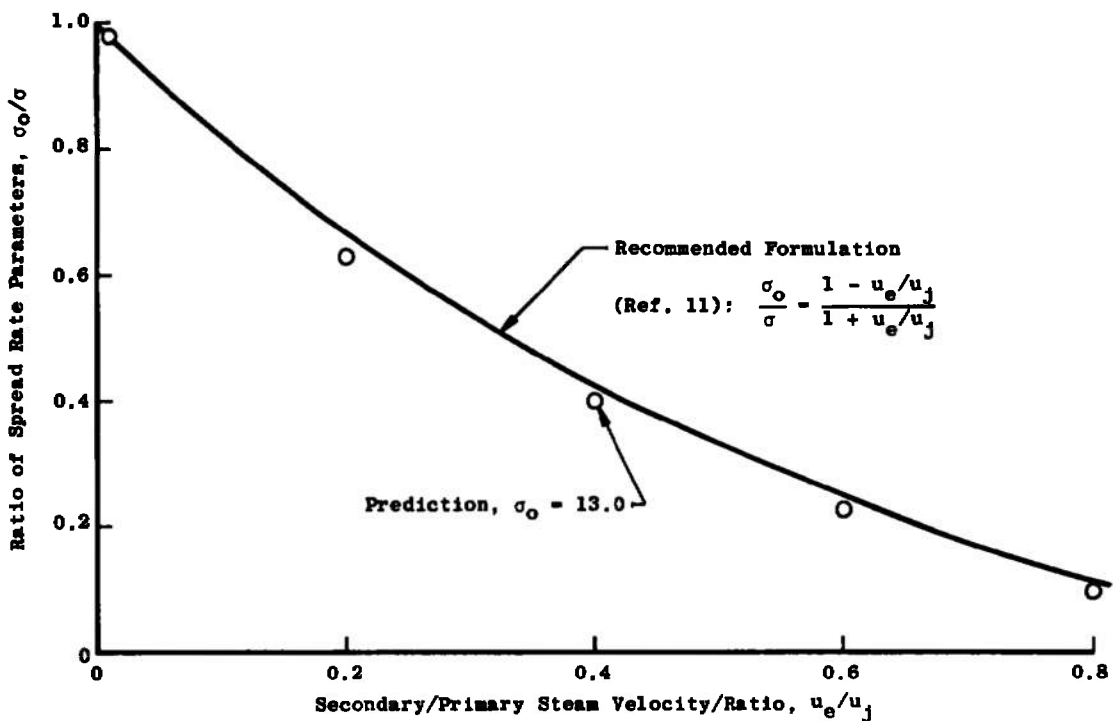


Fig. 6 Predicted Effect of Velocity Ratio on Two-Dimensional Shear-Layer Spread Rate, NASA Case 1

The variation of the spreading parameter σ with Mach number is still a controversial issue, although the proper prediction of this spread parameter is crucial to the correct prediction of the length of the potential core in a supersonic jet. However, a recommended set of data for the variation of σ with Mach number emerged from the NASA Conference, and these data, together with the prediction made by the present model, are shown in Fig. 7. As described in Section 2.3.3, these computations were used to develop the a_2 - R_T expressions, Eqs. (20) through (22). Except for the point at $M = 1$, the agreement is quite good. (There is some evidence, primarily sonic jet core lengths, that the spread rate data point at $M = 1$ represents a value of σ which is too low; thus, in developing Eqs. (20) through (22), which in effect control the shape of the curve of σ_0/σ versus M , more attention was paid to proper prediction of the data at $M = 2$ and higher.)

The predicted variation of σ with density ratio is shown on Fig. 8. Here the correct physical behavior is again controversial, and there are no data available which are directly comparable (i.e., with $u_e/u_j = 0.2$) with these predictions. However, the data discussed in Ref. 11 at other velocity ratios appear to show a smaller variation of σ with density ratio, than that observed with Mach number. This is supported by these calculations, at least for $1/8 \leq \rho_j/\rho_e \leq 14$. Two curves illustrating the effect of Prandtl number change are shown. The calculations were made with a density variation created through a temperature difference between the streams. Within the framework of the present analysis, and assuming a Lewis number of unity, the same effects would be observed if the density difference were caused by molecular weight differences between the streams.

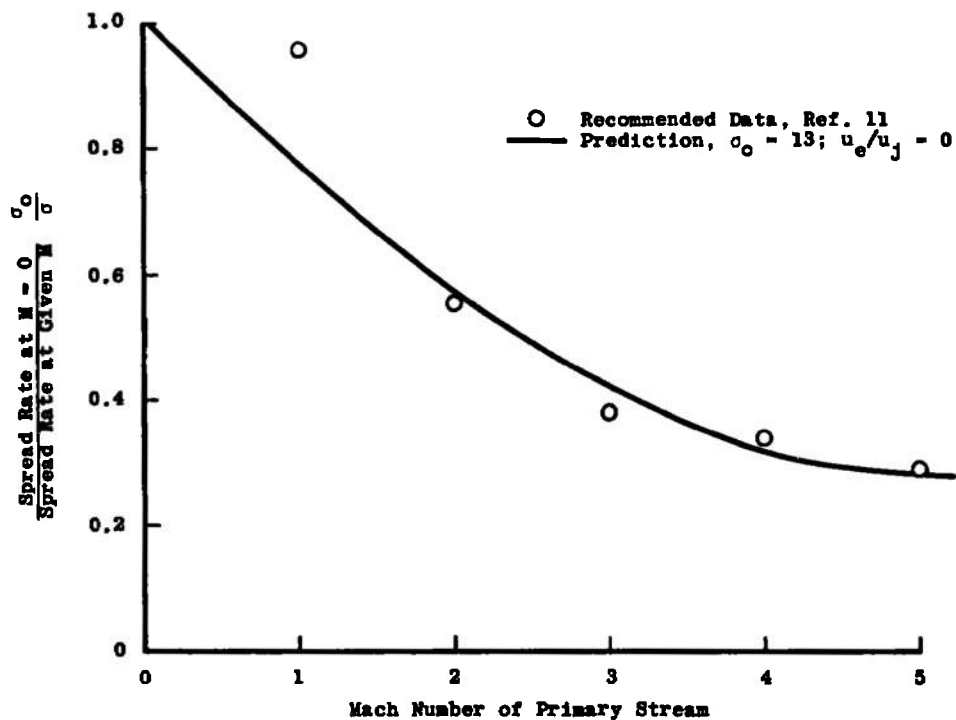


Fig. 7 Predicted Variation of Spread Parameter with Mach Number,
 NASA Case 2

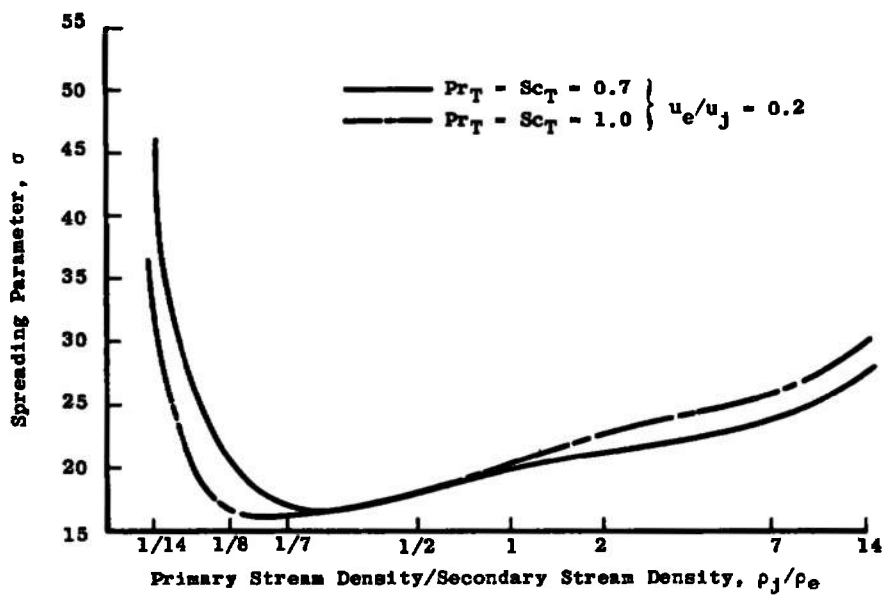


Fig. 8 Variation of Spreading Parameter, with Density Ratio,
 NASA Case 3

These three cases so far discussed have all involved fully developed free shear layers. In the next two cases, computations have been made of the developing free shear layer. Figure 9 shows a comparison of the predicted development of an incompressible two-stream free shear layer with experimental data, while Fig. 10 provides the same comparison for a compressible free shear layer. The agreement in both cases is excellent. In common with the other boundary layer solutions, this computational technique does not satisfy the proper boundary conditions for these nonsymmetric, two-dimensional flows. The effect of this is that the spatial orientation of the computed profiles is not known, and so for the comparison the experimental and theoretical profiles have been matched at the point at which the velocity is equal to the average velocity of the two streams. It should also be noted that because the numerical method utilizes a variable x-step, the axial locations of the predicted and measured profiles will not agree exactly in general.

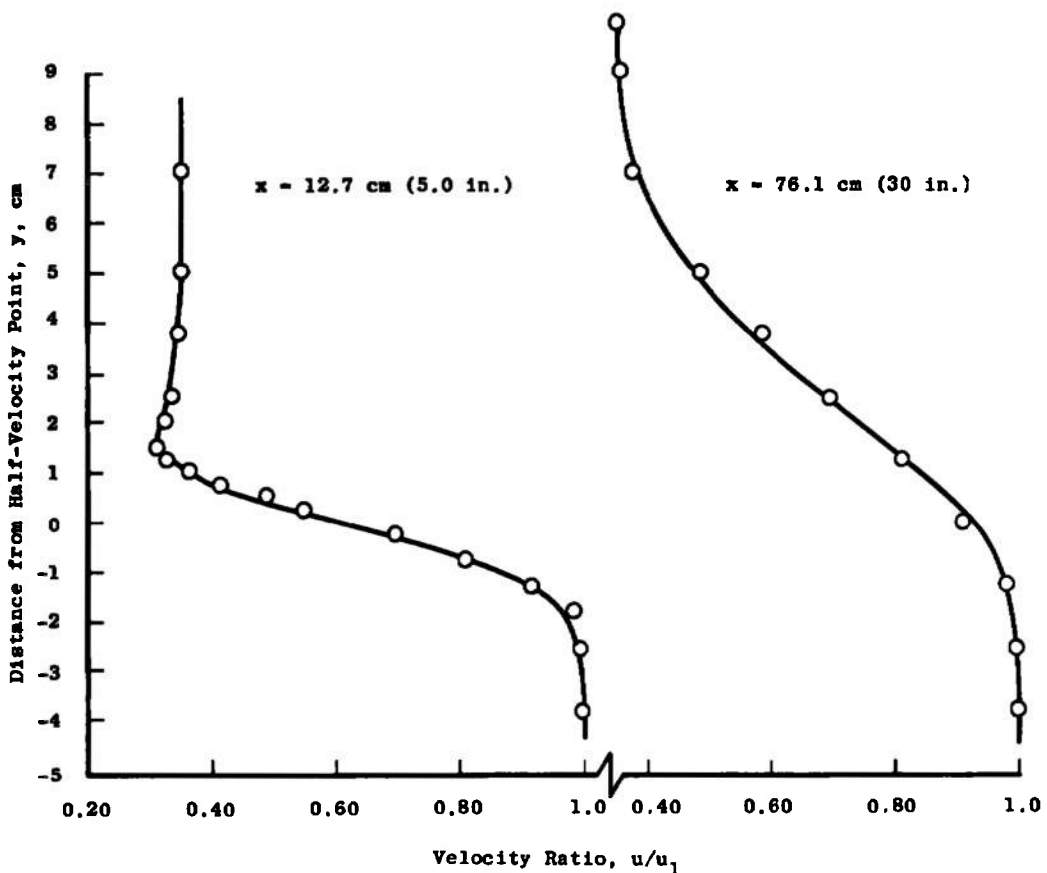


Fig. 9 Comparison of Experimental and Theoretical Velocity Profiles for NASA Case 4 (Incompressible Two-Dimensional Shear Layer, $u_2/u_1 = 0.357$)

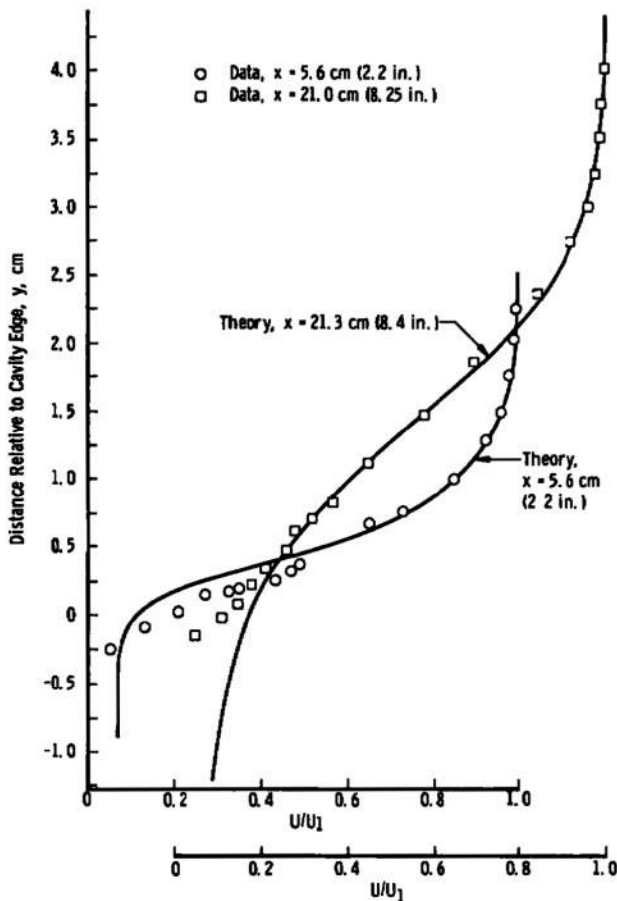


Fig. 10 Comparison of Theoretical and Experimental Profiles, Case 5, Compressible ($M = 2$) Two-Dimensional Shear Layer

4.4 THE CIRCULAR JET

The prediction of the asymptotic behavior of an incompressible circular jet (NASA Conference Case 18) is shown in Fig. 11, from which it can be seen that although the prediction of the centerline velocity is proportional to $(x/D)^{-1}$, as is required by similarity considerations, the proportionality constant does not agree exactly with that which may be obtained from the data of Albertson, et al. (Ref. 25). As discussed in Ref. 2, the data proposed for the comparison in NASA Case 18 do not fully represent an asymptotic jet. For this reason the data of Ref. 25 have been used for this comparison. As can be seen from Fig. 12, the width scale of the flow is also too small, which agrees with the overprediction of the similar-region centerline velocity illustrated in Fig. 11. Comparing the profiles of velocity and turbulent kinetic energy with the data used for Case 18 (from Wygnanski and Fiedler, Ref. 26) also shows that the predicted turbulent kinetic energy is too low compared to the experiment on the centerline. This would indicate that the TKE diffusion is somewhat too small near the centerline in the asymptotic jet. Other computations of this flow, not shown herein, indicate that a lateral variation of the TKE Prandtl number may be required to obtain better agreement.

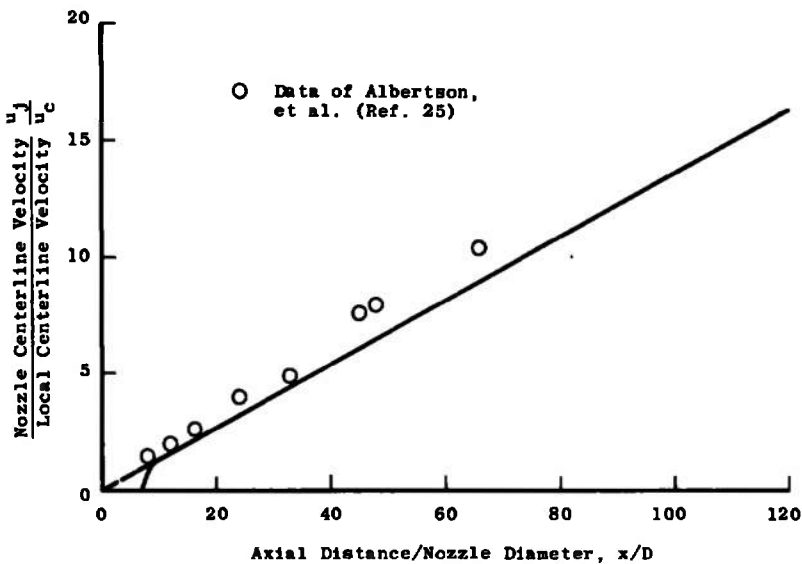


Fig. 11 Comparison of Prediction with Experimental Data, NASA Case 18, Asymptotic Circular Jet

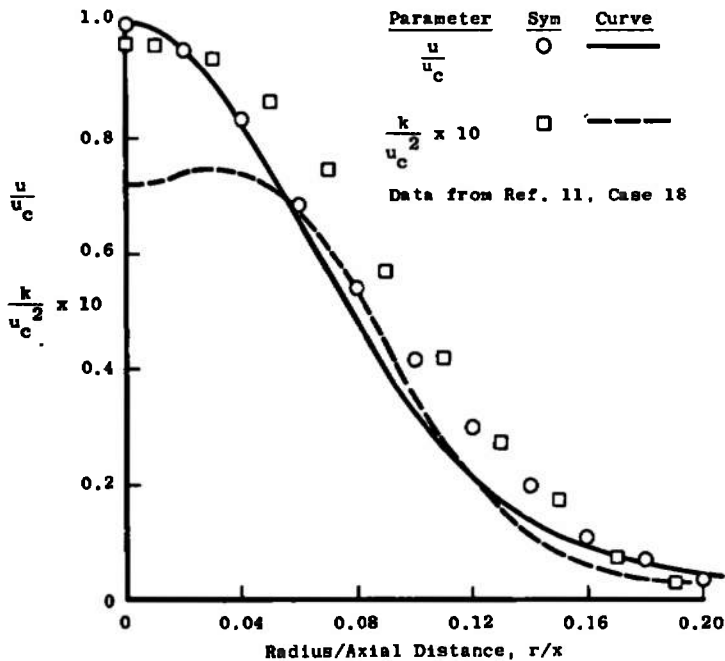


Fig. 12 Comparison of Profile Predictions with Experimental Data, NASA Case 18, Asymptotic Circular Jet

Circular jet predictions were also required for NASA Cases 6, 7, 8 and 19, under varying conditions. The performance of the present model in predicting these cases is shown in Figs. 13-16. The jet Mach number for these cases ranged from 0.6 to 2.22, and as these figures show, the present model provides satisfactory predictions in each case. There appears to be a general trend in these predictions to underpredict the centerline

velocity, which may be traced in Cases 6 and 7 to a slight underprediction of the velocity potential core length.

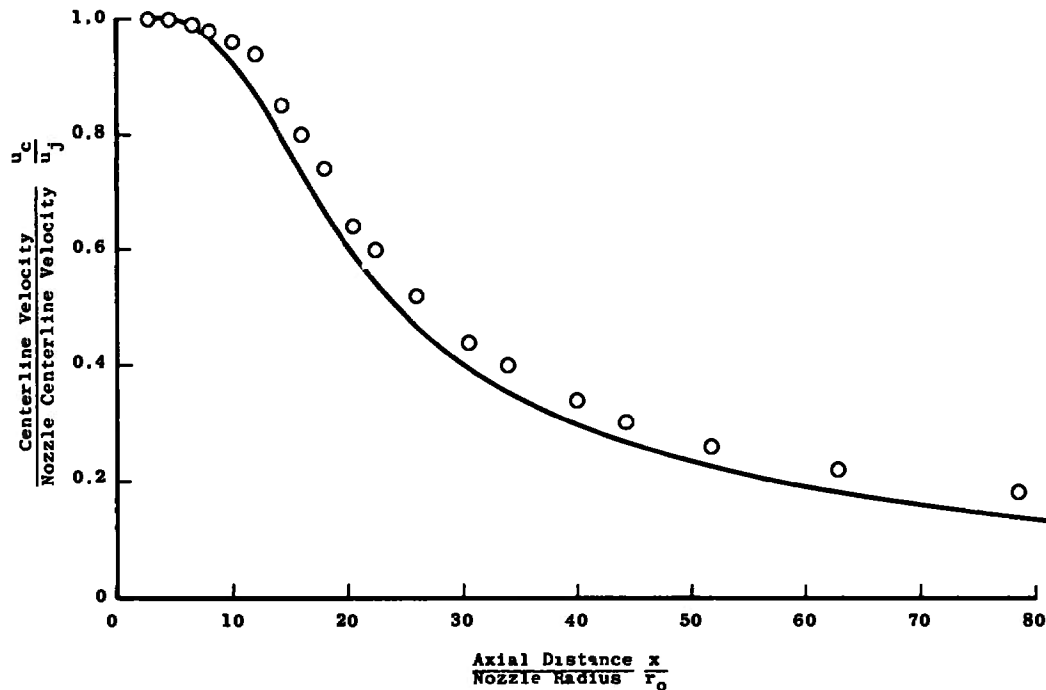


Fig. 13 Comparison of Prediction with Experimental Data for $M = 0.6$
Circular Jet, NASA Case 6

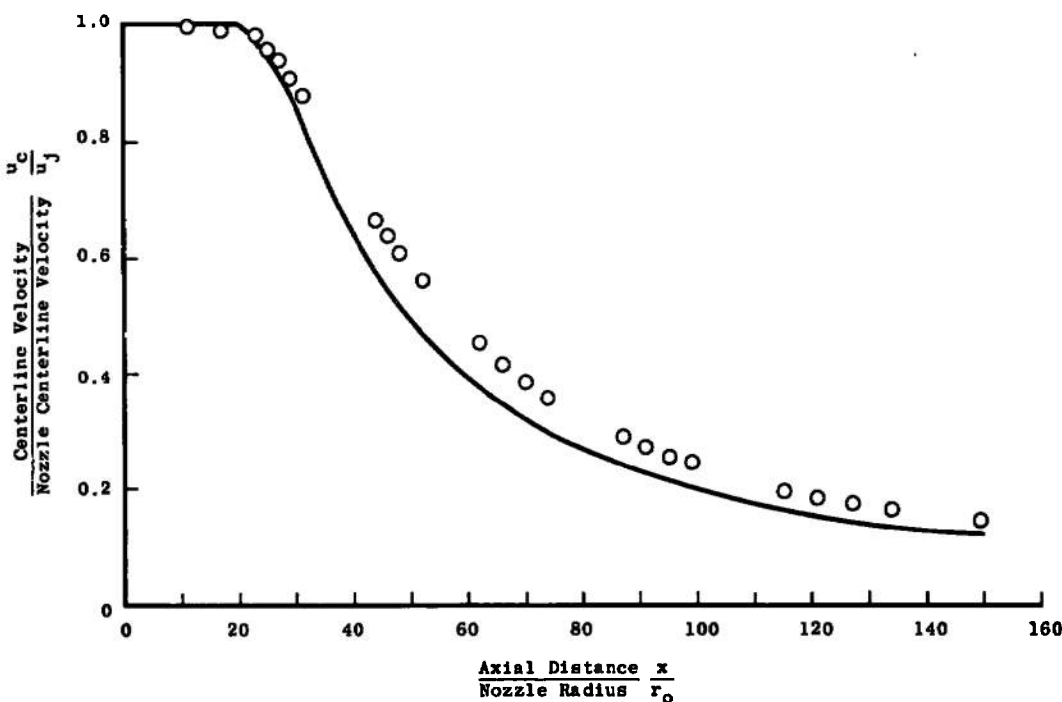


Fig. 14 Comparison of Prediction with Experiment, $M = 2.22$ Jet, NASA Case 7

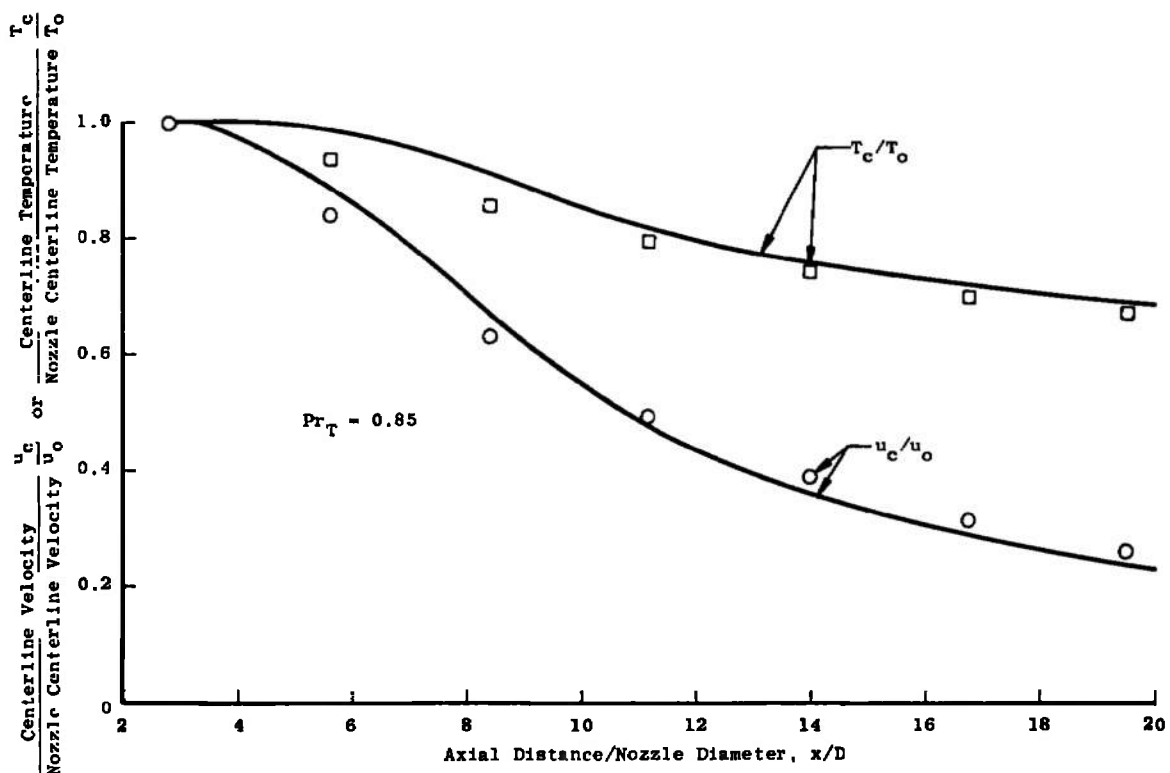


Fig. 15 Comparison of Prediction with Experiment, NASA Case 8, Heated $M = 0.7$ Circular Jet

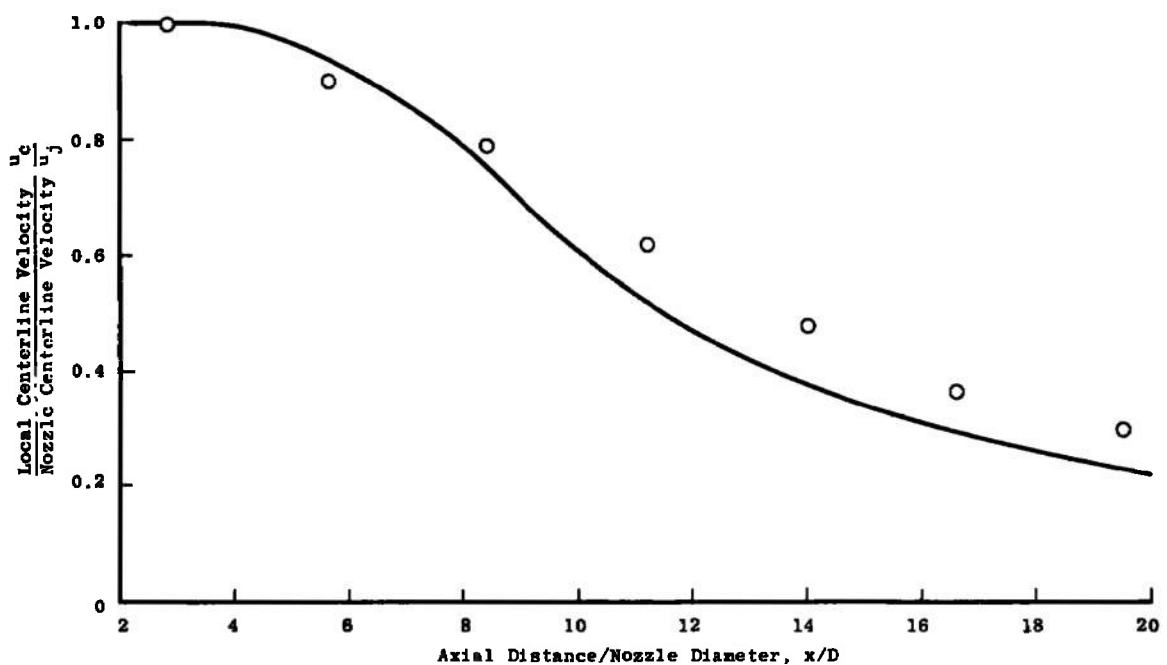


Fig. 16 Comparison of Prediction with Experiment, NASA Case 19, $M_j = 1.4$ Circular Jet

4.5 TWO-STREAM JETS

The eight cases of two-stream jet data selected for the NASA Conference can be divided into three subgroups: momentum transport alone; momentum and energy transport; and momentum, energy, and mass transport. The simplest configurations were the two-stream, two-dimensional mixing process represented by Case 13, and the coaxial two-stream process represented by Cases 9 and 20. In the latter two cases energy and mass tracers were included, but in small enough quantity that the overall flow field was not affected.

As Figs. 17 and 18 show, the prediction of both the two-dimensional flow of Case 13 and the coaxial configuration of Case 9 is excellent. The prediction of the coaxial flow of Case 20 (Fig. 19) is not good; the results of the conference showed that this flow was quite difficult for most of the models presented to predict.

The supersonic mixing configuration represented by NASA Case 11 represented a flow with momentum and energy transfer. This particular case was further complicated by the presence of extremely thick boundary layers at the nozzle exit, and the wake-like character of the flow in which the outer stream velocity is greater than that of the jet velocity. A prediction of this case by the present model is shown in Fig. 20, which demonstrates a good prediction of the boundary-layer-dominated mixing process.

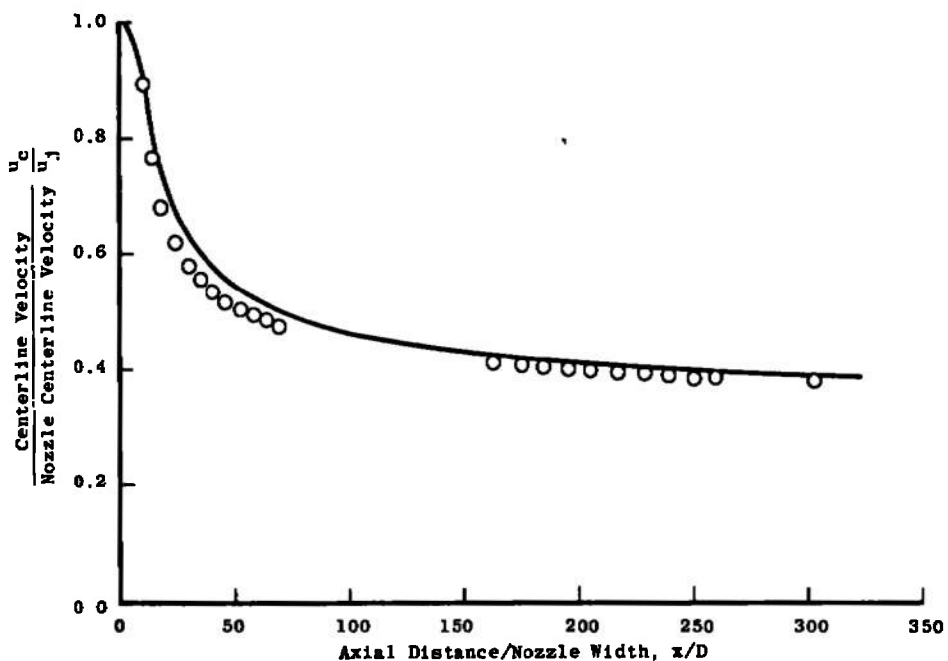


Fig. 17 Comparison of Prediction with Experiment, NASA Case 13,
Two-Dimensional Jet in Moving Stream, $u_j/u_e = 3.29$

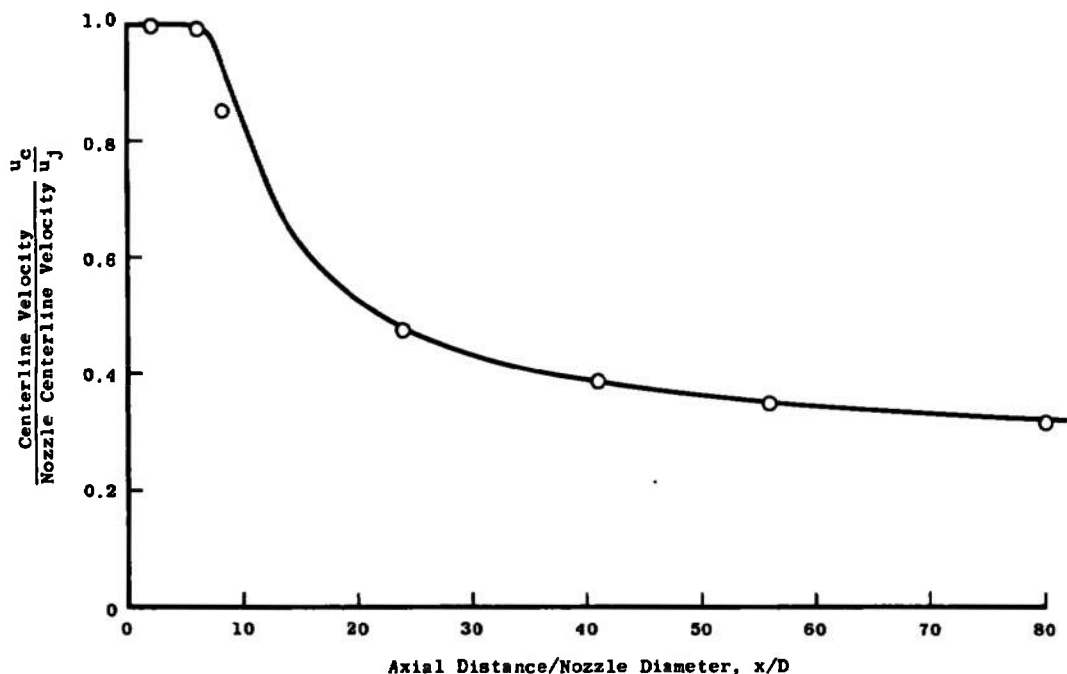


Fig. 18 Comparison of Prediction with Experiment, NASA Case 9,
Coaxial Air Jets

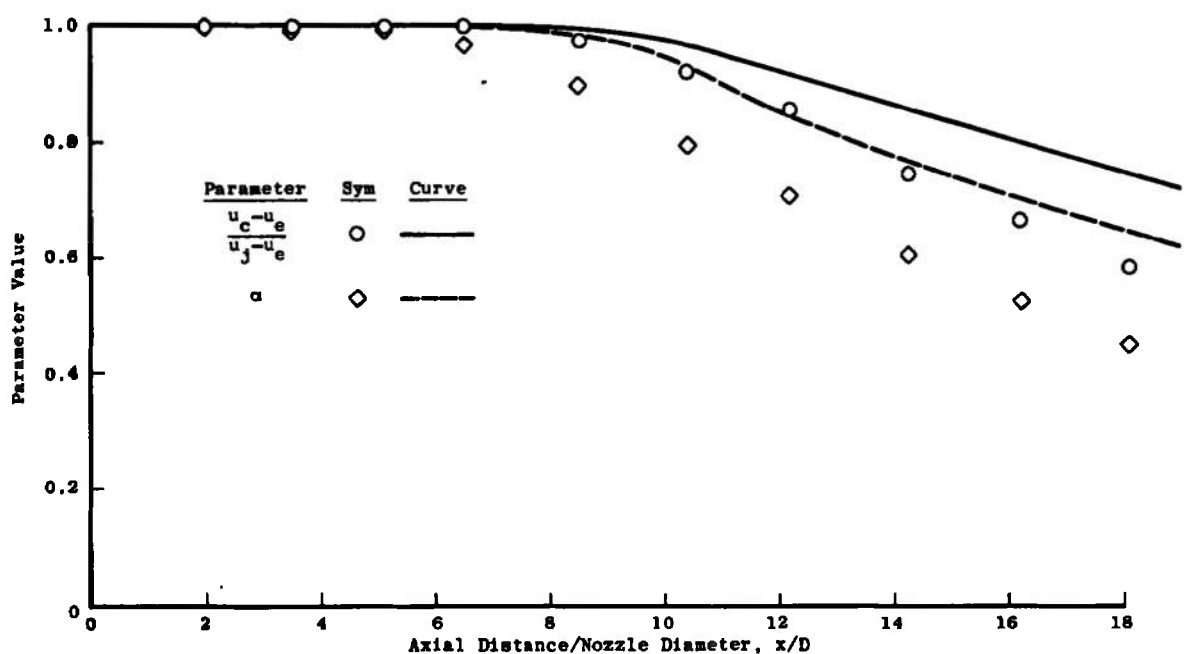


Fig. 19 Comparison of Prediction with Experiment, NASA Case 20,
Coaxial Air Jets

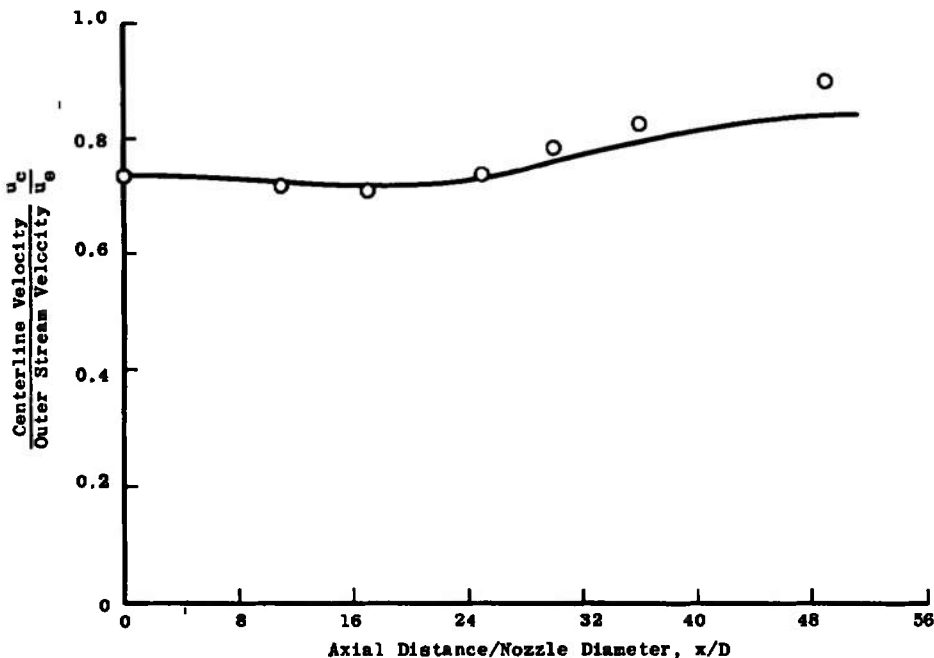


Fig. 20 Comparison of Prediction with Experiment, NASA Case 11,
Axisymmetric Jet in Moving Stream, $M_1 = 0.90$, $M_\infty = 1.30$

Mixing with momentum, energy, and mass transfer was represented by four cases, and predictions of the present model for all of these cases are shown in Figs. 21 through 24. Cases 10 and 21 (Figs. 21 and 22) involve the prediction of the subsonic mixing of coaxial jets of hydrogen and air. Both of these cases involve start points downstream of the nozzle exit. Because the start region in both cases was in the region of transition between first and second regime behavior, a special start technique was used for them. This special technique involved the use of Eqs. (12) and (13) in the development of the initial kinetic energy profile from the initial eddy viscosity profile used as a start condition, and the subsequent use of Eqs. (12) and (13) to obtain the shear stress from the TKE profile even where $U_c > 0.9 U_p$. The reason for this alteration of the standard procedure is that the late start point (in terms of flow field development) did not allow the buildup of centerline turbulent kinetic energy to occur. The calculation normally predicts such a buildup in the transition region. The use of Eqs. (12) and (13) to increase the TKE level near the centerline over that which the assumed constant eddy viscosity would produce, in conjunction with Eq. (11), compensated for the lack of centerline buildup, at least in a crude fashion.

Figures 23 and 24 illustrate the predictions of the model for NASA Cases 12 and 22. Both of these cases were dominated by thick boundary layers and a strongly wake-like character produced by the low momentum flux of the central hydrogen stream. In both cases the initial decay rate is overpredicted, but the qualitative agreement with the data for Case 22, in which the centerline velocity decreases below the outer stream velocity and then slowly increases, is noteworthy.

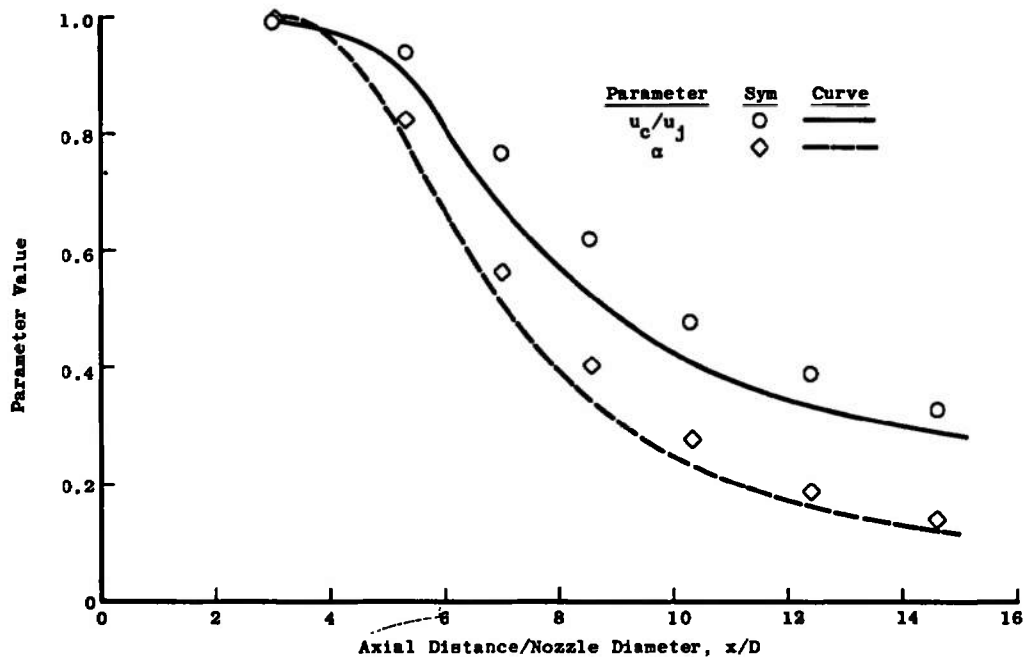


Fig. 21 Comparison of Predictions with Experiment, NASA Case 10,
Hydrogen-Air Jets

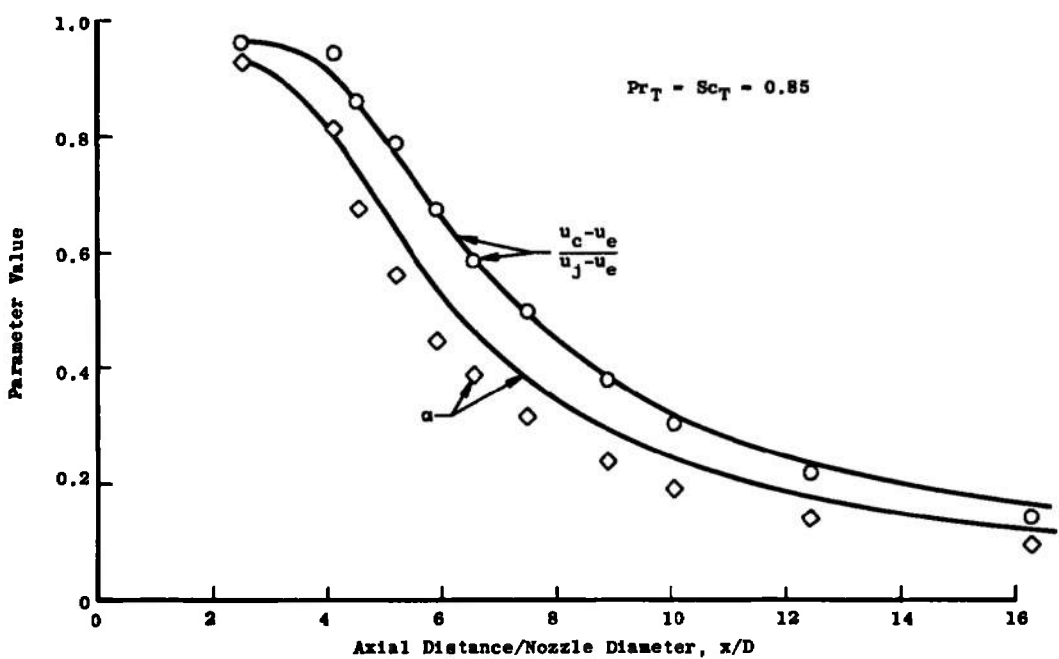


Fig. 22 Comparison Theory with Experiment, NASA Case 21,
Hydrogen-Air Jets

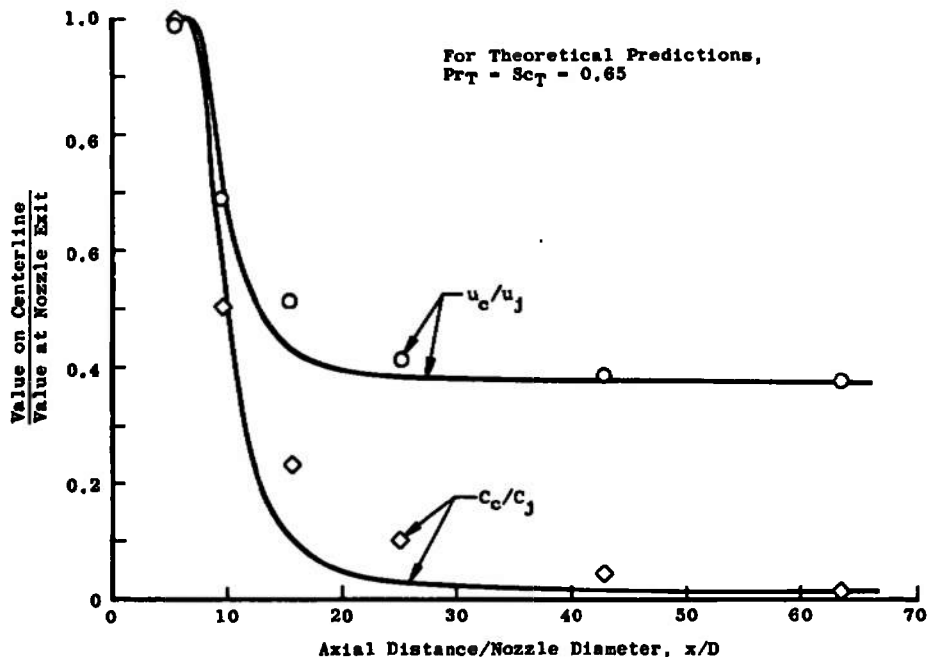


Fig. 23 Comparison of Predictions with Experimental Data, NASA 12, Hydrogen-Air Jets

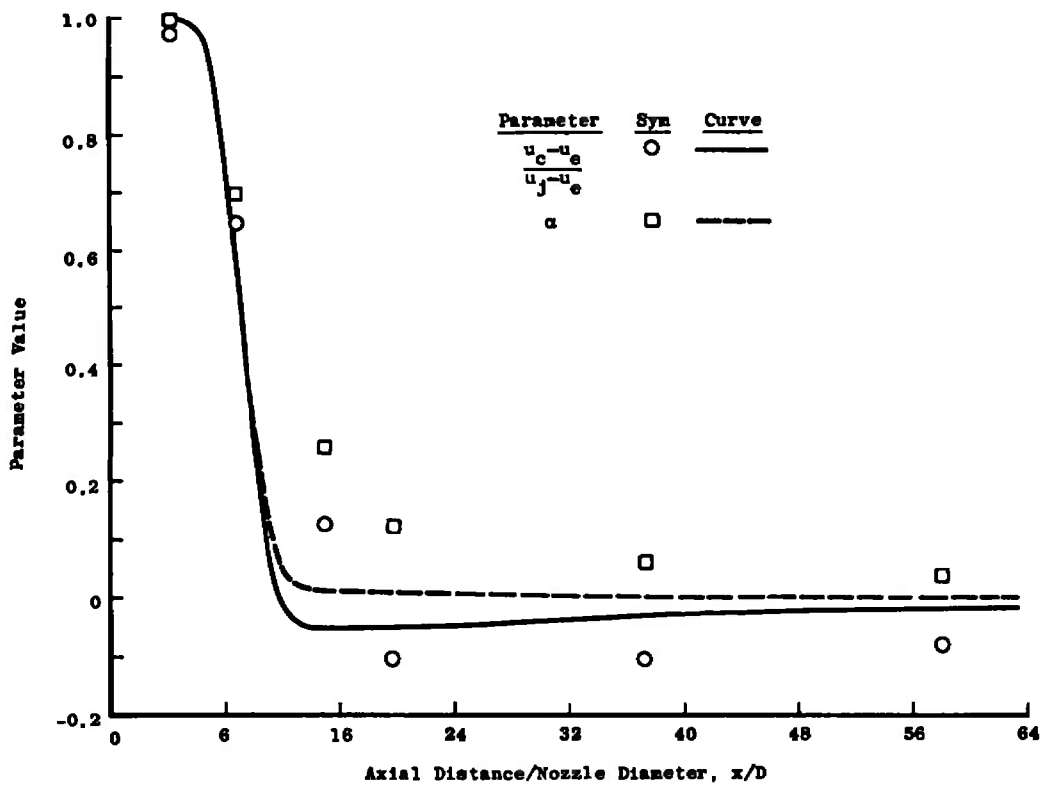


Fig. 24 Comparison of Predictions with Experiment, NASA Case 22, Supersonic Hydrogen-Air Jets

4.6 WAKES

Four wake flows were included in the test cases of Ref. 11, including two-dimensional and axisymmetric, incompressible and compressible flows. The predictions of the present model for these cases are shown in Figs. 25 through 30.

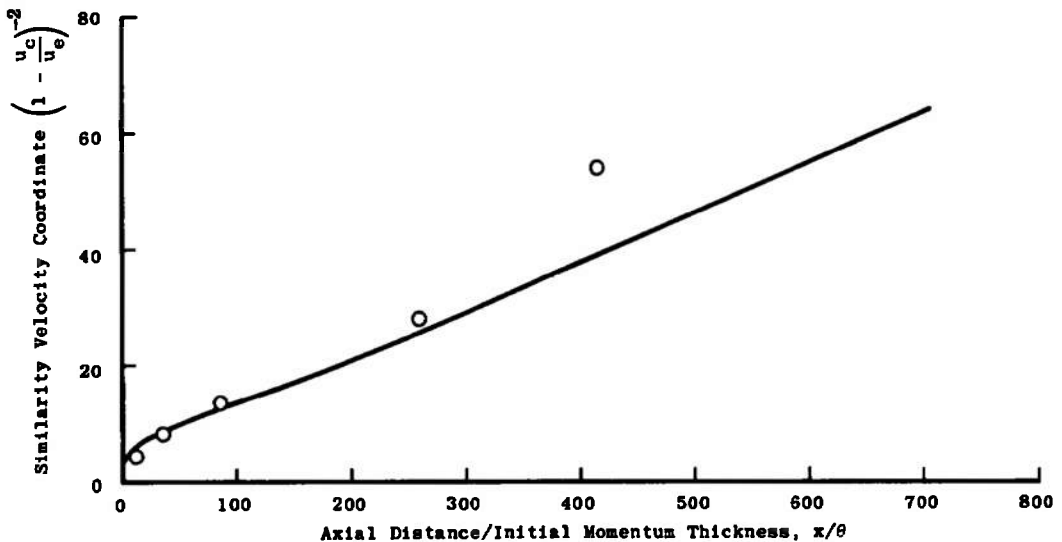


Fig. 25 Comparison of Prediction with Experiment, NASA Case 14, Two-Dimensional Incompressible Wake

The prediction of the centerline velocity for the incompressible planar wake is shown in Fig. 25, plotted in similarity coordinates. From similarity considerations, the curve of $[1 - (u_c/u_e)]^{-2}$ versus x/θ should be a straight line, and Fig. 25 shows that the prediction is a straight line in these coordinates. However, the slope of this curve may be somewhat too low, indicating too slow an approach to the true asymptotic condition. This effect was also seen in the axisymmetric jet, and it is interesting to note that the prediction of these asymptotic flows made by this model are quite similar to the predictions of the "k" model of Launder, et al. (Ref. 27) as presented at the NASA conference. The "k" model of these authors uses an eddy viscosity-type relationship between the shear stress and the kinetic energy and an algebraic length scale formulation. Thus the similar behavior of the two models in asymptotic flow indicates that the length scale formulation may be at fault; i.e., it may be necessary to use a more sophisticated formulation including a transport equation for dissipation (such as the formulation of Hanjalic and Launder, Ref. 19) in order to properly model the transition to asymptotic flow.

Figures 26 and 27 present a comparison of predicted and measured velocity and shear stress profiles for the incompressible two-dimensional wake. In general, the velocity profile prediction is good, although a tendency exists to underpredict the wake width (which is consistent with the underprediction of the velocity decay rate). Figure 27 shows

that the prediction of the peak shear stress is quite reasonable (and it should be remembered that these calculations begin with estimated rather than experimental shear stress profiles), but the profile width is again underpredicted.

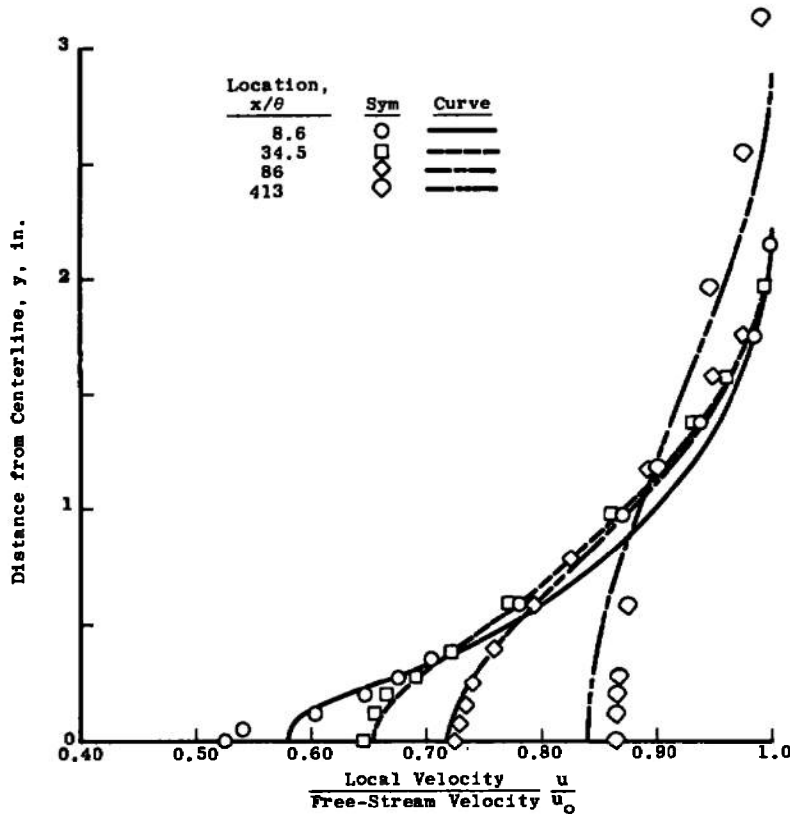


Fig. 26 Comparison of Measured and Predicted Velocity Profiles, NASA Case 14, Two-Dimensional Wake

For the axisymmetric incompressible wake, similarity considerations require that the curve of $[1-(u_c/u_e)]^{-3/2}$ versus x/D be a straight line, and Fig. 28 shows that such a curve is predicted by this model. It might, however, be noted that asymptotic conditions for axisymmetric wakes have not been experimentally demonstrated (Ref. 1), and thus a judgment as to the proper slope of the decay curve cannot be made from the evidence of Fig. 28.

Figure 29 shows that the asymptotic prediction of the centerline velocity for the compressible two-dimensional wake again shows too low a rate of increase of the centerline velocity. This is again consistent with the "k" model of Ref. 27. On the other hand, the prediction of the axisymmetric compressible wake, Fig. 30, which, as discussed above, may not be an asymptotic flow, is considerably better, and also considerably better than the "k" model of Ref. 27.

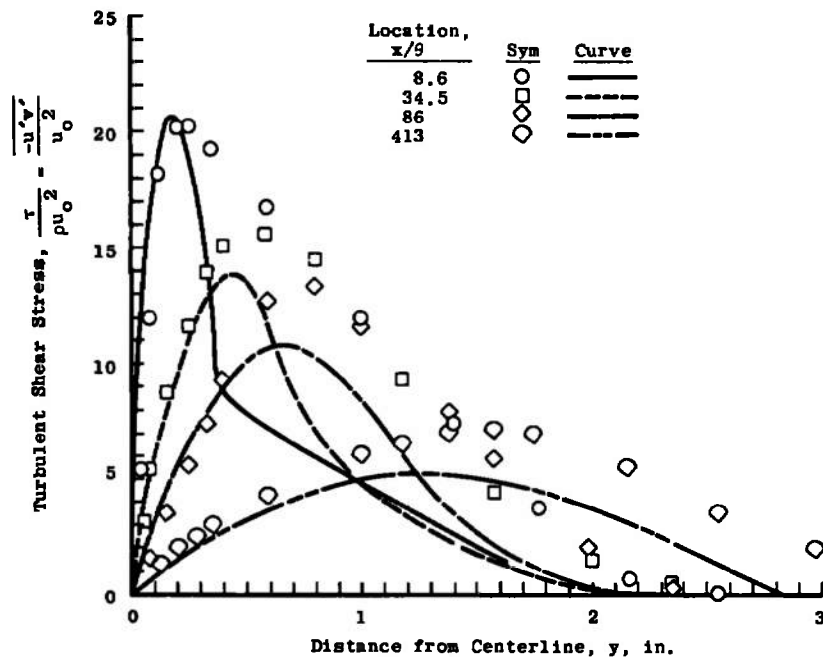


Fig. 27 Comparison of Turbulent Shear Stress Profiles, NASA Case 14,
Two-Dimensional Wake

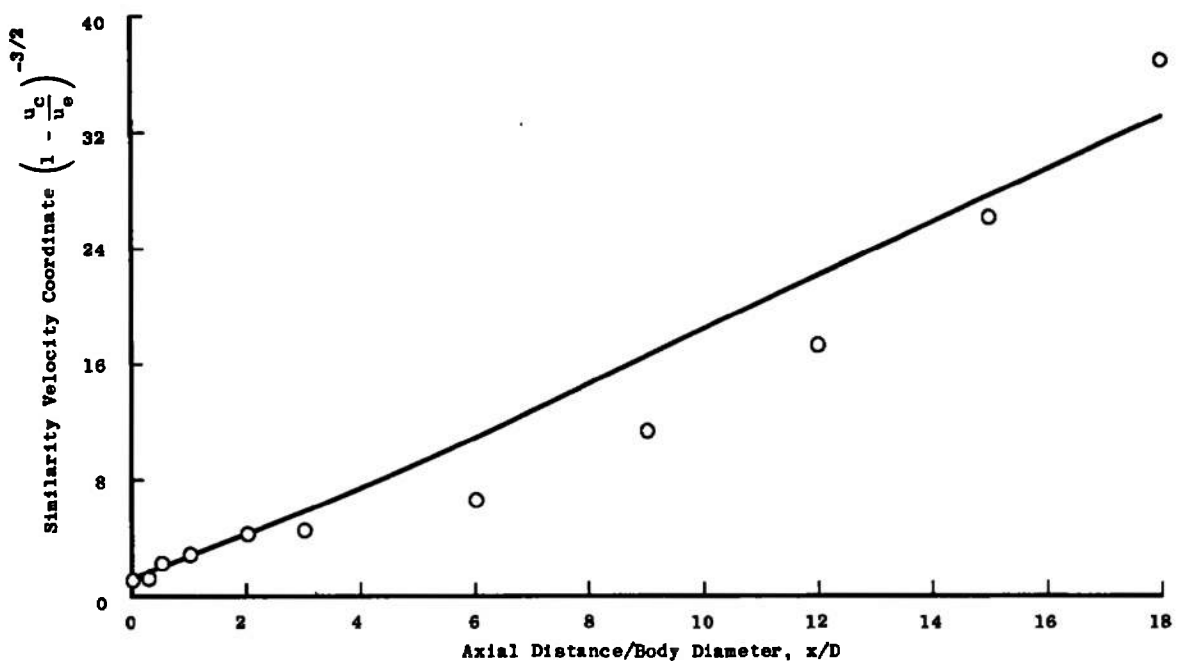


Fig. 28 Comparison of Prediction with Experimental Data, NASA Case 15,
Axisymmetric Incompressible Wake

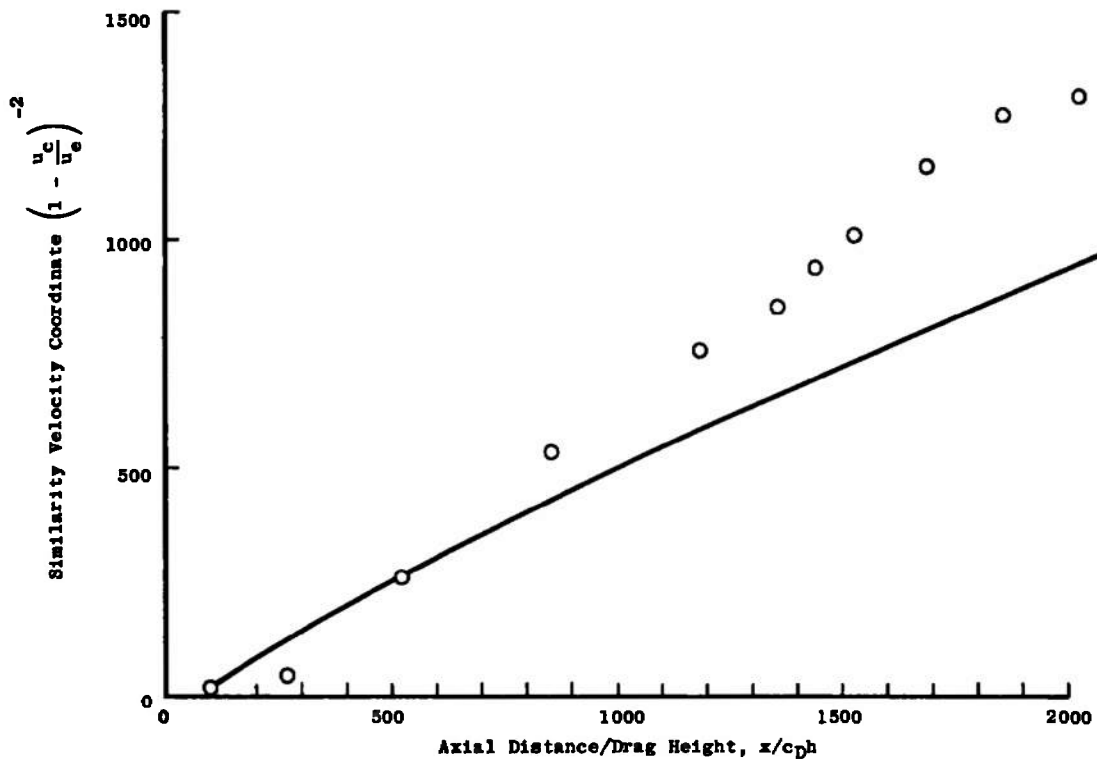


Fig. 29 Comparison of Prediction with Experiment, NASA Case 16,
Compressible ($M = 2.88$) Two-Dimensional Wake

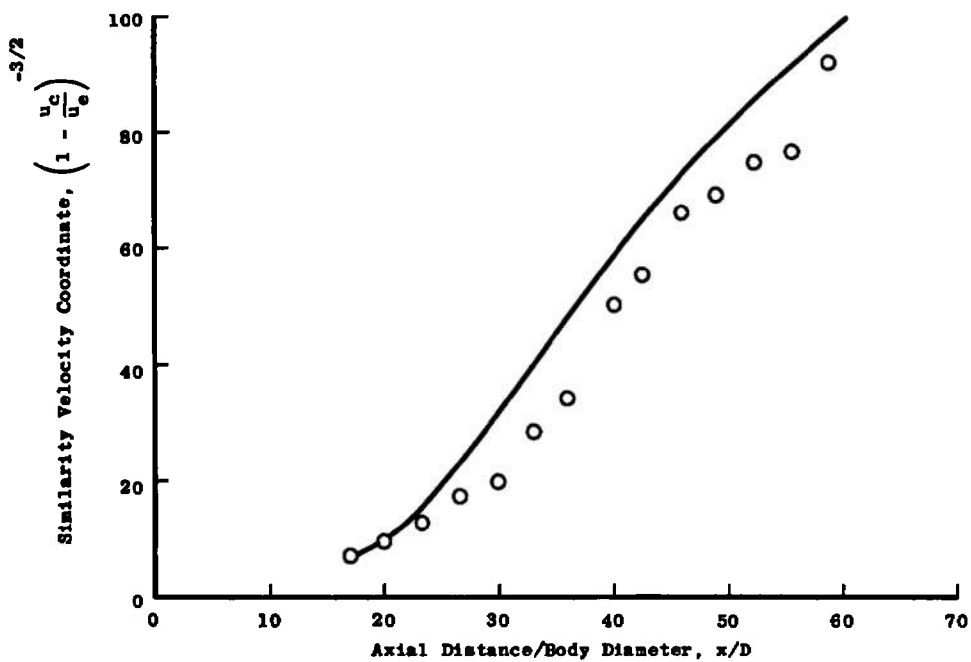


Fig. 30 Comparison of Prediction with Experiment for NASA Case 17,
Compressible Axisymmetric Wake

4.7 CONCLUSIONS AND COMPARISONS WITH OTHER MODELS

The predictions shown above have demonstrated that the present model is capable of accurate predictions of a variety of flows of engineering interest. Its major failures appear to be in the prediction of the asymptotic circular jet and the asymptotic circular wake. In this respect the present model can be compared to the similar "k" model of Ref. 27, but the present model provides considerably better prediction than the "k" model of such flows as the axisymmetric wake and the two-dimensional, two-stream jet. This may indicate that in asymptotic flows the algebraic length scale formulation is in error, since in such weak shear flows the dissipation term in the turbulent kinetic energy equation dominates. On the other hand, the improvement of the present model over the "k" model of Ref. 27 in strong shear flows may indicate that the shear stress formulation used for this model is more accurate than the eddy viscosity formulation of Ref. 27. It should also be noted that all of the present calculations were begun from estimated initial conditions, whereas the calculations of Ref. 27 were begun by iterating on the initial condition until the data at the first downstream station were matched.

The calculations made using the present method may also be compared to the closely-related integral model calculation of Ref. 12, also presented at the NASA conference. In general, the integral model cannot handle the developing part of the first regime, in which boundary-layer-like profiles are developing into profiles characteristic of a free shear layer. However, in flow regions where the assumption of cosine profiles used in formulating the integral model is satisfactory, the integral model predictions are as good as those shown here. Further, the integral model prediction of the asymptotic jet (the two-dimensional wake was not attempted in Ref. 12) is quite good. The difference between the integral calculation and the present model in this flow is that the TKE profiles assumed in the integral model imply a much greater diffusion rate of TKE at the centerline than is predicted in the finite-difference model. Thus, although a comparison of the present model and the "k" model of Ref. 27 put the length-scale formation for an asymptotic jet under suspicion, a comparison of the present model with the integral formulation indicates that the proper behavior could also be obtained through use of a variable TKE diffusion coefficient.

In general, however, the predictions of the present model for flows of engineering interest are quite adequate; they are certainly better than those obtainable with eddy viscosity models (Ref. 1). The present model is also adaptable to more complex cases, such as reacting turbulent flows, using both conventional and unconventional models for the appropriate chemistry (Refs. 28 and 29). It does not predict asymptotic flows adequately, but in view of the behavior of more sophisticated models (Refs. 19 and 27) in these flows, it does not seem worthwhile to attempt to improve the present model for asymptotic predictions which are of limited utility.

SECTION V

THE COMPUTER PROGRAM

5.1 MECHANICS OF THE NUMERICAL PROCEDURE

The sequence of operations performed by the computer program is shown schematically in Fig. 31. From this figure, it can be seen that the operations are broken down into a number of subroutines, so that only the subroutines involved need be altered if a modification is desired. In general, information is passed between the subroutines through the use of labeled common blocks, and thus some care in making modifications needs to be exercised to avoid altering information needed elsewhere. Table IV lists the variables stored in common blocks and their use in each subroutine. It may be noted from this table that several variables defined in the original program (Ref. 13) are no longer used, but the appropriate blocks have been retained. Little effort has been expended to optimize this program with respect to run time; however, a typical time for one of the computations described in the preceding section is one minute on an IBM 370/155, and the program occupies 86K bytes of storage.

The sequence of computer operations for a typical run begins with those operations that are only performed once in the solution of a particular problem. Referring to Fig. 31, the appropriate values of the material constants, such as the gas constant and the specific heat, are established in CONST. The heading is read, and all other operations for which no specific subroutine name is shown are performed, in the MAIN program. This heading, which may consist of up to 80 characters (blanks included), is printed out at the top of each page of output for identification.

Subroutine BEGIN also falls into the category of subroutines called only once in a given problem. In this subroutine the initial profiles of velocity, eddy viscosity, total enthalpy, and concentration of jet species are read in; coefficients are initialized; and the lateral grid spacing in nondimensional stream function (ω) coordinates is computed, using subroutine DENSTY to obtain the densities appropriate to the initial composition and enthalpy.

Length scales; the mixing region width YL, defined as the distance between the points at which the local velocity is a specified function of each edge velocity (see Eq. (17)); and the half-velocity width YMU, defined as the distance from the centerline to the point at which the velocity is equal to the average of the free-stream and centerline velocities, (see Eq. (19)) are defined in subroutine LENGTH. A third length scale, based on an assumed cosine profile shape, will also be computed in subroutine SHEARS, using Eq. (18). These length scales are necessary for the computation of the TKE dissipation rate, which is carried out in subroutine SOURCE.

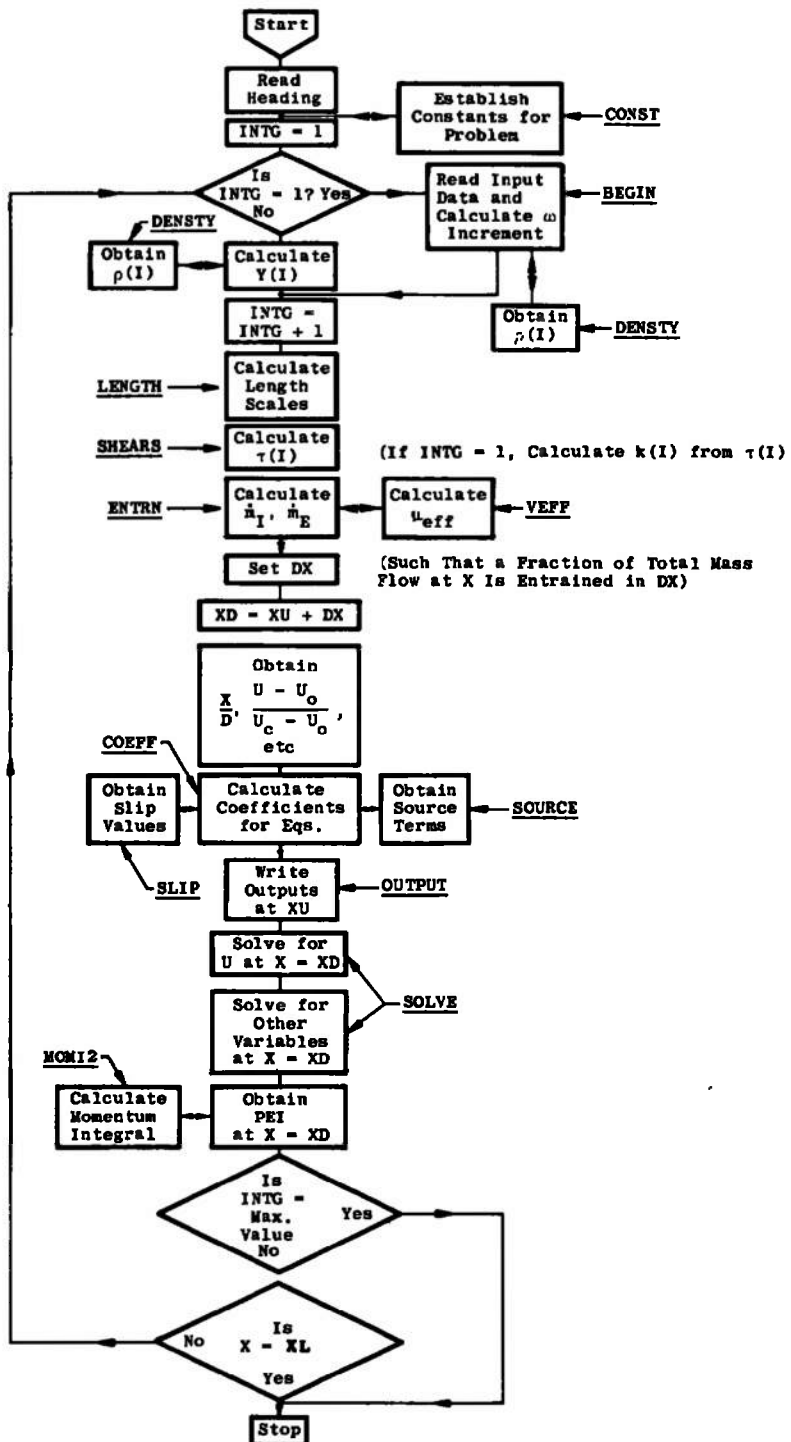


Fig. 31 Computer Program Flow Diagram

TABLE IV
VARIABLES STORED IN COMMON BLOCKS

Block	Variable	MAIN	BEGIN	COEFF	CONST	DENSTY	ENTRN	LENGTH	MOM12	OUTPUT	RAD	READY	SHEARS	SLIP	SOURCE	VEFF
AEMU	EMUA															
ASD	ASD1		I													
	ASD2		I													
AUXP	TEMP															
AUXY	YY															
	XXU															
C	RR1															
	SC	G	M													
	AU	G	M													
	BU	G	M													
	CU	G	M													
	A	G	M													
	B	G	M													
CPS	C	G	M													
	CP1															
	CP2															
	GC1															
	GC2															
DCON	DXC	I	G													
DENC																
DUD	C															
	DUDOM															
	DUDY															
	ADUDY															
	ADUDYM															
GEN	PEI	M	U	G	G	U	G	U		U	U	U	U	U	U	
	AMI	U	U	U	U	U	U	U								
	AME	U	U	U	U	U	U	U								
	DPDX															
	PREF															
	PR															
	P															
	DEN															
	AMU															
	XU	M	G	G	G	U	U	U		U	U	U	U	U	U	
	XD	G	G	G	G	U	U	U		U	U	U	U	U	U	
	XP	G	G	G	G	U	U	U		U	U	U	U	U	U	
	XL	G	G	G	G	U	U	U		U	U	U	U	U	U	
	DX	G	G	G	G	U	U	U		U	U	U	U	U	U	
	CSALFA	G	I	I	I	M	U	U		U	U	U	U	U	U	
	XPC6															
	INTG															

TABLE IV (Continued)

Block	Variable	MAIN	BEGIN	COEFF	CONST	DENSITY	ENTRN	LENGTH	MOM12	OUTPUT	RAD	READY	SHEARS	SOURCE	SLIP	VEFF
HED I	HEAD	I	I	G			U	U				U	U	U	U	
	N	U	G	G			U	U	U			U	U	U	U	
	NP1	U	G	I			U	U	U			U	U	U	U	
	NP2	U	G	I			U	U	U			U	U	U	U	
	NP3	U	G	I			U	U	U			U	U	U	U	
	NEQ	U	G	I			U	U	U			U	U	U	U	
	NPH	U	G	I			U	U	U			U	U	U	U	
	KEX	U	G	I			U	U	U			U	U	U	U	
	KIN	U	G	I			U	U	U			U	U	U	U	
	KASE	U	G	I			U	U	U			U	U	U	U	
	KRAD	U	I	I			U	U	U			U	U	U	U	
	KPRAN	G	I	I			U	U	U			U	U	U	U	
IDIN IW	INDIC	G	I	I			U	U	U			U	U	U	U	
	KWAKE	U	I	I			U	U	U			U	U	U	U	
KJU L	ISL	G	I	I			U	U	U			U	U	U	U	
	KMU	U	I	I			U	U	U			U	U	U	U	
	AK	G	I	I			U	U	U			U	U	U	U	
LIME	ALMG	U	I	I			U	U	U			U	U	U	U	
L1	II	G	I	I			U	U	U			U	U	U	U	
	IE	U	I	I			U	U	U			U	U	U	U	
	YL	G	I	I			U	U	U			U	U	U	U	
	UMAX	U	I	I			U	U	U			U	U	U	U	
	UMIN	G	I	I			U	U	U			U	U	U	U	
	FR	G	I	I			U	U	U			U	U	U	U	
	YIP	G	I	I			U	U	U			U	U	U	U	
	YEM	G	I	I			U	U	U			U	U	U	U	
OUT	UP	G	I	I			U	U	U			U	U	U	U	
	US	G	I	I			U	U	U			U	U	U	U	
	PHIUC	G	I	I			U	U	U			U	U	U	U	
	PSIU	G	I	I			U	U	U			U	U	U	U	
	XOD	G	I	I			U	U	U			U	U	U	U	
	UGU	G	I	I			U	U	U			U	U	U	U	
	UGD	G	I	I			U	U	U			U	U	U	U	
PR	IPRNT	G	I	I			U	U	U			U	U	U	U	
RADI	RO	G	I	I			U	U	U			U	U	U	U	
	RI	G	I	I			U	U	U			U	U	U	U	
RUH RT	RAAUH	G	I	I			U	U	U			U	U	U	U	
	RTM	G	I	I			U	U	U			U	U	U	U	
	YUK	G	I	I			U	U	U			U	U	U	U	
	SHEAR	G	I	I			U	U	U			U	U	U	U	
	SCSH	G	I	I			U	U	U			U	U	U	U	

TABLE IV (Concluded)

Block	Variable	MAIN	BEGIN	COEFF	CONST	DENSTY	ENTRN	LENGTH	MOM12	OUTPUT	RAD	READY	SHEARS	SLIP	SOURCE	VEFF
TEM	TOJO	U				G					G	U				
TWOD	YI	U				U		G	U	U	U	U	U	U	U	
UMUM	YMU	G	I	U		U	U	U	U	U	U	U	U	U	U	
V	U	G	I	U		U	U	U	U	U	U	U	U	U	U	
F		G	I	U		G	U	U	U	U	U	M	U	U	U	
R		U	G	U		U	U	U	U	U	U	U	U	U	U	
RHO		U	U	G		G	U	U	U	U	U	G	U	U	U	
OM		U	I													
Y																U

Legend: G - Generated in subroutine

M - Modified in subroutine

U - Used in subroutine

I - Input data to subroutine

NOTE: Subroutine SOLVE does not use common block storage

After the length scale computation the turbulent shear stress SHEAR (I) is computed from the turbulent kinetic energy F(1,I) in subroutine SHEARS. In the first step of the computation, an additional calculation is also carried out in SHEARS in order first to compute the value of SHEAR(I) from the input profiles of eddy viscosity and velocity, and then to compute the turbulent kinetic energy. The value of the turbulent Reynolds number, RTM, at the step, which is used in computing ASD2 and the TKE dissipation, is also obtained in SHEARS.

Subroutine ENTRN is next called to establish the viscous-region mass increase over the next step. As explained in Section III, this subroutine is fundamental to the computational scheme, yet any reasonable method of obtaining the entrainment rates is acceptable.

With the entrainment for the next step computed, the step size is obtained, in MAIN, by demanding that the step size be such that the mass increase in the viscous region be a specified fraction (FRA) of the viscous region mass at the beginning of the step. Because this length, uncontrolled, can be too large for good accuracy, the step length is externally limited in MAIN to a specified fraction, DXCN, of the mixing region length scale.

The coefficients necessary for a solution of the equations at $X = XD = XU + DX$ are then obtained in COEFF based on values of the dependent variables at $X = XU$. To obtain these coefficients, COEFF calls two additional subroutines, SOURCE, in which

the source terms in the transport equations are computed and SLIP, in which the coefficients at the points 2 and $N + 2$ across the stream are evaluated. Special evaluations are made at these points since they are designed to produce not the proper values of the dependent variables at 2 and $N + 2$, but the proper gradients.

This point marks the end of a computational step, and thus profiles of the dependent variables and some of the coefficients are printed out through subroutine OUTPUT. To start the calculations at the next step, all of the equations involved are solved simultaneously (except for the momentum equation which does not involve other variables) in SOLVE. Two passes through SOLVE are made, the first obtaining the downstream values of the velocity, and the second, the downstream values of the other variables. After this computation, the calculated profiles are inspected for possible errors, such as negative values of a positive-definite quantity, and any errors encountered are corrected.

With new profiles of the dependent variables known, the downstream value of the viscous-layer mass flux is obtained. On the first step, this is accomplished by summing the contributions of the entrained mass flux and the mass flux at the start of the step. For all subsequent steps the condition that the integral momentum flux increment be a constant is used, which involves use of subroutine MOM12.

The values of the physical coordinate $Y(I)$ which correspond to the nondimensional coordinates $OM(I)$ and the computed values of the velocity, total enthalpy, and concentration are now established in subroutine READY. This in turn involves subroutines RAD, in which the radius of the inner edge of the mixing layer is obtained and DENSTY, in which the density $RHO(I)$ corresponding to the computed values of velocity, total enthalpy, and concentration is evaluated. With all values of the dependent and independent variables known at the new X -station, which now becomes XU , the computation is repeated. The sequence is continued until either the maximum number of steps is exceeded or until the input maximum value of $X(XL)$ is achieved.

5.2 INPUT DEFINITIONS

All initial profile data are read in either the main program or subroutine BEGIN. The first card read, from MAIN, defines NCASE, the number of cases to be computed on this run of the program. A case is defined as a complete calculation of a particular flow field. NCASE is read on an 15 format. The second card supplies the heading, with a maximum of 80 characters, blanks included. Finally, the last card read in MAIN supplies the values of XODI and URAT. These variables are used in the case when a calculation is begun at some x/D downstream (XODI) with a nonunity ratio of local centerline velocity to jet velocity. The variable URAT then relates the computed velocity ratio to the jet velocity. These are read on a 2E12.5 format.

The remaining data needed to start a calculation are read in subroutine BEGIN. The first of these is a set of 10 integers which control the calculation, read on a 10I5 format. These variables, and their values, are as follows:

TABLE V
INTEGER CONTROL INPUTS

KRAD	= 0 plane flow = 1 axisymmetric flow
KIN	= 1 inside edge of flow (I = 1) a wall = 2 inside edge of flow (I = 1) a free stream = 3 inside edge of flow (I = 1) an axis of symmetry
KEX	Similar to KIN, but applies to outer edge of flow (I = NP3)
NEQ	Number of equations to be solved = 2 momentum and TKE = 3 momentum, TKE, and total enthalpy = 4 momentum, TKE, total enthalpy, and species
N	Number of cross-stream input points less one
ISL	= 0 flow is a 2-D shear layer = 1 any other flow field type
KPRAN	Not used in present formulation
KSST	= 1 single-stream flow, US = 0 = 2 no effect
KSEV	= 0 UP = U(1) = 1 UP = UW
IWAKE	= 1 flow is a wake = 2 any other flow

After these variables are defined, a set of real variable controls are read. The definitions of these follow in Table VI; they are read on an 11F5.0 format.

The input profiles of $Y(I)$, in feet, $U(I)$, in ft/sec, $F(1, I)$, at this point the eddy viscosity, in ft^2/sec , $F(2, I)$, the total enthalpy, in ft^2/sec^2 , and the jet species concentration, $F(3, I)$, (dimensionless) are next read in using a sequence of statements in BEGIN. They are read sequentially, using a 7F10.5 format. With these data stored, the calculation begins.

TABLE VI
REAL VARIABLE CONTROL INPUTS

XL	Length to which calculation is to be carried, ft
XPC6	Not used
ASD1	Value of a_1 , normally 0.3
ASD2	Initial value of a_2 , normally 1.69
PREF(1)	TKE Prandtl number, normally 0.7
PREF(2)	Mean energy turbulent Prandtl number, 0.7-0.85
PREF(3)	Turbulent Schmidt number, normally equal to PREF(2)
DXC	Step size control, generally 0.5-1.0
RO	Jet nozzle radius, ft — 0.5
RI	Inner boundary-layer thickness, ft — 6.2
CW	Characteristic velocity, normally nozzle exit velocity

5.3 VARIABLE NAMES AND LISTING

A complete list of the FORTRAN variable names used in the program and their meanings follows as Table VII. Appendix I provides a complete FORTRAN listing of the program used to compute all of the test cases of Section IV.

TABLE VII
FORTRAN VARIABLE NAMES

FORTRAN Name	Mathematical Equivalent	Description	Defining Subroutine
A(J,I)	A	Coefficient in difference equation	COEFF
*ADUDY(I)	$ \partial u / \partial y $	Absolute value of velocity gradient	SHEARS
*ADUDYM	$ \partial u / \partial y _M$	Maximum value of $ \partial u / \partial y $ at x-station	SHEARS
*AM	$\int_0^1 (u - u_e) dw$	Momentum increment/mass flux at x-station	MOM12
*AMCHK	$(\psi_E - \psi_I) \int_0^1 (u - u_e) dw$	Momentum increment at x-station	MAIN
*AMD	---	Value of AM at XD	MAIN
AME	\dot{m}'_E	Mass flux/unit area entrained in Δx at external boundary	ENTRN
AMI	\dot{m}'_I	As above, but internal boundary	ENTRN
*AMUP	---	Value of AM at XU	MAIN
*ASD1	a_1	Parameter in $\tau - k$ relation, Eq. (9)	SHEARS
*ASD2	a_2	Parameter in TKE dissipation, Eq. (14)	SHEARS
AU(I)	Au	Coefficient in velocity difference equation	COEFF
B(J,I)	B	Coefficient in difference equation	COEFF
BETA	---	Not used	BEGIN
BU(I)	Bu	Coefficient in velocity difference equation	COEFF
*C	c_1	Density correction to TKE dissipation (Eqs. (23 and 24))	SHEARS
C(J,I)	C	Coefficient in difference equation	COEFF
CPF	C_p_f	Frozen value of constant pressure specific heat	DENSTY
CP1	---	Jet specific heat	CONST
CP2	---	Free-stream specific heat	CONST
CSALFA	$\cos \alpha$	Cosine of angle between flow and axis of symmetry	RAD
CU	Cu	Coefficient in velocity difference equation	COEFF
DEN	ρ_{ref}	Reference value of density, not used	---
DPDX	dP/dx	Pressure gradient, here = 0	MAIN
DUDOM	$\partial u / \partial w$	Velocity gradient in w coordinates	MAIN
*DUDY	$\partial u / \partial y$	Velocity gradient, ft/sec/ft	SHEARS
DX	Δx	Axial step, ft	MAIN
*DXC	---	Max step length factor	MAIN
*DXCN	---	$DXC/2$	MAIN
*DXI	---	Value of DX before limiting	MAIN
*EPSI	ϵ_I	Constant eddy viscosity near inside edge	SHEARS
*EPSO	ϵ_E	Constant eddy viscosity near outside edge	SHEARS
EMU	μ_T	Turbulent dynamic viscosity	VEFF
F(1,I)	k	Turbulent kinetic energy, k , (ft/sec) ²	SOLVE
F(2,I)	H	Total enthalpy (ft/sec) ²	SOLVE
F(3,I)	C	Jet species concentration, dimensionless	SOLVE
FRA	---	Constant in DX expression	MAIN

TABLE VII (Continued)

FORTRAN Name	Mathematical Equivalent	Description	Defining Subroutine
GC1	R_1	Gas constant for jet	CONST
GC2	R_2	Gas constant for free stream	CONST
*READ	---	Heading (20A4) format	MAIN
*IE	---	Outer edge point at which entrainment is calculated	ENTRN
*IECSE	---	Print control	MAIN
*II	---	As IE, for inside edge	ENTRN
*IKMAX	---	Point in profile where $\tau = \tau_{\max}$	SHEARS
*IMAX	---	Point in profile where $DUDY = DUDY_{\max}$	SHEARS
*INDIC	---	Determines case number	MAIN
INTG	---	Axial step number	MAIN
*IPRNT	---	Print control step counter	MAIN
*ISL	---	Shear-layer indicator	BEGIN
*IWAKE	---	Wake indicator	
KASE	---	Free- or wall-flow indicator	
KEX	---	External boundary designator	
KIN	---	Internal boundary designator	
*KPRAN	---	Not used	
KRAD	---	2-D or axisymmetric indicator	
*KSEV	---	Characteristic velocity control	
*KSST	---	Single-stream indicator	
N	---	Number of increments across stream	MAIN
*NCASE	---	Number of flows to be computed	
NEQ	---	Number of transport equations to solve	BEGIN
NPH	---	NEQ-1	BEGIN
NP1	---	$N + 1$	
NP2	---	$N + 2$	BEGIN
NP3	---	$N + 3$	
OM(I)	$(\psi - \psi_I) / (\psi_E - \psi_I)$	Independent cross-stream coordinate (non-dimensional stream function)	BEGIN
OMD	$\omega_{i+1} - \omega_{i-1}$	Increment in ω	COEFF
P(I)	---	Not used	---
PEI	$\psi_E - \psi_I$	Mass flux in mixing region	MAIN
*PEI1	---	PEI at XU	MAIN
*PEI2	---	PEI at XD	MAIN
*PHIUC	$(u_c - u_e) / (u_j - u_e)$	Nondimensional centerline velocity ratio	MAIN
PR(I)	---	Not used	---
PREF(1)	Pr_k	TKE Prandtl number	BEGIN
PREF(2)	Pr_T	Turbulent Prandtl number (mean energy)	BEGIN
PREF(3)	Sc_T	Turbulent Schmidt number	BEGIN
*PS1IE	$(U_{1E} - u_e) / (u_c - u_e)$	Nondimensional velocity at outer entrainment point	ENTRN

TABLE VII (Continued)

FORTRAN Name	Mathematical Equivalent	Description	Defining Subroutine
*PSIII	$(u_{II} - u_e)/(u_c - u_e)$	As PSII, at inner entrainment point	ENTRN
*PSIU	$(u - u_e)/(u_c - u_e)$	Nondimensional velocity	MAIN
*PSIUD	$(\bar{u} - u_e)/(u_c - u_e)$	Desired nondimensional velocity at given entrainment point	ENTRN
R(I)	r	Radial coordinate = RI + Y(I)*CSALFA	READY
*RAAUH(I)	$r^2 \rho u$	---	SHEARS
RBAR	R	Mixture gas constant	DENSTY
*RD	r_D	Inner edge radius at XD	MAIN
RHO(I)	ρ	Density (lbm/ft ³)	DENSTY
RI	r_I	Radius to inner edge of mixing region, ft	RAD
RO	r_o	Nozzle radius, ft	BEGIN
*RR1	---	Turbulent Reynolds number	SHEARS
*RU	r_u	Inner edge radius at XU	MAIN
SC(I)	c	Coefficient in diffusion term of general equation	ENTRN
*SCSH(I)	---	Modified coefficient	ENTRN
*SHEAR(I)	τ	Turbulent shear stress	SHEARS
*SIGMA	σ	2-D shear layer growth rate	SHEARS
TEMP(I)	t	Local static temperature	DENSTY
*TOJO	T_{oj}/T_{oe}	Centerline/free-stream total temperature ratio	OUTPUT
U(I)	u	Velocity, ft/sec	SOLVE
*UDES	\bar{u}	Value of u desired at given lateral point at downstream stations	ENTRN
*UGD	---	Free-stream velocity at XD	MAIN
*UGU	---	Free-stream velocity at XU	MAIN
*UMAX	---	Maximum velocity in a given profile	LENGTH
*UMIN	---	Minimum velocity in a given profile	LENGTH
*UP	u_j	Centerline velocity at $X = 0$	BEGIN
*URAT	---	Coefficient modifying PHIUC	MAIN
*US	u_e	Secondary stream velocity at $X = 0$	BEGIN
*UTOL	---	Minimum velocity difference at a step	LENGTH
*UW	---	Reference velocity	BEGIN
X	x	Axial position, ft	MAIN
XD	x_D	Axial position at downstream station	MAIN
XL	L	Value of x at vehicle to stop calculation	BEGIN
*XOD	x/D	Nondimensional axial coordinate	MAIN
*XODI	x/D_i	Initial value of x/D	MAIN
XP	---	X at last step	MAIN
*XPC6	---	Not used	---

TABLE VII (Concluded)

FORTRAN Name	Mathematical Equivalent	Description	Defining Subroutine
*XSTA	---	X at which eddy viscosity profile modifications are used	SHEARS
XU	x_u	Axial position at upstream station	MAIN
*XXU	---	XU, in.	MAIN
Y(I)	y	Physical lateral coordinate, ft	READY
*YD	y_D	Value of YI at downstream step	MAIN
*YI	y_I	Distance to inner edge of 2-D mixing region	RAD
*YL	ℓ	2-D region width scale, Eq. (17)	LENGTH
*YLK	ℓ_k	Dissipation length scale, Eq. {17 through 19}	SHEAR
*YMU	$y_{1/2}$	Value of y at which $u = 1/2 (u_c + u_e)$	LENGTH
*YY(I)	---	As Y(I), in.	MAIN
*YU	---	Value of YI at upstream step	MAIN

*Indicates variable not used in original program (Ref. 13)

REFERENCES

1. Harsha, Philip Thomas. "Free Turbulent Mixing: A Critical Evaluation of Theory and Experiment." AEDC-TR-71-36 (AD718956), February 1971.
2. Harsha, Philip T. "Prediction of Free Turbulent Mixing Using a Turbulent Kinetic Energy Method," in Free Turbulent Shear Flows, Vol. I, Conference Proceedings, NASA SP-321, 1973, p. 463-521.
3. Schlichting, Herman N. "Boundary Layer Theory" (Fourth Edition). McGraw-Hill Book Company, Inc., New York, New York, 1960.
4. Prandtl, L. "Bemerkungen zu Theorie der freien Turbulenz" Zeitschrift für Angewandte Mathematik und Mechanik, Vol. 22, October 1942, pp. 241-243.
5. Taylor, G.I., Fage, A., and Falkner, U.M. "Transport of Vorticity and Heat through Fluids in Turbulent Motion." Proceedings of the Royal Society of London, Series A, Vol. 135, April 1, 1932, pp. 685-702.
6. Reichardt, Hans. "On a New Theory of Free Turbulence." Journal of the Royal Aeronautical Society, Vol. 47, 1942, pp. 167-176.
7. Schetz, Joseph. "Turbulent Mixing of a Jet in a Coflowing Stream." AIAA Journal, Vol. 6, No. 10, October 1968, pp. 2008-2010.

8. Nee, V.W. and Kovasznay, L.S.G. "Simple Phenomenological Theory of Turbulent Shear Flows." The Physics of Fluids, Vol. 12, No. 3, March 1969, pp. 473-484.
9. Rodi, W. and Spalding, D.B. "A Two-Parameter Model of Turbulence, and Its Application to Free Jets." Wärme- und Stoffübertragung, Vol. 3, No. 2, 1970, pp. 85-95.
10. Donaldson, Coleman duP. and Rosenbaum, H., "Calculation of Turbulent Shear Flows Through Closure of the Reynolds Equations by Invariant Modeling." ARAP Report 127, Aeronautical Research Associates of Princeton, Princeton, New Jersey, 1968.
11. Free Turbulent Shear Flows. Vol. I. Conference Proceedings. Vol. II, Summary of Data. NASA SP-321 (NASA Langley Research Center, Hampton, Virginia, July 20-21, 1972), 1973.
12. Peters, C.E. and Phares, W.J. "An Integral Turbulent Kinetic Energy Analysis of Free Shear Flows" in Free Turbulent Shear Flows, Vol. I, Conference Proceedings, NASA SP-321, 1973, p.577-628.
13. Patankar, S.V. and Spalding, D.B. "Heat and Mass Transfer in Boundary Layers" (Second Edition). Intertext Textbook Co., Ltd. London, England, 1970.
14. Dryden, H.L. Advances in Applied Mechanics, Vol. 1, Academic Press, New York, New York. 1948, pp. 1-40.
15. Bradshaw, P., Ferriss, D.H. and Atwell, N.P. "Calculation of Boundary Layer Development Using the Turbulent Energy Equation." Journal of Fluid Mechanics, Vol. 28, Part 3, May 1967, pp. 593-616.
16. Harsha, P.T. and Lee, S.C. "Correlation between Turbulent Shear Stress and Turbulent Kinetic Energy." AIAA Journal, Vol. 8, No. 8, August 1970, pp. 1508-1510.
17. Kolmogorov, A.N. "The Equations of Turbulent Motion in an Incompressible Fluid." Izvestiya Academy of Sciences, USSR: Physics, Vol. 6, Nos. 1 and 2, 1942, pp. 56-58.
18. Reynolds, W.C. "Computation of Turbulent Flows - State-of-the-Art, 1970." Report MD-27, Thermosciences Division, Stanford University, Stanford, California, October 1970.
19. Hanjalić, K. and Launder, B.E. "A Reynolds Stress Model of Turbulence and its Application to Asymmetric Boundary-Layers." Report TM/TN/A/8, Department of Mechanical Engineering, Imperial College, London, England, March 1971.

20. Laster, M.L. "Inhomogeneous Two-Stream Turbulent Mixing Using the Turbulent Kinetic Energy Equation." AEDC TR-70-134 (AD705578), May 1970.
21. Maise, George, and McDonald, Henry. "Mixing Length and Kinematic Eddy Viscosity in a Compressible Boundary Layer." AIAA Journal, Vol. 6, No. 1, January 1968, pp. 73-80.
22. Chriss, D.E. and Pault, R.A. "Summary Report, An Experimental Investigation of Subsonic Coaxial Free Turbulent Mixing." AEDC-TR-71-236, AFOSR TR 72-0237 (AD737098), February 1972.
23. Demetriades, A. "Compilation of Numerical Data on the Mean Flow from Compressible Turbulent Wake Experiments." Report U-4970, Aeroneutronic Division, Philco-Ford Corp., October 1, 1971.
24. Bradshaw, P., Ferriss, D.H., and Johnson, R.F. "Turbulence in the Noise-Producing Region of a Circular Jet." Journal of Fluid Mechanics, Vol. 19, Part 4, August 1964, pp. 591-624.
25. Albertson, M.L., Dai, Y.B., Jensen, R.A., and Rouse, Hunter. "Diffusion of Submerged Jets." Paper No. 2409, Transactions ASCE, Vol. 115, 1950, pp. 643-664.
26. Wygnanski, I., and Fielder, H. "Some Measurements in the Self-Preserving Jet." Journal of Fluid Mechanics, Vol. 38, Part 3, September 18, 1969, pp. 577-612.
27. Launder, B.E., Morse, A., Rodi, W., and Spalding, D.B. "Prediction of Free Shear Flows - A Comparison of the Performance of Six Turbulence Models" in Free Turbulent Shear Flows, Vol. I, Conference Proceedings, NASA SP-321, 1973, pp. 361-426.
28. Rhodes, R.P. and Harsha, P.T. "On Putting the 'Turbulent' in Turbulent Reacting Flow." AIAA Paper 72-68, AIAA 10th Aerospace Sciences Meeting, San Diego, California, January 1972.
29. Rhodes, R.P., Harsha, P.T., and Peters, C.E. "Turbulent Kinetic Energy Analyses of Hydrogen-Air Diffusion Flames" presented at 4th International Colloquium on Gas Dynamics of Explosions and Reactive Systems, La Jolla, California, July 10-13, 1973.
30. Heskestad, G. "Hot-Wire Measurements in a Plane Turbulent Jet." Journal of Applied Mechanics, Vol. 32, December 1965, pp. 721-724; erratum, Journal of Applied Mechanics, Vol. 33, September 1966, p. 710.

31. Bradbury, L.J.S. "The Structure of a Self-Preserving Turbulent Plane Jet." Journal of Fluid Mechanics, Vol. 23, Part 1, September 1965, pp. 31-64.
32. Van der Hegge Zijnen, B.G. "Measurements of Turbulence in a Plane Jet of Air by the Diffusion Method and by the Hot-Wire Method." Applied Scientific Research, Section A, Vol. 7, No. 4, 1958, pp. 293-313.
33. Chevray, R. "The Turbulent Wake of a Body of Revolution." Journal of Basic Engineering, Transactions ASME. Vol. 90, Series D, No. 2, June 1968, pp. 275-284.
34. Lee, S.C. and Harsha, P.T. "Use of Turbulent Kinetic Energy in Free Mixing Studies." AIAA Journal, Vol. 8, No. 6, June 1970, pp. 1026-1032.

**APPENDIX
FORTRAN LISTING**

```

0001      IMPLICIT REAL*8(A-H,O-Z)
0002      RFAL*4 HEAD
0003      COMMON /GEN/PET,AMI,AME,DPDX,PREF(3),PR(3),P(3),DEN,AMU,XU,XD,XP,
1XL,DX,CSALFA,XPC6,INTG
1/T/N,NPI,NP2,NP3,NEQ,NPH,KEX,KIN,KASE,KRAD,KPRAN
1/V/U(43),F(3,43),R(43),RHO(43),OM(43),Y(43)
1/C/SC(43),AU(43),BU(43),CU(43),A(3,43),B(3,43),C(3,43)
0004      COMMON/PR/UGJ,UGD
0005      COMMON/U4UM/YMU
0006      COMMON/AUXY/YY(43),XXU,RR1
0007      COMMON /SHEAR/ SHEAR(43),SCSH(43)
0008      COMMON/L1/YL,UMAX,UMIN,FR,YIP,YEM
0009      COMMON /ASD/ ASD1,ASD2
0010      COMMON/TWOD/YI
0011      COMMON /IDYN/ INDIC
0012      COMMON/IW/KWAKE,ISL
0013      COMMON/DUD/DUDCM(43),DUDY(43),ADUDY(43),ADUDVM
0014      COMMON/DCDN/DXC
0015      -/ COMMON/HED/HEAD(20)
0016      COMMON/RT/RTM,YLK
0017      COMMON/RADI/RO,RI
0018      COMMON/JUT/UP,US,PHIUC(501),PSIU(43),XOD(501)
0019      COMMON/PRNT/PRNT
0020      DIMENSION AMCHK(501)
0021      INDIC=0
C SUBROUTINE TO LIMIT NUMBER OF DIVIDE CHECK MESSAGES TO 50. A LIBRARY
C SUBROUTINE
0022      CALL EKRSET(209,250,50,0)
0023      READ(5,8000) NCASE
0024      8000 FORMAT (15)
0025      16 CONTINUE
0026      READ(5,8001) HEAD
0027      8001 FCFMTT(20A4)
0028      READ(5,3002) XOD1,URAT
0029      8002 FORMATT(2E12.5)
0030      INDIC=1,NCIC+1
0031      X = 0.0
0032      INTG=0
0033      PRNT=1
0034      IEC SF=0
0035      IEC SE=1
0036      FPA=.025
0037      CALL CINST
0038      CALL REGIN
0039      TOJ=F(12,1).
0040      DXCN=DXC/2.
0041      AMI=0.
0042      AME=0.
0043      SHEAR(1)=0.
0044      SHEAP(NP3)=0.
0045      CU TII 25
0046      15 CALL PRNT.
0047      IF(Y(1NP3).LT.0.) GOTO 85
0048      25 CONTINUE

```

define C_p air C_p hydrogen
Rain R hydrogen

$INTG = INTG_i + 1$
 C IF IECSE = 1, PRINT EACH STEP
 0050 IF((FCSE.EQ.1) GO TO 6
 0051 IF((INTG.EQ.1) GO TO 5
 0052 IF((INTG/5.GT.INTG)) GO TO 5
 0053 IPRNT=0
 0054 GO TO 6
 0055 5 INTGL=INTG/5
 0056 IPRNT=1
 0057 6 CONTINUE
 0058 DO 102 I=2,NP2
 0059 102 DUDOM(I)=(U(I+1)-U(I-1))/(OM(I+1)-OM(I-1))
 0060 DUDOM(1)=0.
 0061 DUDOM(NP3)=0.
 0062 DO 91 I=1,NP3
 0063 PSIU(I)=(U(I)-U(NP3))/(U(1)-U(NP3))
 0064 91 CONTINUE
 0065 CALL LENGTH
 0066 CALL SHEARS
 0067 CALL ENTRN
 C CHOICE OF FORWARD STEP
 0068 DX=DABS(FRA *PEI/(R(1)*AM1-R(NP3)*AME))
 0069 DX1=DX
 0070 IF(DX.GT.OXCN*YLK) OX=OXCN*YLK
 0071 IF(DX.LE.0.) GO TO 85
 0072 AME=AME*DX/DX1
 0073 XD=XU+DX
 0074 77 CONTINUE
 C CALCULATES CHANGE IN FREE STREAM VELOCITY
 C FOR NONZERO PRESSURE GRADIFNT MAKE CHANGES HERE
 0075 UGO=U(NP3)
 0076 UGU = UGD
 0077 DPDX=0.
 0078 CALL COEFF
 C CONVERT UNITS TO INCHES FOR PRINTOUT
 0079 7 ~~XXU=12.0*XU~~
 0080 RR1=12.0*R(1)
 0081 ~~IF(XU.EQ.0.) XU=.001~~
 0082 DO 90 I=1,NP3
 C FOR 2D SHEAR LAYER, NASA CASES 1-3
 C 90 YY(I)=(Y(I)-YMU)/(XU+XODI)
 0083 90 YY(I)=12.*Y(I)
 0084 XOD(INTG)=XU/(2.*R0)+X001
 0085 PHIUC(INTG)=U(1)/UP
 0086 AMCHK(INTG)=AM*PEI+RHO(1)*R(1)*U(1)*(U(1)-U(NP3))*R(1)/2.
 0087 IF(KPAD.NE.0) GO TO 93
 0088 AMCHK(INTG)=AM*PEI+RHC(1)*U(1)*(U(1)-U(NP3))*YI
 0089 93 CONTINUE
 0090 IF(IPRNT.EQ.0) GO TO 21
 0091 CALL OUTPUT
 0092 21 CONTINUE
 C SETTING UP VELOCITIES AT A FREE BOUNDARY
 0093 IF(KFX.EQ.2)U(NP3)=DSQRT(U(NP3)*U(NP3)-2.*((XD-XU)*DPDX/RHO(NP3))
 0094 IF(KIN.EQ.2)U(1)=DSQRT(U(1)*U(1)-2.*((XD-XU)*DPDX/RHO(1))
 0095 CALL SOLVE(AJ,BU,CU,U,NP3)
 C THIS LOOP USES UMIN FROM LAST STEP. ALWAYS .LE. UMIN THIS STEP
 0096 DO 705 I=1,NP3
 0097 705 IF(U(I).LT.UMIN) U(I)=0.5*(U(I+1)+U(I-1))

```

C SETTING UP VELOCITIES AT A SYMMETRY LINE
0098  IF(KIN.NE.3) GO TO 71
0099  U(1)=U(2)
0100  IF(KRAD.EQ.0)U(1)=.75*U(2)+.25*U(3)
0101  71 IF(KEX.EQ.3)U(NP3)=.75*U(NP2)+.25*U(NP1)
0102  -72 CONTINUE
0103  IF(NEQ.LQ.1) GO TO 30
0104  DO 45 J=1,NPH
0105  DO 46 I=2,NP2
0106  AU(I)=A(J,I)
0107  EU(I)=R(J,I)
0108  46 U(I)=C(J,I)
0109  DO 47 I=1,NP3
0110  47 SC(I)=F(J,I)
0111  CALL SLLVE(AU,RU,CU;SC,NP3)
0112  DO 48 I=1,NP3
0113  48 F(J,I)=SC(I)
0114  81 IF(KIN.NE.3) GO TO P2
0115  -F(J,1)=F(J,2)
0116  -IF(KRAD.EQ.0)F(J,1)=.75*F(J,2)+.25*F(J,3)
0117  -82 IF(KFX.EQ.3)F(J,NP3)=.75*F(J,NP2)+.25*F(J,NP1)
0118  45 CONTINUE
0119  30 XP=XU
0120  DO 455 I=2,NP2
0121  455 IF(FT(I,I).LT.0.) F(I,I)=0.5*(F(I,I+1)+F(I,I-1))
0122  XU=XD
0123  PF11=PE1
0124  PE1=PE1+DX*(R(1)*AM1-R(NP3)*AM1)
0125  IF(1SL.EQ.0) GO TO 32
C CALCULATION OF VALUE OF PE1 WHICH SATISFIES REQUIREMENT THAT
C INTEGRATED MOMENTUM INCREMENT = CONSTANT
0126  IF(INTG.EQ.1) GO TO 31
0127  AMUP=AMD
0128  RU=RD
0129  YU=YD
0130  31 CALL MOMI2(AM)
0131  PD=R(1)
0132  YD=YI
0133  AM0=AM
0134  IF(INTG.EQ.1) GO TO 32
0135  PET2=PE11*AMUP/AMD
0136  IF(KRAD.EQ.0) GO TO 315
0137  IF(KIN.EQ.2) PE12=PE12+RHO(1)*U(1)*(U(1)-U(NP3))*(RU**2.
I-RD**2.)/(2.*4MD)
0138  GO TO 316
0139  315 PE12=PE12+RHO(1)*U(1)*(U(1)-U(NP3))*(YU-YD)/AMD
0140  316 CONTINUE
0141  WRITE(6,1003)PE11,PE12,PE1
0142  1003 FORMAT(3E15.5)
0143  PF1=PF12
0144  32 CONTINUE
C THE TERMINATION CONDITION
0145  IF(INTG.EQ.500) GO TO 85
0146  IF(XU-XL)15,85,85
0147  85 CONTINUE
0148  IF(1SL.EQ.0) GO TO 86
0149  WPITE(6,1003)
0150  1000 FORMAT(1HO,7X,3HX/D,8X,5HPHIUC,4X,5HAMCHK/)
0151  WPITE(6,1001) (X0D(I),PHIUC(I),AMCHK(I),I=1,INTG)
0152  1001 FORMAT(1H 1P2D12.3,D17.7)
0153  86 CONTINUE
0154  IF (INIC.NE.NCASE) GO TO 16
0155  STOP
0156  END

```

```

0001      SUBROUTINE BEGIN
0002      IMPLICIT REAL*8(A-H,O-Z)
0003      COMMON /GEN/PE1,AM1,AME,DPDX,PREF(3),PR(3),P(3),DEN,AMU,XU,XD,XP,
1XL,DX,CALFA,XPC6,INTG
1/V/N,NP1,NP2,NP3,NEQ,NPH,KEX,KIN,KASE,KRAD,KPRAN
1/V/1(43),F(3,43),R(43),RHO(43),OM(43),Y(43)
0004      COMMON/ASD/ ASD1,ASD2
0005      COMMON/CPS/CP1,CP2,GCL,GC2
0006      COMMON /SHEAR/ SHEAR(43),SCSH(43)
0007      COMMON/DCON/DXC
0008      COMMON/IW/IWAKE,ISL
0009      COMMON/OUT/UP,US,PHIUC(501),PSIU(43),XOD(501)
0010      COMMON/RADI/RO,RI
      C  PROBLEM SPECIFICATION
0011      READ(5,42) KRAD,KIN,KEX,NEQ, N,ISL ,KPRAN,KSST,KSEV,IWAKE
0012      42 FORMAT(10I5)
0013      READ(5,43) XL,XPC6,ASD1,ASD2,PREF(1),PREF(2),PREF(3),DXC,RO,RI,UW
0014      43 FORMAT(11F5.0)
0015      44 FORMAT(2F10.5)
0016      KASE=2
0017      IF(KIN.EQ.1.OR.KEX.EQ.1)KASE=1
0018      XU=0.
0019      NPH=NEQ-1
0020      NP1=N+1
0021      NP2=N+2
0022      NP3=N+3
0023      READ (5,444) Y(1), (Y(I), I=3,NP1), Y(NP3)
0024      READ (5,444) U(1), (U(I), I=3,NP1), U(NP3)
0025      READ(5,444) F(1,1), (F(1,I),I=3,NP1), F(1,NP3)
0026      IF(NEQ.LT.3) GO TO 109
0027      READ(5,444) F(2,1), (F(2,I),I=3,NP1), F(2,NP3)
0028      IF(NEQ.EQ.3) GO TO 109
0029      READ(5,444) F(3,1), (F(3,I),I=3,NP1), F(3,NP3)
0030      GO TO 109
0031      444 FORMAT (7F10.5)
0032      109 CONTINUE
0033      446 CONTINUE
0034      IF(IWAKE.EQ.1) GO TO 447
0035      UP=UW
0036      US=U(NP3)
0037      IF(KSEV.EQ.0) UP=U(1)
0038      IF(KSST.EQ.1) US=0.
0039      GO TO 448
0040      447 UP=UW
0041      US=0.
0042      448 CONTINUE
      C  CALCULATION OF SLIP VELOCITIES AND DISTANCES
0043      BETA=.143
0044      GO TO (71,72,73),KIN
0045      71 CONTINUE
0046      GO TO 74
0047      72 U11=U(1)*U(1)
0048      U13=U(1)*U(3)
0049      U33=U(3)*U(3)
0050      SQ=84.*U11-12.*U13+9.*U33
0051      U(2)=(16.*U11-4.*U13+U33)/(2.*U(1)+U(3)+DSQRT(SQ))

```

```

0052      Y(2)=Y(3)*(U(2)+U(3)-2.*U(1))+.5/(U(2)+U(3)+U(1))
0053      GO TO 74
0054      73 IF(KRAD.NE.0) GO TO 89
0055      U(2)=(4.*U(1)-U(3))/3.
0056      Y(2)=0.
0057      GO TO 74
0058      89 U(2)=U(1)
0059      Y(2)=Y(3)/3.
0060      74 GO TO (75,76,77),KEX
0061      75 CONTINUE
0062      GO TO 78
0063      76 U11=U(NP1)*U(NP1)
0064      U13=U(NP1)*U(NP3)
0065      U33=U(NP3)*U(NP3)
0066      SQ=84.*U33-12.*U13+9.*U11
0067      U(NP2)=(16.*U33-4.*U13+U11)/(2.*U(NP1)+U(NP3))+DSQRT(SQ))
0068      Y(NP2)=Y(NP3)-(Y(NP3)-Y(NP1))**U(NP2)+U(NP1)-2.*U(NP3))**.5/
0069      L(U(NP2)+U(NP1)+U(NP3))
0070      GO TO 78
0071      77 U(NP2)=(4.*U(NP3)-U(NP1))/3.
0072      Y(NP2)=Y(NP3)
0073      78 CCNTINUE
0074      IF(NEQ.EQ.1) GO TO 45
0075      C CALCULATION OF CORRESPONDING SLIP VALUES
0076      DO 88 J=1,NPH
0077      GO TO (81,82,83),KIN
0078      81 CONTINUE
0079      GO TO 84
0080      82 G=(U(2)+U(3)-8.*U(1))/(5.*U(2)+U(3))**8.*U(1))
0081      GF=(1.-PREF(J))/(1.+PREF(J))
0082      GF=(G+GF)/(1.+G*GF)
0083      F(J,2)=F(J,3)*GF*(1.-GF)*F(J,1)
0084      GO TO 84
0085      83 F(J,2)=F(J,1)
0086      IF(KRAD.EQ.0)F(J,2)=(4.*F(J,1)-F(J,3))**3.
0087      84 GO TO (85,86,87),KEX
0088      85 CONTINUE
0089      GO TO 88
0090      86 G=(U(NP2)+U(NP1)-8.*U(NP3))/(5.*U(NP2)+U(NP1))+8.*U(NP3))
0091      GF=(1.-PREF(J))/(1.+PREF(J))
0092      GF=(G+GF)/11.*G*GF)
0093      F(J,NP2)=F(J,NP1)*GF*(1.-GF)*F(J,NP3)
0094      GO TO 88
0095      87 F(J,NP2)=(4.*F(J,NP3)-F(J,NP1))/3.
0096      88 CONTINUE
0097      45 CCNTINUE
0098      CALL DENSITY
0099      C CALCULATION OF RAOI
0100      CALL RAD(XU,R(1),CSALFA)
0101      IF(CSALFA.EQ.0..OR.KRAD.EQ.0) GO TO 27
0102      DO 28 I=2,NP3
0103      28 R(I)=R(1)+Y(I)*CSALFA
0104      GO TO 29
0105      27 DO 30 I=2,NP3
0106      30 P(I)=R(1)
0107      29 CONTINUE
0108      C CALCULATION OF OMEGA VALUES
0109      OM(1)=0.
0110      OM(2)=0.
0111      DO 49 I=3,NP2
0112      49 OM(I)=OM(I-1)+.5*(RHO(I)*U(I)*R(I)+RHO(I-1)*U(I-1)*R(I-1))*
0113      L(Y(I)-Y(I-1))
0114      PFI=OM(NP2)
0115      DO 59 I=3,NP1
0116      59 OM(I)=OM(I)/PFI
0117      OM(NP2)=1.0
0118      OM(NP3)=1.
0119      RETURN
0120      END

```

```

0001      SUBROUTINE COEFF
0002      IMPLICIT REAL*8(A-H,O-Z)
0003      COMMON /GEN/PEI,AMI,AME,DPDX,PREF(3),PR(3),P(3),DEN,AMU,XU,XD,XP,
1XL,DX,CSALFA,XPC6,INTG
0004      1/V/N,NP1,NP2,NP3,NEG,NPH,KEX,KIN,KASE,KRAD,KPRAN
0005      1/V/U(43),F(3,43),RI(43),RHO(43),OM(43),Y(43)
0006      1/C/SC(43),AU(43),BU(43),CU(43),A(3,43),B(3,43),C(3,43)
0007      COMMON /SHEAR/ SHEAR(43),SCSH(43)
0008      COMMON/DUO/DUODOM(43),DUDY(43),ADUDY(43),ADUDYH
0009      DIMENSION G1(43),G2(43),G3(43),D(3,43),S1(43),S2(43),S3(43)
0010      C CALCULATION OF SMALL C'S
0011      C THE CONVECTION TERM
0012      SA=R(1)*AMI/PEI
0013      SB=IR(NP3)*AME-R(1)*AMI/PEI
0014      DX=XD-XU
0015      DO 71 I=3,NP1
0016      DMD=OM(I+1)-OM(I-1)
0017      P2=.25/DX
0018      P3=P2/DMD
0019      P1=(OM(I+1)-OM(I))*P3
0020      P3=(OM(I)-OM(I-1))*P3
0021      P2=3.*P2
0022      Q=SA/DMD
0023      R2=-SB*.25
0024      R3=R2/CMD
0025      R1=-(OM(I+1)+3.*CM(I))*R3
0026      R3=(OM(I-1)+3.*CM(I))*R3
0027      G1(I)=P1+Q+R1
0028      G2(I)=P2+R2
0029      G3(I)=P3-Q+R3
0030      CU(I)=-P1*U(I+1)-P2*U(I)-P3*U(I-1)
0031      C THE DIFFUSION TERM
0032      AU(I)=2./OMO
0033      BU(I)=SC(I-1)*AU(I)/(CM(I)-CM(I-1))
0034      CUI(I)=SC(I)*AU(I)/(CM(I+1)-CM(I))
0035      IF(NEQ.EQ.1) GO TO 33
0036      DO 34 J=1,NPH
0037      C(J,I)=-P1*F(J,+1)-P2*F(J,I)-P3*F(J,I-1)
0038      CALL SOURCE(CS,D(J,I),J,I)
0039      C(J,I)=-C(J,)+CS-F(J,I)+O(J,I)
0040      A(J,I)=AU(I)/PREF(J)
0041      BIJ,I)=BU(I)/PREF(J)
0042      34 CONTINUE
0043      C SOURCE TERM FOR VELOCITY EQUATION
0044      33 PHI = 0.0
0045      S1(I) = (DPDX + PHI)*DX
0046      S2(I)=P2*S1(I)/(RHO(I)*U(I))
0047      S3(I)=P3*S1(I)/(RHO(I-1)*U(I-1))
0048      S1(I)=P1*S1(I)/(RHO(I+1)*U(I+1))
0049      CUI(I)=CUI(I)-2.*IS1(I)+S2(I)+S3(I)
0050      S1(I)=S1(I)/U(I+1)
0051      S2(I)=S2(I)/U(I)
0052      S3(I)=S3(I)/U(I-1)
0053      71 CONTINUE
0054      C COEFFICIENTS IN THE FINAL FORM
0055      DO 91 I=3,NP1
0056      RL=1./(G2(I)+AU(I)+BU(I)-S2(I))
0057      AU(I)=(AU(I)+S1(I)-G1(I))*RL
0058      BU(I)=(BU(I)+S3(I)-G3(I))*RL
0059      91 CU(I)=CU(I)*RL
0060      76 CALL SLIP
0061      RETURN
0062      END

```

```

0001      SUBROUTINE CONST
0002      IMPLICIT REAL*8(A-H,O-Z)
0003      COMMON /GEN/PE1,AM1,AM2,DPDX,PREF(3),PR(3),P(3),DEN,AMU,XU,XD,XP,
1XL,DX,CSALFA,XPC6,INTG
0004      I/I/N,NP1,NP2,NP3,NEQ,NPH,REX,KIN,KASE,KRAD,KPRAN
0005      I/L1/YL,UMAX,UMIN,FR,YIP,YEM
0006      COMMON /ASD/ASD1,ASD2
0007      COMMON/CPS/CP1,CP2,GC1,GC2      — Change
0008      FR=.10
0009      PR(3) = 0.35
0010      PR(1)=1.
0011      PR(2)=.7
0012      AMU = 0.000012
0013      CP1=3.42
0014      CP2=0.24
0015      GC1=766.6
0016      GC2=53.35
0017      RETURN
      END
      CALL XEUNIT( 100,D1,D2,D3,D4)
      FORMAT (4E12.0)

```

READ(S,9) T₁, T₂, CP₁, CP₂, GC₁, GC₂,
P₁, P₂

in hydrogen-min

```

0001      SUBROUTINE DENSTY
0002      IMPLICIT REAL*8(A-H,O-Z)
0003      COMMON /GEN/PEI,AMI,AME,DPDX,PREF(3),PK131,P(31),DEN,AMU,XU,XD,XP,
1XL,DX,CSALFA,XPC6,INTG
0004      1/V/U(43),F(3,43),RT(43),RHCT43),CM(43),Y(43)
0005      1/I/N,NP1,NP2,NP3,NEQ,NPH,KEX,KIN,KASE,KRAD,KPRAN
0006      COMMON/AUXP/TEMP(43)
0007      COMMON/TEM/TOJO
0008      COMMON/CPS/CPL,CP2,GC1,GC2 replace
0009      COMMON/IW/IWAKE
0010      COMMON/IDIN/INDIC
0011      COMMON/DENC/C
0012      DIMENSION RBAR(43)
0013      PINF=14.7*144. PINF = P0A * 144.
0014      DO 45 I=1,NP3
0015      IF (NPH.LT.3) GO TO 46
0016      CPF=CP1*F(3,I)+CP2*(1.-F(3,I)) drop
0017      CPF=CPF*25000.0
0018      RBAR(I)=GC1*F(3,I)+GC2*(1.-F(3,I))
0019      GO TO 44
0020      46 CPF=.24*25000.
0021      F(3,I)=1.
0022      RBAR(I)=53.35
0023      IF(NPH.LT.2) F(2,I)=CPF*520.
0024      44 TEMP(I)=(F(2,I)-.5*U(I)*U(I))/CPF
0025      RHOII=PINF/(TEMP(I)*RBAR(I))
0026      IF(I.EQ.1) T1=F(2,I)/CPF
0027      IF(I.EQ.NP3) T2=F(2,NP3)/CPF
0028      45 CONTINUE
0029      TOJO=T1/T2
0030      IF(INTG.NE.0) GO TO 50
0031      C CHECK THAT GAS CONSTANTS CORRESPOND PROPERLY. 2=LOW SPEED SIDE
0032      IJ=1
0033      IA=NP3
0034      47 CONTINUE
0035      IF(RHO(IJ).LE.RHO(IA)) GO TO 48
0036      TRAT=T2/T1
0037      IF(IJ.EQ.NP3) TRAT=T1/T2
0038      C=0.95+.05*RBAR(IA)*TRAT/RBAR(IJ)
0039      GO TO 50
0040      48 C=0.984+.016*RHO(IA)/RHO(IJ)
0041      50 CONTINUE
0042      RETURN
0043      END

```

CALL XFUNT (F(3,I), TEMP(I), CPF, RBAR(I))

$$: P(I.EQ.1) T1 = TEMP(I)$$

$$: IFC(I.EQ.NP3) T2 = TEMP(I)$$

$$: TEMP(I) = TEMP(I) - U(I)*U(I)$$

$$: 50077.*CPF$$

$$: RT(I) = PINF*(TEMP(I)*RBAR(I))$$

$$: GO TO 45$$

$$: 46 CPF = .24*25000.$$

$$: F(3,I) = 1.$$

$$: RBAR(I) = 53.35$$

$$: IF (NPH.LT.2) F(2,I) = CPF*520.$$

$$: 45 CONTINUE$$

$$: T(I) = T1/12$$

$$: etc.$$

```

0011      SUBROUTINE ENTRN
0012      IMPLICIT REAL*8(A-H,O-Z)
0013      REAL*4 HEAD
0014      COMMON /GEN/ PEI,AMI,AME,DPDX,PREF(3),PR(3),P(3),DEN,AMU,XU,XD,XP,
0015      1XL,DX,CSALFA,XPC6,INTG
0016      1/V(43),F(3,43),R(43),RHC(43),QM(43),Y(43)
0017      1/I/N,NPI,NP2,NP3,NEQ,NPH,KEX,KIN,KASE,KRAD,KPRAN
0018      1/C/SC(43),DUMM(516)
0019      1/L1/Y/L,UMAX,UMIN,FR,Y1P,YEM
0020      COMMON /SHEAR/ SHEAR(43),SCSH(43)
0021      COMMON /RUAH/ RAAUH(43)
0022      COMMON/LIME/I,I,E
0023      COMMON/PRNT/ IPRNT
0024      COMMON /ASD/ ASD1,ASD2
0025      COMMON/HED/HEAD(20)
0026      DO 99 I=2,NP2
0027      CALL VEFF(EMU,I,I+1)
0028      SC(1)=RAAUH(I)*EMU/(PEI*PEI)
0029      99 CONTINUE
0030      SC(1)=0.D+0
0031      SC(NP3)=0.D+0
0032      IF(IPRNT.EQ.0) GO TO 10
0033      WRITE(6,1001) HEAD
0034      1001 FORMAT('1DATA FROM ENTRN ',20A4)
0035      WRITE(6,1002) KIN,KEX,KPRAN,NEQ,XU
0036      1002 FORMAT(' KIN=',I2,'KEX=',I2,'KPRAN=',I2,'NEQ=',I2,'XU=',F8.5)
0037      10 CONTINUE
0038      GO TO (11,12,31),KIN
0039      11 GO TO 40
0040      C
0041      12 IF(XU.EQ.0.) GO TO 30
0042      C
0043      13 UFR=I.01
0044      14 TF(U(I))/U(NP3).LE.0.1) UFR=I.10
0045      DO 25 I=4,N
0046      I)=
0047      IF(DABS(U(I))-U(I+1)).GT..0001*UMAX) GO TO 26
0048      25 CONTINUE
0049      26 CONTINUE
0050      C
0051      IF(U(I)).LT.U(1))GO TO 251
0052      IF(U(I)).GT.U(1))GO TO 252
0053      IF(U(I+1)).LT.U(I))GO TO 251
0054      IF(U(I+1)).GT.U(I))GO TO 252
0055      C THE VALUE OF INDEX MAY BE VARIED TO SUIT PROBLEM
0056      251 UDES=0.99*U(1)
0057      PSIUD=UDES
0058      IF(U(I)).GT.UDES) UDES=U(I)
0059      GO TO 253
0060      252 UDES=UFR*U(1)
0061      IF(UDES.EQ.0.) UDES=0.9*U(I)
0062      PSIUD=UDES
0063      IF(U(I)).LT.UDES) UDES=U(I)
0064      253 CONTINUE
0065      226 GI=(2.*PEI/(U(I+1)-U(I-1)))*((SC(I-1)*(U(I+1)-U(I)))/(OM(I+1)

```

```

1)-OM(I1)))-(SC(I1-1)*(U(I1)-U(I1-1))/[OM(I1)-OM(I1-1))]-[OM(I1+1)
0047   GI=DABSIG1)
0048   PSIUD={PSIUD-U(NP3)}/(U(1)-U(NP3))
0049   PSIII={U(I1)-U(NP3)}/(U(I1)-U(NP3))
0050   GRAT=(1.-PSIII)/[1.-PSIUD)
0051   IF(GRAT.GT.1..OR.GRAT.LE.0.) GRAT=L.
0052   GI=GI*GRAT
0053   IF(GI.GT.50.) GI=50.
0054   IF(I1.GT.5) GI=0.1*GI
0055   IF(IPRNT.EQ.0) GO TO 40
0056   400 WRITE(6,1000)I1,U(I1),U(I1+1),OM(I1-1),OM(I1),OM(I1+1),SC(I
0057   I1-1),SC(I1),SC(I1+1),GI
0058   1000 FORMAT(' IN ORDER I1, U(3),CM(3),SC(3),GI'/I3,10D11.4)
0059   GO TO 40
C
0059   30 AMI=DABSI(SHEART2)+SHEART3)-2.*SHEART1)
1   [U(2)+U(3)-2.*U(1))]
0060   GO TO 40
C
0061   31 AMI=0.
C
0062   40 GO TO (41,42,75),KEX
0063   41 IF(KPRAN.EQ.1.OR.NEQ.EQ.I.OR.XU.EQ.0.)GO TO 43
0064   IFIKIN.EQ.2)AMI=(GI-OM(I1))*R(NP3)*AME/[1.0-OM(I1)*R(1))
0065   43 GO TO 80
C
0066   42 IF(XU.EQ.0.) GO TO 70
C
0067   DO 56 I=3,N
0068   J=NP3-I
0069   IE=J
0070   IF(DABS(U(J)-U(J+1)).GT..0001*UMAX) GO TO 57
0071   56 CONTINUE
0072   57 CONTINUE
C
0073   IF(U(IE).LT.U(NP3))GO TO 551
0074   IF(U(IE).GT.U(NP3))GO TO 552
0075   IF(U(IE-1).LT.U(IE))GO TO 551
0076   IF(U(IE-1).GT.U(IE))GO TO 552
C THE VALUE OF UDES MAY BE VARIED TO SUIT PROBLEM
0077   551 UDES=0.99*U(NP3)
0078   PSIUD=UDES
0079   IF(U(IE).GT.UDES) UDES=U(IE)
0080   GO TO 553
0081   552 UDES=1.01*U(NP3)
0082   PSIUD=UDES
0083   IF(U(IE).LT.UDESI UDES=U(IE)
0084   553 CONTINUE
0085   556 GE=(2.*PEI/[U(IE+1)-U(IE-1)))*[({SC(IE)}*(U(IE+1)-U(IE))/
1/[OM(IE+1)-OM(IE)))-(SC(IE-1)*(U(IE)-U(IE-1))/
1/[OM(IE)-OM(IE-1)))-(CM(IE+1)-OM(IE-1))*(UDES
0086   -U(IE))]/
1/(DX*2.))
0087   GE=-1.*DABSI(GE)
  PSIUD={PSIUD-U(NP3)}/(U(1)-U(NP3))

```

```

0088      PSIIE=(U(IE)-U(NP3))/(U(1)-U(NP3))
0089      GRAT=PSIIE/PSIUD
0090      IF(GRAT.GT.1..OR.GRAT.LE.0.) GRAT=1.
0091      GE=GF*GRAT
0092      IF(IE.LT.(NP3-5)) GE=0.1*GE
0093      IF(GE.LT.-100.) GE=-100.
0094      IF(IPRNT.EQ.0) GO TO 60
0095      500 WRITE(6,1003)IE,U(IE-1),U(IE),U(IE+1),OM(IE-1),OM(IE),OM(IE+1),SC(IE-1),SC(IE),SC(IE+1),GE
0096      1003 FORMAT(' IN ORDER IE, U(3),CM(3),SC(3),GE/I3,10D11.4)
C
0097      60 IF(KIN.EQ.1)AME=(GE+(GM(IE)-1.)*R(1)*AMI)/(R(NP3)* OM(IE))
0098      IF(KIN.EQ.2)GO TO 65
0099      IF(KIN.EQ.3)AME=GE/(R(NP3)*GM(IE))
0100      GO TO 80
C      BOTH BOUNDARIES ARE FREE
0101      65 AMI=(GI*OM(IE)-GE*OM(1))/((OM(IE)-OM(1))*R(1))
0102      AME=((1.-OM(1))*GE-(1.-OM(IE))*GI)/((OM(IE)-OM(1))*R(NP3))
0103      IF(IPRNT.EQ.0) GO TO 80
0104      WRITE(6,1004)AMI,AME,PEI
0105      1004 FORMAT(' AT 65 AMI=',D11.4,'AME=',D11.4,'PEI=',D11.4)
0106      GO TO 80
0107      TO AME=-DABS((SHEAR(NP2)+SHEAR(NP1)-2.*SHEAR(NP3))/((U(NP2)+U(NP1)-2.*U(NP3)))
0108      1 IF(IPRNT.EQ.0) GO TO 80
0109      702 WRITE(6,1005)AMI,AME,PEI
0110      1005 FORMAT(' AT 70 AMI=',D11.4,'AME=',D11.4,'PEI=',D11.4)
0111      GO TO 80
0112      75 AME=0.
0113      IF(XU.EQ.0.) GO TO 80
0114      IF(KIN.EQ.2)AMI=GI/((1.-OM(1))*R(1))
0115      80 RETURN
0116      END

```

```

0001      SUBROUTINE LENGTH
0002      IMPLICIT REAL*8(A-H,O-Z)
0003      COMMON /GEN/PE1,AMI,AME,DPDX,PREF(3),PR(3),P(3),DEN,AMU,XU,XD,XP,
1XL,DX,CSALFA,XPC6,INTG
1/V/U(43),F(3,43),R(43),RHC(43),OM(43),Y(43)
1/I/N,NP1,NP2,NP3,NEQ,NPH,KEX,KIN,KASE,KRAD,KPRAN
1/L1/YL,UMAX,UMIN,FL,YIP,YEM
0004      COMMON/UMUM/YMU
0005      COMMON/KJU/KMU
C SEARCH FOR THE MAXIMUM AND MINIMUM VELOCITIES
0006      KMU=0
0007      40 UMAX=U(1)
0008      UMIN=U(1)
0009      DO 41 J=3,NP3
0010      IF(J.EQ.NP2)GO TO 41
0011      IF(U(J)).GT.UMAX)UMAX=U(J)
0012      IF(U(J).LT.UMIN) UMIN=U(J)
0013      GO TO 41
0014      42 UMIN=U(J)
0015      YMU=Y(J)
0016      KMU=J
0017      41 CONTINUE
0018      UTOL=.01*DABST(U(1)-U(NP3))
0019      IF(U(1).LT.U(NP3)) GO TO 410
0020      IF(DABS(UMIN-U(NP3)).LT.UTOL) UMIN=U(NP3)
0021      GO TO 4101
0022      410 IF(DABS(UMIN-U(1)).LT.UTOL) UMIN=U(1)
0023      4101 CONTINUE
0024      IF(U(1).LT.UTNP3) GO TO 425
0025      IF(UMIN.LT.U(NP3)) GO TO 61
0026      GO TO 426
0027      425 IF(UMIN.LT.U(1)) GO TO 61
0028      426 CONTINUE
0029      UM=.5*(U(1)+U(NP3))
0030      UMUZZ=DABS(U(1)-UM)
0031      DO 21 K=3,NP1
0032      UMUZ=DABS(U(K)-UM)
0033      IF(UMUZ.LT.UMUZZ) UMUZZ=UMUZ
0034      21 CONTINUE
0035      UMU=UM+UMUZZ
0036      KRAZY=1
0037      20 DO 22 K=3,NP1
0038      IF(U(K).NE.UMU) GO TO 22
0039      GO TO 24
0040      22 CONTINUE
0041      UMU=UM-UMUZZ
0042      KRAZY=KRAZY+1
0043      IF(KRAZY.EQ.2) GO TO 20
0044      24 KKU=K
0045      IF(U(KKU).EQ.UM) YMU=Y(KKU)
0046      IF(U(1).GT.U(NP3)) GO TO 25
0047      IF(U(KKU).GT.UM) GO TO 28
0048      25 IF(U(KKU).LT.UM) GO TO 27
0049      27 IF(U(KKU).GT.UM) GO TO 27
0050      28 IF(U(KKU).LT.UM) GO TO 28
0051      27 YMU=Y(KKU)+(UM-U(KKU))*(Y(KKU+1)-Y(KKU))/(UM-KKU+1)-U(KKU))

```

```

0052      GO TO 61
0053      28 YMU=Y(KKU)+(UM-U(KKU))*{Y(KKU-1)-Y(KKU)}/{U(KKU-1)-U(KKU)}
0054      61 CONTINUE
0055      DIF=DABS(UMAX-UMIN)*FR
0056      C SEARCH NEAR THE I BOUNDARY
0057      IF(KIN.NE.2) GU TO 43
0058      47 J=2
0059      48 J=J+1
0060      UJ1=U(J)-U(1)
0061      IF(DABS(UJ1).GE.DIF)GO TO 49
0062      GO TO 48
0063      49 AI=1.
0064      IF(UJ1.LT.0.)AI=-1.
0065      YIP=Y(J-1)+{Y(J)-Y(J-1)}*{U(1)+AI*DIF-U(J-1)}/{U(J)-U(J-1)}
0066      GO TO 44
0067      43 YIP=0.
0068      C SEARCH NEAR THE E BOUNDARY
0069      44 IF(KEX.NE.2) GO TO 45
0070      50 J=NP2
0071      51 J=J-1
0072      UJ1=U(J)-U(NP3)
0073      IF(DABS(UJ1).GE.DIF)GO TO 52
0074      GO TO 51
0075      52 AI=1.
0076      IF(UJ1.LT.0.)AI=-1.
0077      YEM=Y(J+1)+{Y(J)-Y(J+1)}*{U(NP3)+AI*DIF-U(J+1)}/{U(J)-U(J+1)}
0078      GO TO 46
0079      45 YEM=Y(NP3)
0080      46 YL=YEM-YIP
0081      RETURN
0082      END

```

```

0001      SUBROUTINE M0M12(AM)
0002      IMPLICIT REAL*8(A-H,O-Z)
0003      C M0M12 CALCULATES INTEGRAL MOMENTUM INCREMENT IN OMEGA COORDINATES
0004      COMMON/V/ U(43),F(3,43), R(43), RHO(43),OM(43),Y(43)
0005      1/I,N,NP1,NP2,NP3,NEQ,NPH,KEX,KIN,KASE,K,KPRAN
0006      UD25=0.5*(U(1)+U(3)-2.*U(NP3))
0007      UDNP25=0.5*(U(NP1)-U(NP3))
0008      OM25=0.5*OM(3)
0009      OMNP25=0.5*(OM(NP1)+1.)
0010      C
0011      EMI=0.5*OM25*(UD25+U(1)-U(NP3))
0012      DO 10 I=4,NP1
0013      10 EMI=EMI+0.5*(OM(I)-OM(I-1))*(U(I)+U(I-1)-2.*U(NP3))
0014      EMI=EMI+0.5*OMNP25*U0NP25
0015      C
0016      AM=EMI
0017      RETURN
0018      END

```

```

0001      SUBROUTINE OUTPUT
0002      IMPLICIT REAL*8(A-H,O-Z)
0003      COMMON /GEN/PEI,AMI,AME,DPDX,PREF(3),PR(3),DEN,AMU,XU,XD,XP,
1XL,DX,CSALFA,XPC6,INTG
1/V/U(43),F(3,43),R(43),RHO(43),OM(43),V(43)
1/C/SC(43),AU(43),BU(43),CU(43),A(3,43),B(3,43),C(3,43)
1/LI/YL,UMAX,UMIN,FR,YIP,YEM
1/I/N,NP1,NP2,NP3,NEQ,APH,KEX,KIN,KASE,KRAD,KPRAN
0004      COMMON/AUXP/TEMP(43)
0005      COMMON/AUXY/YY(43),XXU,RR1
0036      COMMON /SHEAR/ SHEAR(43),SCSH(43)
0007      COMMON /IDIN/ INOIC
0008      COMMON/DUD/DUD00M(43), DUDY(43), ADUDY(43), ADUDYM
0009      COMMON /ASD/ ASD1,ASD2
0010      COMMON/TEM/TOJO
0011      COMMON/UMUM/YMU
0012      COMMON/RADI/R0,RI
0013      COMMON/OUT/UP,US,PHIUC(501),PSIU(43),XOD(501)
0014      COMMON/TWOD/YI
0015      DIMENSION AMACH(43)
0016      DIMENSION TEMPE(43)
0017      IF(INTG.NE.1) GO TO 15
0018      DO 11 I=1,NP3
0019      AMACH(I)=0.
0020      11 CONTINUE
0021      WRITE(6,49)(OM(I),I=1,NP3)
0022      49 FORMAT(24H1THE VALUES OF CMEGA ARE/(11F10.4))
0023      15 CONTINUE
0024      IF (U(NP3).EQ.0.) GO TO 16
0025      UJUD=U(1)/U(NP3)
0026      GO TO 17
0027      16 UJUD=0.
0028      17 RHJO=RHO(1)/RHO(NP3)
0029      IF(KRAD.EQ.0) GO TO 605
0030      DO 60 I=1,NP3
0031      TEMPE(I)=R(I)/R0
0032      60 CONTINUE
0033      GO TO 615
0034      605 DO 610 I=1,NP3
0035      610 TEMPE(I)=Y(I)/R0
0036      615 CONTINUE
0037      AMACH(I)=0.
0038      AMACH(NP3)=0.
0039      DO 62 I=2,NP2
0040      IF(DUDY(I).EQ.0.) GO TO 62
0041      AMACH(I)=SHEAR(I)/(RHC(I)*DUDY(I))
0042      62 CONTINUE
0043      WRITE(6,51) XXU,RR1
0044      51 FORMAT('0 XU= ',2P011.2,' RI = ',2P011.2,' IN')
0045      WRITE(6,55) UJUD,RHJC,TOJO,PREF(1),PREF(2),PREF(3),ASD1,ASD2
0046      55 FORMAT(1H0,
1       6HUJ/U0=F6.3,2X,8HRHJ/RHC=F6.3,2X,7HTOJ/TO=F6.3,2X,6HPREF1
1=F5.3,2X,6HPREF2=F5.3,2X,6HPREF3=F5.3,2X,5HASD1=F6.3,2X,5HASD2=F6.
23)
0047      WRITE(6,54)
0048      WRITE(6,52)
0049      52 FORMAT(1H0,8X,1HY,11X,1HU,11X,1HH,12X,1HC,9X,2HKE,8X,4HR/R0,8X,
15HSHEAR,9X,3HEPS,9X,3HRHO,6X,5SHD/U/Y,7X,4HPSIU/
29X,2HIN,7X,6HFT/SEC,3X,12HFT**2/SEC**2,
313X,11H(FT/SEC)**2,10X,13HL8M/FT-SEC**2,
42X,9HFT**2/SEC,3X,9HL8M/FT**3,3X,9HFT/SEC/FT//)
0050      53 FORMAT(1H 1P11D12.3 )
0051      54 FORMAT(1H0 )
0052      DO 10 J1=1,NP3
0053      J2=NP2-J1+2
0054      WRITE(6,53) YY(J2),U(J2),F(2,J2),F(3,J2),F(1,J2),TEMPE(J2),
ISHEAR(J2),AMACH(J2),RHOU(J2),DUDY(J2),PSIU(J2)
0055      10 CONTINUE
0056      RETURN
0057      END

```

```

0001      SUBROUTINE RAD(X,R1,CSALFB)
0002      IMPLICIT REAL*8(A-H,C-Z)
0003      C      APPLICABLE TO AXISYMMETRIC MIXING LAYER AND JET
0003      COMMON /GEN/PE1,AMI,AME,DPDX,PREF(3),PR(3),P(3),DEN,AMU,XU,XD,XP,
0003      IXL,DX,CSALFA,XPC6,INTG
0003      1/V/UL43),F(3,43),R(43),RHO(43),UM(43),Y(43)
0003      L/I/N,NP1,NP2,NP3,NEQ,NPH,KEX,KIN,KASE,KRAD,KPRAN
0004      COMMON/RADI/RD,RI
0005      COMMON/TWOD/YI
0006      COMMON/IW/IWAKE,ISL
0007      CSALFB=1.
0008      IF (KRAD.EQ.0) GO TO 18
0009      IF(KIN.EQ.3) GO TO 17
0010      IF(X.EQ.0.) GO TO 15
0011      R1=R(1)*(R(1)-2.*AMI*(X-XP)/(RHO(1)*U(1)))
0012      IF(R1.LT.0.) R1=0.
0013      RI=DSQRT(R1)
0014      RETURN
0015      15 R1=RD-RI
0016      RETURN
0017      17 R1=0.
0018      RETURN
0019      C      APPLICABLE TO 2D JET
0020      18 R1=1.
0020      IF(X.EQ.0.) GO TO 19
0021      IF(ISL.EQ.0) RETURN
0022      IF(KIN.EQ.3) GO TO 20
0023      YI=YI-AMI*(X-XP)/(RHO(1)*U(1))
0024      IF(YI.LT.0.) YI=0.
0025      RETURN
0026      19 YI=RD-RI
0027      IF(ISL.EQ.0) YI=1.
0028      RETURN
0029      20 YI=0.
0030      RETURN
0031      END

```

```

0001      SUBROUTINE READY
0002      (IMPLICIT REAL*8(A-H,O-Z)
0003      COMMON /GEN/PE1,AMI,AME,OPDX,PREF(3),PR(3),P(3),DEN,AMU,XU,XD,XP,
0004      1XL,DX,CSALFA,XPC6,INTG
0005      1/V/U(43),F13,43),R(43),RHCI43),OM(43),Y(43)
0006      1/I/N,NP1,NP2,NP3,NEQ,NPH,KEX,KIN,KASE,KRAD,KPRAN
0007      COMMON/TWOD/YI
0008      CALL DENSTY
0009      CALL RAD(XU,R(1),CSALFA)
0010      C Y NEAR THE I BOUNDARY
0011      IF (R(1).EQ.0.) K(N=3)
0012      IFIKRAD.EQ.1) GO TO 70
0013      IF(YI.EQ.0.) KIN=3
0014      70 CONTINUE
0015      GO TO (71,72,73),KIN
0016      71 CONTINUE
0017      GO TO 74
0018      72 Y(2)=12.*OM(3)/(I3.*RHC(2)+RHO(3))*(U(2)+U(3)+4.*U(1)))
0019      GO TO 74
0020      73 Y(2)=.5*OM(3)/IRHO(1)*U(1))
0021      74 Y(3)=Y(2)+.25*OM(3)*I1./(RHC(3)*U(3))+2./IRHO(3)*U(3)+RHO(2)*U(2))
0022      1)
0023      C Y 'S' FOR INTERMEDIATE GRID POINTS
0024      DO 50 I=4,NP1
0025      50 Y(I)=Y((-1)+.5*IOM(I)-CP(I-1))*I1./IRHO(I)*U(I))+1./IRHO(I-1)*
0026      1U(I-1))
0027      C Y NEAR THE E BOUNDARY
0028      Y(NP2)=Y(NP1)+.25*(OM(NP2)-OM(NP1))*(1./IRHO(NP1)*U(NP1))+2./
0029      1(RHO(NP1)*U(NP1)+RHO(NP2)*U(NP2)))
0030      GO TO (81,82,83),KEX
0031      81 CONTINUE
0032      GO TO 84
0033      82 Y(NP3)=Y(NP2)+12.*OM(NP2)-OM(NP1))/(RHO(NP1)+3.*RHO(NP2))*(U(NP2)
0034      1)+U(NP1)+4.*U(NP3))
0035      GO TO 84
0036      83 Y(NP3)=Y(NP2)+.5*(OM(NP2)-OM(NP1))/(RHO(NP3)*U(NP3))
0037      84 IF(CSALFA.EQ.0..OR.KRAD.EQ.0) GO TO 51
0038      DO 52 I=2,NP3
0039      52 Y(I)=2.*Y(I)*PE1/(R(I)+DSCRT(R(I))*R(I)+2.*Y(I)*PE1*CSALFA)
0040      GO TO 56
0041      51 DO 54 I=2,NP3
0042      54 Y(I)=PE1*Y(I)/R(I)
0043      55 Y(2)=2.*Y(2)-Y(3)
0044      C CALCULATION OF RADII
0045      DO 57 I=2,NP3
0046      IFIKRAD.EQ.0) R(I)=R(1)
0047      57 IF(KRAD.NE.0) R(I)=R(1)+Y(I)*CSALFA
0048      57 CONTINUE
0049      69 RETURN
0050      END

```

```

0001      SUBROUTINE SHEARS
0002      IMPLICIT REAL*8(A-H,O-Z)
0003      COMMON /GEN/PEI,AMI,APE,DPOX,PREF(3),PR(3),P(3),DEN,AMU,XU,XD,XP,
0004      1XL,DX,CSALFA,XPC6,INTG
0005      1/I/N,NP1,NP2,NP3,NEQ,APH,KEX,KIN,KASE,KRAD,KPRAN
0006      1/V/U(43),F(3,43),R(43),RHC(43),GM(43),Y(43)
0007      1/L/YL,UMAX,UMIN,FR,YIP,YEM
0008      COMMON/OUT/UP,US,PHIUC(501),PSIU(43),XOD(501)
0009      COMMON /SHEAR/ SHFAR(43),SCSH(43)
0010      COMMON /ASD/ ASD1,ASD2
0011      COMMON/AEMU/E4UA
0012      COMMON/DENC/C
0013      COMMON/RT/RT4,YLK
0014      COMMON/DUDOM(43),DUDY(43),ADUDY(43),ADUDYM
0015      COMMON /KUH/ RAAUH(43)
0016      COMMON/KJU/KHU
0017      COMMON/IW/IWAKE,ISL
0018      COMMON/UMUM/YMU
0019      COMMON/I0IN/INDIC
0020      IKMAX=0
0021      TAUM=.0001
0022      ADUDYM=.0001
0023      DO 98 I=2,NP1
0024      RA=.5*(R(I+1)+R(I))
0025      RH=.5*(RHO(I+1)+RHO(I))
0026      UM=.5*(U(I+1)+U(I))
0027      RAAUH(I)=RA*RA*RH*UM
0028      SCSH(I)=R(I)*RHO(I)*U(I)/PEI
0029      DUDY(I)=DUDOM(I)*SCSH(I)
0030      99 CONTINUE
0031      SCSH( 1)=R( 1)*RHO( 1)*U( 1)/PEI
0032      SCSH(NP2)=R(NP2)*RHC(NP2)*U(NP2)/PEI
0033      SCSH(NP3)=R(NP3)*RHO(NP3)*U(NP3)/PEI
0034      DUDY( 1)=DUDOM( 1)*SCSH( 1)
0035      DUDY(NP2)=DUDOM(NP2)*SCSH(NP2)
0036      DUDY(NP3)=DUDOM(NP3)*SCSH(NP3)
0037      RAAUH(NP2)=SCSH(NP2)*R(NP2)*PEI
0038      DO 97 I=1,NP3
0039      ADUDY(I)=DABS(DUDY(I))
0040      97 CONTINUE
0041      IF(INTG.NE.1) GO TO 1066
0042      C F(1,I) INPUT IS EDDY VISCOSITY = EPS = SO THAT TAU=RHO*EPS*DUDY
0043      C AND TKE=EPS*DUDY/A1
0044      DO 1045 I=2,NP2
0045      C FOR THIS CALCULATION INPUT IS EPS (FT**2/SEC)
0046      1045 F(1,I)=F(1,I)*ADUDY(I)/ASD1
0047      F(1,1)=0.
0048      FT(1,NP3)=0.
0049      IF(K(N.EQ.3)F(1,1)=F(1,2)/2.
0050      XSTA=Y(NP3)*10.
0051      ICHK=7*NP3/10

```

```

0050      RTM=1.
0051      1066 CONTINUE
0052      IF(IIMAX.GT.ICHK) IIMAX=ICHK
0053      SIGN=DUDY(3)/DUDY(NP1)
0054      DO 101 I=2,NP2
0055      33 SHEAR(I)=ASD1*RHO(I)*F(1,I)*DUCY(I)/ADUDY(I)
0056      IF(IKIN.EQ.2) GO TO 101
0057      IF(IWAKE.EQ.11) GO TO 333
0058      IF(I.LT.IMAX.AND.U(I).LT.0.9*UP)
0059      1SHEAR(I)=SHEAR(I)*ADUCY(I)/ADUDY(I)
0060      GO TO 101
0061      333 IF(SIGNI101,334,334
0062      334 IF(I.LT.IMAX) SHEAR(I)=SHEAR(I)*ADUDY(I)/ADUDY(IMAX)
0063      101 CONTINUE
0064      IF(KIN.EQ.3) GO TO 118
0065      IF(XU.LE.XSTAI) GO TO 118
0066      IF(UN(I).LT.U(NP3)) GO TO 102
0067      IF(UMIN.LT.U(NP3)) GO TO 118
0068      GO TO 103
0069      102 IF(UMIN.LT.U(I)) GO TO 118
0070      103 CONTINUE
0071      DELU=U(NP3)-U(I)
0072      C0 110 I=1,NP3
0073      IF(U(I).GT.U(NP3)) GO TO 111
0074      IF((U(I)-U(I)).GT..05*DELU) GO TO 112
0075      GO TO 110
0076      111 IF((U(I)-U(NP3)).LT.-.95*DELU) GO TO 112
0077      110 CONTINUE
0078      112 I=I-1
0079      IF(IIN.LT.2) IIN=2
0080      DO 113 I=1,NP3
0081      IF(U(I).GT.U(NP3)) GO TO 114
0082      IF((U(I)-U(I)).GT..95*DELU) GO TO 115
0083      GO TO 113
0084      114 IF((U(I)-U(NP3)).LT.-.05*DELU) GO TO 115
0085      113 CONTINUE
0086      115 IOUT=I
0087      IF(IOUT.EQ.NP3) IOUT=NP2
0088      EPSI=SHEAR(IIN)/(RHO(IIN)*DUDY(IIN))
0089      EPS0=SHEAR(IOUT)/(RHO(IOUT)*DUDY(IOUT))
0090      DO 116 I=1,NP3
0091      IF(I.GT.IIN) GO TO 117
0092      SHEAR(I)=RHU(I)*EPSI*DUDY(I)
0093      GO TO 116
0094      117 IF(I.LT.IOUT) GO TO 116
0095      SHEAR(I)=RHO(I)*EPS0*DUDY(I)
0096      116 CONTINUE
0097      118 CONTINUE
0098      DO 125 I=1,NP3
0099      TAUL=TAUM
0100      TAU=DABS(SHEAR(I))
0101      IF(TAU.GT.TAUM) TAUM=TAU
0102      IF(TAUM.GT.TAUL) IKMAX=I
0103      125 CONTINUE
0104      RTML=RTM
0105      EMUM=SHEAR(IKMAX)/(RHO(IKMAX)*DUDY(IKMAX))

```

```

0105      RTM=DABS(U(1)-U(NP3))/EMUM
0106      YLK=1.5708*DABS(U(1)-U(NP3))/ADUDY(IKMAX)
0107      IF(YLK.LT.YL) YLK=YL
0108      IF(YLK.GT.1.57*YL) YLK=1.57*YL
0109      IF(PSIU(IKMAX).LT.0.4) YLK=1.57*YL
0110      IF(KIN.FQ.3.AND.KRAD.NE.0) YLK=2.*YMU
0111      RTM=RTM*YLK
0112      IF(XU.LE.XSTA) GO TO 126
0113      IF(INTG.EQ.1) RTML=RTM
0114      IF(RTM.GT.1.02*RTML) RTM=1.02*RTML
0115      126 CONTINUE
C      ****
C      RAMP(6)
C      ****
0116      IF(XU.LE.XSTA) GO TO 144
0117      IF(RTM.GT.185.) GO TO 131
0118      ASD2=1.69
0119      GO TO 145
0120      131 ASD2=0.46+.00762*RTM
0121      IF(ASD2.GT.3.20) ASD2=3.20
0122      GO TO 145
0123      144 ASD2=1.69
0124      145 CONTINUE
C      ****
0125      ASD2=ASD2/C
0126      SIGMA=1.855*XU/YL
0127      WRITE(6,1000) INTG,RTM,ASD2,SIGMA
0128      1000 FORMAT(1H , ' FROM SHEARS, AT STEP ',14,'RTM= ',1PE14.5,' ASD2= ',1,
I1PE14.5,' SIGMA= ',1PE14.5)
0129      WRITE(6,1001) YL,YLK,IKMAX
0130      1001 FORMAT(1H , ' YL= ',1PE14.5,' YLK= ',1PE14.5,' IKMAX= ',13)
0131      FMUA=DABS(SHEAR(3)/DUDY(3))
0132      RETURN
0133      END

```

```

0001      SUBROUTINE SLIP
0002      IMPLICIT REAL*8(A-H,O-Z)
0003      (COMMON /GEN/PE1,AM1,AM2,DPDX,PHEF(3),PK(3),P(3),DEN,AMU,XU,XD,XP,
0004      1XL,DX,CSALFA,XPC6,INTG
0005      1/1/N,NP1,NP2,NP3,NEC,NPH,KEX,KIN,KASE,KRAD,KPRAN
0006      1/V/U(43),F(3,43),R(43),RHO(43),OM(43),Y(43)
0007      COMMON/AEMU/EMUA
0008      COMMON /L/AK,ALMG
0009      1/C/SC(43),AU(43),BU(43),CU(43),A(3,43),B(3,43),C(3,43)
0010      C SLIP COEFFICIENTS NEAR THE I BOUNDARY FOR VELOCITY EQUATION
0011      C NOTE-- U(1) MAY BE ZERO ONLY IF DPDX=0.
0012      CU(2)=0.
0013      CU(NP2)=0.
0014      GO TO (71,72,73),KIN
0015      71 CONTINUE
0016      GO TO 74
0017      72 SQ=84.*U(1)*U(1)-12.*U(1)*U(3)+9.*U(3)*U(3)
0018      BU(2)=8.*(2.*U(1)+U(3))/(2.*U(1)+7.*U(3)+DSQRT(SQ))
0019      AU(2)=1.-BU(2)
0020      GO TO 74
0021      73 BU(2)=0.
0022      IF(U(1).EQ.0.) GO TO 735
0023      AK1=1./DX-DPDX/(RHO(1)*U(1)*U(1))
0024      AK2=-U(1)*AK1+DPDX/(RHO(1)*U(1))
0025      GO TO 7355
0026      735 AK1=1./DX
0027      AK2=0.
0028      7355 CONTINUE
0029      AJ=RHO(1)*U(1)*.25*(Y(2)+Y(3))**2/EMUA
0030      IF(KPAU.EQ.0) GO TO 75
0031      AU(2)=2./(2.+AJ*AK1)
0032      CU(2)=-.5*AJ*AK2*AU(2)
0033      GO TO 74
0034      75 CU(2)=1./(2.+3.*AJ*AK1)
0035      AU(2)=CU(2)*(2.-AJ*AK1)
0036      CU(2)=-CU(2)*4.*AJ*AK2
0037      C SLIP COEFFICIENTS NEAR THE E BOUNDARY FOR VELOCITY EQUATION
0038      C NOTE-- U(NP3) MAY BE ZERO ONLY IF DPDX=0.
0039      74 GO TO (81,82,83),KEX
0040      81 CONTINUE
0041      GO TO 84
0042      82 SQ=84.*U(NP3)*U(NP3)-12.*U(NP3)*U(NP1)+9.*U(NP1)*U(NP1)
0043      AU(NP2)=8.*(2.*U(NP3)+U(NP1))/(2.*U(NP3)+7.*U(NP1)+DSQRT(SQ))
0044      BU(NP2)=1.-AU(NP2)
0045      GO TO 84
0046      83 AU(NP2)=0.
0047      CALL VEFF(FMU,NP1,NP2)
0048      IF(U(NP3).EQ.0.) GO TO 835
0049      PK1=1./DX-DPDX/(RHO(NP3)*U(NP3)*U(NP3))
0050      PK2=-U(NP3)*PK1+DPDX/(RHO(NP3)*U(NP3))
0051      GO TO 8355
0052      835 PK1=1./DX
0053      PK2=0.
0054      8355 CONTINUE
0055      BJ=RHO(NP3)*U(NP3)*.25*(2.*Y(NP3)-Y(NP1)-Y(NP2))**2/EMU
0056      CU(NP2)=1./(2.+3.*BJ*PK1)

```

```

0049      BU(NP2)=CU(NP2)*(2.-BJ*BK1)
0050      CU(NP2)=-CU(NP2)*4.*BJ*BK2
0051  84 IF(NEQ.Q,FQ,1)RETURN
C   SLIP COEFFICIENTS NEAR THE I BOUNDARY FOR OTHER EQUATIONS
0052      PI 54 J=1,NPH
0053      C(J,2)=0.
0054      C(J,NP2)=0.
0055      GO TO (41,42,43),KIN
0056      41 CONTINUE
0057      GO TO 44
0058      42 A(J,2)=(U(2)+U(3)-8.*U(1))/(5.*(U(2)+U(3))+8.*U(1))
0059      GF=(1.-PREF(J))/(1.+PREF(J))
0060      A(J,2)=(A(J,2)+GF)/(1.+A(J,2)*GF)
0061      B(J,2)=1.-A(J,2)
0062      GO TO 44
0063      43 B(J,2)=0.
0064      CALL SOURCE(CS,DS,J,1)
0065      AK1=1./DX-DS
0066      AK2=-AK1*F(J,1)-CS
0067      AJF=AJ*PREF(J)
0068      (F(KRAD,EQ,0) GU TO 45
0069      A(J,2)=2./ (2.+AJF*AK1)
0070      C(J,2)=-.5*AJF*AK2*A(J,2)
0071      GO TO 44
0072      45 C(J,2)=1./(2.+3.*AJF*AK1)
0073      A(J,2)=C(J,2)*(2.-AJF*AK1)
0074      C(J,2)=-C(J,2)*4.*AJF*AK2
C   SLIP COEFFICIENTS NEAR THE E BOUNDARY FOR OTHER EQUATIONS
0075      44 GO TO (51,52,53),KEX
0076      51 CONTINUE
0077      GO TO 54
0078      52 B(J,NP2)=(U(NP2)+U(NP1)-8.*U(NP3))/(5.*(U(NP2)+U(NP1))+8.*U(NP3))
0079      GF=(1.-PREF(J))/(1.+PREF(J))
0080      B(J,NP2)=(B(J,NP2)+GF)/(1.+B(J,NP2)*GF)
0081      A(J,NP2)=1.-B(J,NP2)
0082      GO TO 54
0083      53 A(J,NP2)=0.
0084      CALL SOURCE(CS,DS,J,NP3)
0085      BK1=1./DX-DS
0086      BK2=-BK1*F(J,NP3)-CS
0087      BJF=BJ*PREF(J)
0088      C(J,NP2)=1./(2.+3.*BJF*BK1)
0089      B(J,NP2)=C(J,NP2)*(2.-BJF*BK1)
0090      C(J,NP2)=-C(J,NP2)*4.*BJF*BK2
0091      54 CONTINUE
0092      RETURN
0093      END

```

```

0001      SUBROUTINE SOLVE(A,B,C,F,NP3)
0002      IMPLICIT REAL*8(A-H,O-Z)
C   THIS SOLVES EQUATIONS OF THE FORM
C   F(I) = A(I)*F(I+1) + B(I)*F(I-1) + C(I)
C   FOR I=2,NP2
0003      DIMENSION A(NP3),B(NP3),C(NP3),F(NP3)
0004      NP2=NP3-1
0005      B(2) = B(2)*F(1) + C(2)
0006      DO 48 I=3,NP2
0007      T = 1./(1.-B(I)*A(I-1))
0008      A(I) = A(I)*T
0009      48 B(I) = (B(I)*F(I-1) + C(I))*T
0010      DO 50 I=2,NP2
0011      J=NP2-I+2
0012      50 F(J)=A(J)*F(J+1)+B(J)
0013      RETURN
0014      END

```

```

0001      SUBROUTINE SOURCE(ICS,DS,J,1)
0002      IMPLICIT REAL*8(A-H,O-Z)
0003      C FOR CONSERVATION OF STAGNATION ENTHALPY
0004      C CAUTION- USE CONSISTENT UNITS
0005      C THE DOT PRODUCT OF E WITH J IS NEGLECTED
0006      CCOMMON/GEN/PEI,AMI,AME,DPOX,PREF(3),PR(3),P(3),DEN,AMU,XU,XD,XP,
0007      1XL,DX,CSALFA,XPC6,INTG
0008      1/V/U(43),F(3,43),R(43),RHC(43),OM(43),Y(43)
0009      1/I/N,NP1,NP2,NP3,NEU,NPH,KEX,KIN,KASE,KRAD,KPRAN
0010      1/L1/YL,UMAX,UMIN,FR,YIP,YEM
0011      1/C7SC(43),AU(43),BU(43),CUT(43),AL(3,43),BL(3,43),CL(3,43)
0012      CCOMMON/ASD/ASD1,ASD2
0013      COMMON/RT/RTM,YLK
0014      COMMON /SHEAR/ SHEAR(43),SCSH(43)
0015      COMMON/DUD/DUDOM(43), DUDY(43), ADUDY(43), ADUDYM
0016      COMMON/UMUM/YMU
0017      COMMON/UMUM/YMU
0018
0019
0020      IF (J.GT.3) GO TO 12
0021      GO TO (13,11,12),J
0022      11 IF(I.EQ.1) GO TO 12
0023      CS=SC(I)*(U(I+1)*U(I+1)-U(I)*U(I))/(OM(I+1)-OM(I))
0024      CS=CS-SC(I-1)*(U(I)*U(I)-U(I-1)*U(I-1))/(OM(I)-OM(I-1))
0025      CS=(1.0D+0-1.0D+0/PREF(J))*CS/(OM(I+1)-OM(I-1))
0026      CSKE=SC(I)*
0027      1 (OM(I+1)-OM(I))
0028      CSKE=CSKE-SC(I-1)*(F(1,I)-F(1,I-1))/(OM(I)-OM(I-1))
0029      CS=CS+2.0D+0*(1.0D+0/PREF(I)-1.0D+0/PREF(J))*CSKE/(OM(I+1)-OM(I-1))
0030      CS=CS+CSKE
0031      DS=0.0D+0
0032      GO TO 3
0033      12 CONTINUE
0034      CS = 0.0D+0
0035      DS = 0.0D+0
0036      GO TO 3
0037      C SOURCE MODIFICATION NO. 1. D=R**2*RHO*U*EMU*DUDOM**2/PEI**2-DK/RHO*U
0038      13 IF(I.LT.2.OR.I.GT.NP2) GO TO 131
0039      CALL VEFF(EMU,I,I+1)
0040      GO TO I32
0041      131 CS=0.0D+0
0042      GO TO 133
0043      132 CS=RHO(I)*U(I)*EMU * (DUDOM(I)*R(I)/PEI)**2
0044      133 IF(F(I,I).LE.0.0D+0) GO TO 15
0045      IF(U(I).EQ.0.0D+0) GO TO 15
0046      CS=CS-ASD2*F(I,I)**1.5D+0/(YLK*U(I))
0047      DS=-1.5D+0*ASD2*DSQRT(F(I,I))/(YLK*U(I))
0048      GO TO 16
0049      15 DS=0.0D+0
0050      16 CONTINUE
0051      17 RETURN
0052      ENO

```

```

0001      SUBROUTINE VEFF(EMU,I,IPL)
0002      IMPLICIT REAL*8(A-H,O-Z)
0003      COMMON /SHEAR/ SHEAR(43),SCSH(43)
0004      COMMON/DUD/DUDOM(43), DUDY(43), ADUDY(43), ADUDYM
0005      67 EMU=DABSI(SHEAR(I)/DUDY(I))
0006      RETURN
0007      END

```

UNCLASSIFIED

Security Classification

DOCUMENT CONTROL DATA - R & D

(Security classification of title, body of abstract and indexing annotation must be entered when the overall report is classified)

1. ORIGINATING ACTIVITY (Corporate author) Arnold Engineering Development Center Arnold Air Force Station, Tenn. 37389		2a. REPORT SECURITY CLASSIFICATION UNCLASSIFIED
		2b. GROUP N/A
3. REPORT TITLE A GENERAL ANALYSIS OF FREE TURBULENT MIXING		
4. DESCRIPTIVE NOTES (Type of report, and inclusive dates) Final Report - June 1969 through June 1973		
5. AUTHOR(S) (First name, middle initial, last name) Philip T. Harsha, ARO, Inc.		
6. REPORT DATE May 1974	7a. TOTAL NO. OF PAGES 76	7b. NO. OF REFS 34
8a. CONTRACT OR GRANT NO.	9a. ORIGINATOR'S REPORT NUMBER(S) AEDC-TR-73-177	
b. PROJECT NO. 9711	9b. OTHER REPORT NO(S) (Any other numbers that may be assigned this report) ARO-ETF-TR-73-111	
c. Program Element 61102F		
d.		
10. DISTRIBUTION STATEMENT Approved for public release; distribution unlimited.		
11. SUPPLEMENTARY NOTES Available in DDC.	12. SPONSORING MILITARY ACTIVITY Air Force Office of Scientific Research (SERP), 1400 Wilson Blvd. Arlington, VA 22209	
13. ABSTRACT <p>A general analysis applicable to a variety of free mixing flows of engineering interest is described. An empirical relationship between the turbulent shear stress and the turbulent kinetic energy is used. Solution of the turbulent kinetic energy equation as one of the governing equations yields the turbulent shear stress at all points in the flow field. Algebraic relationships are used to obtain the length scales required to close the turbulent kinetic energy equation. The computer program developed to provide the numerical framework for this analysis is described, and a FORTRAN listing and description of required inputs is included. To demonstrate the capabilities of the analysis, a number of experimental free mixing flows have been calculated, and the results of these calculations are discussed.</p>		

UNCLASSIFIED

Security Classification

14. KEY WORDS	LINK A		LINK B		LINK C	
	ROLE	WT	ROLE	WT	ROLE	WT
mixing turbulence						
turbulent flow						
shear stress						
kinetic energy						